

REPUBLIQUE DU CAMEROUN

Paix-Travail-Patrie



DEPARTEMENT DE GENIE CIVIL
DEPARTMENT OF CIVIL ENGINEERING

REPUBLIQUE DU CAMEROUN

Paix-Travail-Patrie



UNIVERSITÀ
DEGLI STUDI
DI PADOVA

DEPARTMENT OF CIVIL, ARCHITECTURAL
AND ENVIRONMENTAL ENGINEERING

INFLUENCE OF HIGH TEMPERATURE ON THE STRUCTURAL BEHAVIOUR OF STEEL STRUCTURES AND SOLUTIONS : CASE OF PANZANI BUILDING

A thesis submitted in partial fulfilment of the requirements for the
degree of Master of Engineering (MEng) in Civil Engineering
Curriculum: Structural Engineering

Presented by :

WAMBA KENFACK ANNE SINCLAIRE

Student number : 15TP20976

Supervised by:

Pr. Carlo PELLEGRINO

Co-supervised by:

Dr. Paolo ZAMPIERI

Dr. Cyrille TETOUGUENI

Academic year : 2019/2020

INFLUENCE OF HIGH TEMPERATURE ON THE STRUCTURAL BEHAVIOUR OF STEEL
STRUCTURES AND SOLUTIONS : CASE OF PANZANI BUILDING

REPUBLIQUE DU CAMEROUN

Paix-Travail-Patrie



DEPARTEMENT DE GENIE CIVIL
DEPARTMENT OF CIVIL ENGINEERING

REPUBLIQUE DU CAMEROUN

Paix-Travail-Patrie



UNIVERSITÀ
DEGLI STUDI
DI PADOVA

DEPARTMENT OF CIVIL, ARCHITECTURAL
AND ENVIRONMENTAL ENGINEERING

INFLUENCE OF HIGH TEMPERATURE ON THE
STRUCTURAL BEHAVIOUR OF STEEL
STRUCTURES AND SOLUTIONS : CASE OF
PANZANI BUILDING

A thesis submitted in partial fulfilment of the requirements for the
degree of Master of Engineering (MEng) in Civil Engineering

Curriculum: Structural Engineering

Presented by :

WAMBA KENFACK ANNE SINCLAIRE

Student number : 15TP20976

Supervised by:

Pr. Carlo PELLEGRINO

Co-supervised by:

Dr. Paolo ZAMPIERI

Dr. Cyrille TETOUGUENI

Academic year : 2019/2020

DEDICATION

To my father
WAMBA FABIEN

ACKNOWLEDGEMENTS

This work would not have been completed without the combined efforts of individuals who contributed directly and/or indirectly to its realization. I wish to express my sincere thanks and gratitude to :

- The **President of the jury**;
- The **Examiner** of this jury for accepting to bring his criticisms and observations to ameliorate this work;
- My supervisors Prof. **Carlo PELLEGRINO**, Dr. **Paolo ZAMPIERI** and Dr. **Cyrille TETOUGUENI** for all the guidance and advice they provide me with, during this thesis work;
- Professors **NKENG George ELAMBO** and **Carmelo MAJORANA** for all their academic and administrative support during these five years spent at ENSTP in the MEng program in partnership with University of Padua in Italy;
- The vice-director of ENSTP, Dr. **BWEMBA Charles Loic** for his perpetual help and advices during our sojourn in this school;
- Prof. **MBESSA Michel**, the head of department of Civil Engineering for his tutoring and valuable advices;
- Dr. Eng. **Guillaume Hervé POH'SIE** for his advice and help which helped me during this work;
- **All the teaching staff of ENSTP and University of Padua** for their good quality teaching and the motivation they developed in us to continue our studies;
- My family and more specially to my mother **WAMBA TCHOUMO Elise**, my uncle **TEMGWA NJEUFACK Rene**, my aunt **DJOUKANG Rachel** and my cousin **DOUNTSOP GUEGIM Martial** for the education and financial support during all these years;
- **All my classmates and all my friends** who were a source of motivation and tenacity. As a team, together we have been able to achieve more.

LIST OF ABBREVIATIONS AND SYMBOLS

ABBREVIATIONS

AISI	American Iron and Steel Institute
ASTM	American Society for Testing and Materials
BCSA	British Constructional Steelwork Association
BHP	Broken Hill Proprietary
BOP	Basic Oxygen Process
BRE	British Research Establishment
BS	British Steel
CHS	Circular Hollow Section
CVUT	Czech Technical University
DETR	Department of Environment and Transport in the Regions
EC	Eurocode
EN	European Norm
FEA	Finite Element Analysis
FASBUS II	Fire Analysis of Steel Building System II
FCFA	Franc of the Financial Community of Africa
FERMENCAM	Cameroonian Fermentation company
HVAC	Heating Ventilation and Air Conditioning
ISO	International Organisation Standardization
NBS	National Building Standards
OLP	Oxygen Lime Powder
RC	Reinforce Concrete
SAP	Structural Analysis Program
SCI	Steel Construction Institute
SLS	Serviceability Limit State
SHS	Square Hollow Section
SONARA	National Refining Company
ULS	Ultimate Limit State
UK	United Kingdom
WSA	World Steel Association

SYMBOLS

A	Area of cross section
A_a	Area of the steel section
A_b	Area of bolt
A_{eff}	Effective area
A_m	Surface area of the member per unit length
A_{net}	Net cross sectional area
A_p	Area of base plate
A_t	Total area of enclosure
A_v	Shear area of the steel profile
A_v	Area of vertical openings
A_s	Tensile stress area of the bolt
c	Specific heat
C_{dir}	Directional factor
$c_e(z)$	Exposure factor
C_{season}	Seasonal factor
$C_o(z)$	Orography factor
$C_r(z)$	Roughness factor
C_{pe}	Pressure coefficient for the external pressure
C_{pi}	Pressure coefficient for the internal pressure
d	Bolt diameter
d_0	Diameter of bolt holes
d_w	Diameter of the washer or the width across points of the bolt head
d_p	Thickness of the fire protective material
E	Young modulus
$E_{fi,d}$	Design effect of actions for the fire design situation
e_c	Edge distance of the column flange
e_p	Edge distance of the end plate
e_1	End distance from the centre of a bolt hole to the adjacent end part measured in the direction of load transfer
e_2	End distance from the centre of a bolt to the adjacent edge end, measured at right angles to the direction of load transfer

INFLUENCE OF HIGH TEMPERATURE ON THE STRUCTURAL BEHAVIOUR OF STEEL
STRUCTURES AND SOLUTIONS : CASE OF PANZANI BUILDING

$F_{b,Rd}$	Bearing resistance
f_{cd}	Design compressive strength of concrete
f_{ck}	Characteristic compressive cylinder strength of concrete
$F_{c,Rd}$	Resistance of the column web in the compressed zone
$F_{T,1Rd}, F_{T,2Rd}, F_{T,3Rd}$	Design resistance for the failure modes 1, failure mode 2 and failure mode 3
f_y	Yielding strength
f_u	Ultimate tensile strength
f_{ub}	Ultimate tensile strength of the bolt
$F_{t,Rd}$	Traction resistance of the bolts
$F_{v,Rd}$	Shear resistance of the bolt
G_k	Permanent loads
h_w	Height of web
$\dot{h}_{net,d}$	Net heat flux per unit area
h_p	Height of the plate
H	Height
I_v	Turbulence intensity
i	radius of gyration
i_s	Influence width
k_b	Conversion factor depending on thermal properties
k_C	Correction factor
k_T	Terrain factor
k_{sh}	Correction factor for the shadow effect
k_1	Turbulence factor
l_b	Length of beam
L_{cr}	Critical buckling length
l_{eff}	Effective length of the equivalent T-stub
$M_{b,Rd}$	Lateral torsional buckling resistance
$M_{c,Rd}$	Resisting moment of the beam
M_{cr}	Elastic critical moment for lateral torsional buckling
M_{Ed}	Design moment
$M_{el,Rd}$	Elastic resisting moment

INFLUENCE OF HIGH TEMPERATURE ON THE STRUCTURAL BEHAVIOUR OF STEEL
STRUCTURES AND SOLUTIONS : CASE OF PANZANI BUILDING

$M_{pl,Rd}$	Plastic resisting moment
$M_{pl,i,Rd}$	Plastic resistance moment of the equivalent T-stub for different modes
$N_{b,Rd}$	Buckling resistance
$N_{C,Rd}$	Resistance to axial compression
N_{Ed}	Design axial load
n_i	Number of bolt rows
$N_{pl,Rd}$	Design plastic resistance of gross cross section
N_{SLS}	Serviceability limit state axial force solicitation
$N_{u,Rd}$	Design ultimate resistance of the net cross section at holes for fasteners
O	Opening factor
p_1	Spacing between the centres bolts in a line in the direction of load transfer
p_2	Spacing between the centres bolts in a line at right angles to the direction of load transfer
q_b	Basic velocity pressure
$q_{f,d}$	Design fire load density
Q_k	Live loads
$q_p(z)$	Peak velocity pressure
$q_{t,d}$	Design fire load density related to total surface area of the enclosure
r	Root radius
$R_{fi,d,t}$	Design resistance of the member for fire design situation at time
t	Time
t_{ed}	Equivalent time of fire exposure for design
t_f	Flange thickness
t_{lim}	minimum value for the duration of the fire based on fire growth rates
t_{wc}	Thickness of the column flange
t_p	Thickness of the plate
t_w	Web thickness
u	Perpendicular distance from the edge of the beam flange to the edge of the column (lever arm)
V	Volume of the member per unit area
V_b	Basic wind velocity
$v_m(z)$	Mean wind velocity

INFLUENCE OF HIGH TEMPERATURE ON THE STRUCTURAL BEHAVIOUR OF STEEL
STRUCTURES AND SOLUTIONS : CASE OF PANZANI BUILDING

V_{Ed}	Design shear
V_{Rd}	Shear resistance of the connectors
$V_{c,Rd}$	Design shear resistance
$V_{pl,Rd}$	Shear resistance of the beam
w_c	Width of column
w_e	External pressure coefficient
W_{el}	Elastic section modulus
W_{eff}	Effective section modulus
w_f	Ventilation factor
w_i	Internal pressure coefficient
W_{pl}	Plastic section modulus
z_e	Reference height for external pressure
z_{min}	Minimum height
z_o	Roughness length
θ	Temperature
α_v	Coefficient depending on ventilation and floor area
ρ	Density
λ	Thermal conductivity
$\Delta\theta$	Variation in temperature
μ_0	Degree of utilization
$\Psi_{i,j}$	Combination coefficient
ε	Coefficient depending on f_y
χ	Reduction factor for the relevant buckling mode
χ_{LT}	Reduction factor for lateral-torsional buckling
α_{LT}	Imperfection factor for buckling
$\bar{\lambda}$	Non-dimensional slenderness with respect to z axis
σ	Compression constraint
$\gamma_{MO}, \gamma_{M1}, \gamma_{M2}$	Partial safety factors
γ	Unit weight
ω	Reduction factor to allow for the possible effects of interaction with shear in the column

ABSTRACT

The main objective of this work was to analyse the structural behaviour of a steel building subjected to fire and to propose some solutions in order to reduce or prevent the damage of such structures due to flames. To achieve this objective, a literature review was done in order to have an overview on steel material, on the different steel structures, on the effect of fire on steel structures and on how structural analysis of fire in a structure can be made. The case study used for the different analyses was a warehouse of the Panzani company located at Tractafric, in the industrial zone of the Bassa district in Douala, which was ravaged by flames. This work started by creating a model of the case study in SAP2000 with all the loads applied on it, in order to get the different solicitations present in the model. These solicitations which were used to statically verify the structure according to Eurocodes norms. Then, the fire analysis using the sequentially coupled thermal analysis method with the help of the software Abaqus/CAE was made on the roofing elements and the structural elements. The standard temperature-time curve ISO 834 was used to represent the evolution of temperature with time due to fire. The results gotten from the analyses made on the roofing elements showed that they were extremely affected by fire, due to high deflection observed and the fact that their melting point arrived rapidly just after the beginning of the fire. Moreover, a global fire analysis was made and it was observed that the most affected structures on it were the purlins, due to their small cross sections as compare to the other structural elements. Afterwards, a local analysis made on a purlin and a column of the case study showed that after one hour of fire, the purlin deflected with a value of 366.5 mm and the column with a value of 866 mm. Then, the local analysis made on the SHS and CHS columns showed that these two columns cross sections are not efficient against fire as compare to an IPE due to their hollow sections. The displacements observed after fire analysis on the SHS and CHS were 1596 mm and 1474 mm respectively. Finally, protective fire systems using fire extinguisher balls, intumescent coatings and solid materials were proposed and the fire analysis made on the partial hybrid steel-timber column, total hybrid steel-timber column, partial hybrid steel-concrete column and total hybrid steel-concrete column showed that they are good fire protective materials for steel and that the total hybrid steel-timber was the best configuration for fire protection.

Keywords: steel, fire, static analysis, sequentially coupled thermal analysis, intumescent coating.

RÉSUMÉ

L'objectif principal de ce travail était d'analyser le comportement structurel d'un bâtiment en acier soumis à un incendie et de proposer quelques solutions afin de réduire ou d'empêcher des incendies d'endommager de telles structures. Pour atteindre cet objectif, une revue de la littérature a été faite afin d'avoir une vue d'ensemble sur l'acier, sur les différentes structures en acier, sur l'effet du feu sur les structures en acier et sur la façon dont l'analyse structurelle du feu dans une structure peut être faite. Le cas d'étude utilisé pour les différentes analyses est un entrepôt de la société Panzani situé à Tractafric, dans la zone industrielle du quartier Bassa à Douala qui a été ravagé par les flammes. Ce travail a commencé par la création d'un modèle du cas d'étude dans le logiciel SAP2000 avec toutes les charges appliquées sur celui-ci, afin d'obtenir les différentes sollicitations présentes dans le modèle. Ces sollicitations ont été utilisées pour la vérification statique de la structure selon les normes Eurocodes. Ensuite, l'analyse incendie utilisant la méthode d'analyse thermique couplée séquentiellement à l'aide du logiciel Abaqus/CAE a été effectuée sur les éléments de toiture et sur les éléments structurels. La courbe standard température-temps ISO 834 a été utilisée pour représenter l'évolution de la température dans le temps sous l'effet du feu. L'analyse réalisée sur les éléments de toiture a montré qu'ils étaient extrêmement affectés par le feu en raison de la forte déflexion observée et du fait que leur point de fusion arrivait rapidement juste après le début de l'incendie. De plus, une analyse globale du feu a été effectuée et il a été observé que les structures les plus affectées étaient les pannes en raison de leurs petites sections par rapport aux autres éléments structurels. Ensuite, une analyse locale effectuée sur une panne et un poteau du cas d'étude a montré qu'après une heure d'incendie, la panne a fléchi avec une valeur de 366.5 mm et le poteau avec une valeur de 866 mm. De plus, l'analyse locale effectuée sur les poteaux SHS et CHS a montré que ces deux sections ne sont pas efficaces contre le feu par rapport à un IPE en raison de leurs sections creuses. Les déplacements observés après une analyse incendie sur le poteau SHS et CHS étaient respectivement de 1596 mm et 1474 mm. Finalement, des systèmes de protection contre le feu consistant à utiliser des boules d'extincteur, des peintures intumescentes et des matériaux solides ont été proposés. Une analyse du feu effectuée sur un poteau hybride partiel acier-bois, hybride total acier-bois, hybride partiel acier-béton et hybride total acier-béton a montré qu'ils sont de bons matériaux de protection contre le feu pour l'acier et que le poteau hybride total acier-bois est la meilleure configuration pour la protection contre le feu.

Mots clés : acier, feu, analyse statique, analyse thermique à couplage séquentiel, peintures intumescentes.

LIST OF FIGURES

Figure 1.1. Melting metal in crucible.....	3
Figure 1.2. Bessemer Converter.....	4
Figure 1.3. Open-hearth furnace	5
Figure 1.4. Oxygen furnace.....	6
Figure 1.5. Section (a) and plan (b) view of an electric arc furnace.....	6
Figure 1.6. Empire State Building	13
Figure 1.7. Amazon spheres.....	14
Figure 1.8. Parts of a bolt.....	14
Figure 1.9. Butt and fillet weld	15
Figure 1.10. Shear connection.....	16
Figure 1.11. Moment connection	16
Figure 1.12. Axial connection.....	17
Figure 1.13. Column base plate connection.....	18
Figure 1.14. Single-storey building.....	18
Figure 1.15. Single span symmetric portal frame	19
Figure 1.16. Lattice truss structure.....	19
Figure 1.17. Types of braced frame: (a) Concrete core, (b) inverted V bracing, (c) alternative types of triangulated bracing.....	20
Figure 1.18. Japoma stadium	20
Figure 1.19. Destroyed McCormick Center.....	23
Figure 1.20. AMA industry in fire	23
Figure 1.21. Yopougon industrial zone in fire	24
Figure 1.22. Industrial area of Sidi Bernoussi	24
Figure 1.23. Damaged SONARA structure	25
Figure 1.24. Damaged structure of Fermencam warehouses	25
Figure 1.25. Damaged structure of Biopharma’s warehouse.....	26

INFLUENCE OF HIGH TEMPERATURE ON THE STRUCTURAL BEHAVIOUR OF STEEL
STRUCTURES AND SOLUTIONS : CASE OF PANZANI BUILDING

Figure 1.26. The Cardington fire tests	28
Figure 2.1. Illustrations of the exposure factor $c_e(z)$ for $c_0=1,0$, $k_1=1,0$	46
Figure 2.2. Pressure on surfaces.....	46
Figure 2.3. Beam shear resisting area	52
Figure 2.4. Buckling curves	56
Figure 2.5. Spacing of the holes on the plate	58
Figure 2.6. Connection geometry.....	59
Figure 2.7. Portal frame eaves connections with bolted end plate.....	60
Figure 2.8. Complete flange yielding.....	60
Figure 2.9. Bolt failure with flange yielding.....	61
Figure 2.10. Bolt failure.....	62
Figure 2.11. Portal frame apex connection with bolted extended end plate	63
Figure 2.12. Tangent lines on the base plate which determine uplift	65
Figure 2.13. Modelling of aluminium sheet.....	67
Figure 2.14. Modelling of purlin IPE80.....	67
Figure 2.15. Assembly model of the roofing elements	71
Figure 2.16. Standard nominal temperature curve	72
Figure 2.17. Predefined ambient temperature and boundary conditions on the roof.....	72
Figure 2.18. Assembly model of the building.....	74
Figure 2.19. Loading and boundary conditions on the building	75
Figure 2.20. Modelling of (a) purlin IPE80 and (b) column IPE400.....	75
Figure 2.21. Faces of the IPE400 column where fire was applied.....	76
Figure 2.22. Faces of the SHS 260/16 column where fire was applied	78
Figure 2.23. Faces of the CHS 323.9/14.2 column where fire was applied.....	78
Figure 2.24. Partial hybrid steel-timber column	80
Figure 2.25. Faces of the partial hybrid steel-timber column where fire was applied.....	80
Figure 2.26. Totally protected steel-timber column.....	80

INFLUENCE OF HIGH TEMPERATURE ON THE STRUCTURAL BEHAVIOUR OF STEEL
STRUCTURES AND SOLUTIONS : CASE OF PANZANI BUILDING

Figure 2.27. Faces of the total hybrid steel-timber column where fire was applied	81
Figure 2.28. Partially protected steel-concrete column.....	82
Figure 2.29. Totally protected steel-concrete column.....	82
Figure 3.1. Map of Douala showing the location of the case study	83
Figure 3.2. Panzani’s warehouse directly after fire damage	85
Figure 3.3. Panzani’s warehouse today	86
Figure 3.4. Site plan showing the store	87
Figure 3.5. Floor plan of the store.....	88
Figure 3.6. Building model from SAP2000	92
Figure 3.7. Front view of temperature distribution in the roofing elements.....	105
Figure 3.8. Back view of temperature distribution in the roofing elements	105
Figure 3.9. Deflection on the roofing elements	106
Figure 3.10. Damaged roofing elements due to fire	107
Figure 3.11. Displacement due to fire on the whole structure	107
Figure 3.12. Zoomed image of the maximum displacement of the structure	108
Figure 3.13. Damaged roof elements of the Panzani’s store	108
Figure 3.14. Temperature distribution in the purlin.....	109
Figure 3.15. Temperature evolution in the IPE80 purlin’s cross section.....	110
Figure 3.16. Undeformed and deformed shape of the purlin	110
Figure 3.17. Temperature distribution in the IPE400 column	111
Figure 3.18. Temperature evolution in the IPE400 column’s cross section	112
Figure 3.19. Displacement of the IPE column due to the fire effect.....	112
Figure 3.20. Temperature distribution in the SHS column due to fire effect	115
Figure 3.21. Temperature evolution in the SHS column’s cross section.....	115
Figure 3.22. Displacement of the SHS column due to fire effect	116
Figure 3.23. Temperature distribution in the CHS column due to fire effect.....	117
Figure 3.24. Temperature evolution in the CHS column’s cross section	117

INFLUENCE OF HIGH TEMPERATURE ON THE STRUCTURAL BEHAVIOUR OF STEEL
STRUCTURES AND SOLUTIONS : CASE OF PANZANI BUILDING

Figure 3.25. Displacement of the CHS column due to fire effect..... 118

Figure 3.26. Temperature distribution in partially protected steel with timber 119

Figure 3.27. Temperature evolution in partially steel-timber cross section..... 119

Figure 3.28. Temperature distribution in totally protected steel with timber 120

Figure 3.29. Temperature evolution in totally steel-timber cross section..... 121

Figure 3.30. Temperature distribution in partially protected steel with concrete 122

Figure 3.31. Temperature evolution in partially steel-concrete cross section 122

Figure 3.32. Temperature distribution in totally protected steel with concrete 123

Figure 3.33. Temperature evolution in totally steel-concrete cross section..... 124

LIST OF TABLES

Table 1.1. Steel classification according to their carbon content	8
Table 1.2. Nominal values of the yield strength and the ultimate tensile strength for bolts ...	15
Table 1.3. Summary of results of the Cardington fire tests	30
Table 2.1. Codes	42
Table 2.2. Terrain categories and terrain parameters	45
Table 2.3. Elastic properties of aluminium zinc	68
Table 2.4. Plastic properties of aluminium zinc	68
Table 2.5. Thermal properties of aluminium zinc	69
Table 2.6. Elastic properties of steel S235	69
Table 2.7. Plastic properties of steel S235.....	70
Table 2.8. Thermal properties of steel S235.....	70
Table 2.9. Density of timber	79
Table 2.10. Thermal properties of timber.....	79
Table 2.11. Thermal properties of concrete.....	81
Table 3.1. Steel structural sections material properties	89
Table 3.2. Concrete and reinforcing steel material properties.....	90
Table 3.3. Wind load calculations	91
Table 3.4. Vertical loads.....	91
Table 3.5. Horizontal loads.....	92
Table 3.6. Solicitation on the purlin	93
Table 3.7. Properties of IPE80.....	93
Table 3.8. Classification of the purlin cross section.....	93
Table 3.9. Design verification of the purlin.....	94
Table 3.10. Solicitation on the rafter	94
Table 3.11. Properties of IPE400.....	94
Table 3.12. Classification of the rafter cross section.....	95

INFLUENCE OF HIGH TEMPERATURE ON THE STRUCTURAL BEHAVIOUR OF STEEL
STRUCTURES AND SOLUTIONS : CASE OF PANZANI BUILDING

Table 3.13. Design verification of the rafter.....	95
Table 3.14. Solicitations on the IPE400 column	96
Table 3.15. Design verification of the IPE400 column	96
Table 3.16. Solicitations on the IPE160 column	97
Table 3.17. Properties of IPE160.....	97
Table 3.18. Classification of the IPE160 column	97
Table 3.19. Design verification of the IPE160 column	98
Table 3.20. Solicitation on the horizontal braces	98
Table 3.21. Properties of L50*50*5	99
Table 3.22. Design verification of the horizontal braces.....	99
Table 3.23. Solicitation on the vertical braces.....	99
Table 3.24. Properties of L80*80*8	100
Table 3.25. Design verification of the vertical braces	100
Table 3.26. Solicitations in the beam to column connection.....	101
Table 3.27. Design verification of the beam-column connection.....	101
Table 3.28. Solicitations in the beam to beam connection	102
Table 3.29. Design verification of the beam-beam connection.....	102
Table 3.30. Solicitations in the beam to beam connection	103
Table 3.31. Design verification of the brace connection	103
Table 3.32. Solicitations at column base connection.....	104
Table 3.33. Design verification of the column base connection.....	104
Table 3.34. Classification of the SHS 260/16 column	113
Table 3.35. Classification of the CHS 323.9/14.2 column	113
Table 3.36. Design verification of the SHS 260/16 column.....	114
Table 3.37. Design verification of the CHS 323.9/14.2 column	114

TABLE OF CONTENTS

DEDICATION	i
ACKNOWLEDGEMENTS	ii
LIST OF ABBREVIATIONS AND SYMBOLS.....	iii
ABSTRACT	viii
RÉSUMÉ.....	ix
LIST OF FIGURES.....	x
LIST OF TABLES	xiv
TABLE OF CONTENTS.....	xvi
GENERAL INTRODUCTION	1
CHAPTER 1: LITERATURE REVIEW	2
Introduction	2
1.1. Steel.....	2
1.1.1. Steelmaking process.....	2
1.1.1.1. Crucible process	3
1.1.1.2. Bessemer process	3
1.1.1.3. Open hearth furnace	4
1.1.1.4. Basic oxygen steelmaking.....	5
1.1.1.5. Electric arc furnace.....	6
1.1.2. Properties of steel	7
1.1.2.1. Tensile strength	7
1.1.2.2. Ductility.....	7
1.1.2.3. Durability	7
1.1.2.4. Conductivity	7
1.1.2.5. Lustre.....	7
1.1.2.6. Magnetic.....	8
1.1.3. Type of steel.....	8

INFLUENCE OF HIGH TEMPERATURE ON THE STRUCTURAL BEHAVIOUR OF STEEL
STRUCTURES AND SOLUTIONS : CASE OF PANZANI BUILDING

1.1.3.1. Carbon steels	8
1.1.3.2. Alloy steels	9
1.1.3.3. Stainless steels	9
1.1.3.4. Tool steels	9
1.1.4. Uses of steel	9
1.1.4.1. Buildings and infrastructure	10
1.1.4.2. Mechanical equipment	10
1.1.4.3. Automotive	10
1.1.4.4. Metal products	10
1.1.4.5. Other transport	10
1.1.4.6. Domestic appliances	11
1.1.4.7. Electrical equipment	11
1.1.5. Defects of steel	11
1.1.6. Prevention of defects	11
1.1.6.1. Metal type	11
1.1.6.2. Protective coating	11
1.1.6.3. Environmental measures	12
1.1.6.4. Metallic coatings	12
1.1.6.5. Corrosion inhibitors	12
1.1.6.6. Design modifications	12
1.2. Steel structures	13
1.2.1. Historical background	13
1.2.2. Steel connecting devices	14
1.2.2.1. Classification based on the connecting medium	14
1.2.2.2. Classification based on the type of internal force	15
1.2.2.3. Classification based on the type of members joining	17
1.2.3. Type of steel structures	18

INFLUENCE OF HIGH TEMPERATURE ON THE STRUCTURAL BEHAVIOUR OF STEEL
STRUCTURES AND SOLUTIONS : CASE OF PANZANI BUILDING

1.2.3.1. Single storey buildings	18
1.2.3.2. Multi-storey buildings	19
1.2.3.3. Special steelwork.....	20
1.2.4. Advantages and disadvantages of steel structures.....	21
1.2.4.1. Advantages of steel structures	21
1.2.4.2. Disadvantages of steel structures	21
1.3. Fire effect on steel structures	22
1.3.1. Overview of structural damaged events due to fire.....	22
1.3.1.1. Damaged structures due to fire in the world	22
1.3.1.2. Damaged structures due to fire in Africa	23
1.3.1.3. Damaged structures due to fire in Cameroon.....	24
1.3.2. Experimental research on the fire performance of structures.....	26
1.3.2.1. AISI and NBS test	26
1.3.2.2. BHP William Street fire test.....	27
1.3.2.3. Cardington fire test.....	27
1.3.3. Numerical research on the Cardington test (PiT Project).....	30
1.4. Structural fire analysis.....	32
1.4.1. Thermal analysis	32
1.4.1.1. Atmosphere temperatures.....	32
1.4.1.2. Member temperatures.....	36
1.4.2. Structural analysis	38
1.4.2.1. Critical temperature method.....	38
1.4.2.2. Resistance method.....	39
1.4.2.3. Advanced calculation method	40
Conclusion.....	40
CHAPTER 2: METHODOLOGY	41
Introduction	41

INFLUENCE OF HIGH TEMPERATURE ON THE STRUCTURAL BEHAVIOUR OF STEEL
STRUCTURES AND SOLUTIONS : CASE OF PANZANI BUILDING

2.1. General site recognition	41
2.2. Site visit.....	41
2.3. Data collection.....	41
2.3.1. Structural data	41
2.3.2. Characteristics of materials	42
2.4. Codes and loads conditions	42
2.4.1. Codes	42
2.4.2. Permanent loads	42
2.4.3. Variable loads.....	43
2.4.3.1. Imposed loads.....	43
2.4.3.2. Wind loads.....	43
2.4.4. Accidental loads	47
2.4.5. Limit states	48
2.4.5.1. Ultimate limit states	48
2.4.5.2. Serviceability limit states	48
2.4.6. Load combinations	48
2.5. Structural design method of steel structures	49
2.5.1. Numerical static analysis tool	49
2.5.1.1. Presentation of the numerical software SAP2000.....	49
2.5.1.2. Analysis steps	50
2.5.2. Classification of the sections.....	50
2.5.3. Members in bending.....	51
2.5.3.1. Uniaxial bending	51
2.5.3.2. Shear resistance	51
2.5.3.3. Lateral torsional buckling.....	53
2.5.4. Members in tension	54
2.5.5. Members in compression	54

INFLUENCE OF HIGH TEMPERATURE ON THE STRUCTURAL BEHAVIOUR OF STEEL
STRUCTURES AND SOLUTIONS : CASE OF PANZANI BUILDING

2.5.5.1. Pure compression	54
2.5.5.2. Buckling resistance	55
2.5.6. Connection design	57
2.5.6.1 Beam-column connection.....	57
2.5.6.2. Beam-beam connection	63
2.5.6.3. Brace connection	64
2.5.6.4. Column base connection	64
2.5.7. Serviceability limit states check for steel members	65
2.6. Numerical fire analysis tool	65
2.6.1. Presentation of the numerical software ABAQUS.....	66
2.6.2. Analysis step	66
2.6.2.1. Local analysis on roofing elements	66
2.6.2.2. Global analysis on structural elements	73
2.6.2.3. Local analysis on structural elements.....	75
2.7. Analysis of two fire protective systems	78
2.7.1. Hybrid steel-timber elements	79
2.7.2. Hybrid steel-concrete elements	81
Conclusion.....	82
CHAPTER 3 : RESULTS AND INTERPRETATION.....	83
Introduction	83
3.1. General presentation of the site	83
3.1.1. Physical parameters.....	83
3.1.1.1. Location.....	83
3.1.1.2. Climate	84
3.1.1.3. Hydrology.....	84
3.1.2. Socio-economical parameters	84
3.1.2.1. Population.....	84

INFLUENCE OF HIGH TEMPERATURE ON THE STRUCTURAL BEHAVIOUR OF STEEL
STRUCTURES AND SOLUTIONS : CASE OF PANZANI BUILDING

3.1.2.2. Economy.....	84
3.1.2.3. Transport	85
3.2. Physical description of the site.....	85
3.3. Presentation of the project.....	86
3.3.1. Presentation of the structural data	86
3.3.2. Characteristics of the materials	89
3.4. Loads determination.....	91
3.4.1. Vertical loads.....	91
3.4.2. Horizontal loads	91
3.5. Design verification of the steel structure.....	92
3.5.1. Purlin design verifications.....	93
3.5.2. Rafter design verifications	94
3.5.3. Column design verifications.....	96
3.5.3.1. IPE400	96
3.5.3.2. IPE160	97
3.5.4. Braces design verifications.....	98
3.5.4.1. Horizontal braces.....	98
3.5.4.2. Vertical braces.....	99
3.5.5. Connections design verifications	100
3.5.5.1. Beam-column connection.....	100
3.5.5.2. Beam-beam connection	102
3.5.5.3. Brace connection	103
3.5.5.4. Column base connection	103
3.6. Result of the fire analysis on the project.....	105
3.6.1. Local analysis on the roofing elements	105
3.6.2. Global analysis on the structural elements	107
3.6.3. Local analysis on the structural elements.....	109

INFLUENCE OF HIGH TEMPERATURE ON THE STRUCTURAL BEHAVIOUR OF STEEL
STRUCTURES AND SOLUTIONS : CASE OF PANZANI BUILDING

3.6.3.1. Results of purlin	109
3.6.3.2. Results of column.....	111
3.7. Result of the analysis on the fire protective systems	118
3.7.1. Results of the hybrid steel-timber elements	119
3.7.2. Results of the hybrid steel-concrete elements	121
Conclusion.....	125
GENERAL CONCLUSION	126
BIBLIOGRAPHY	127
WEBOGRAPHY.....	130
ANNEXES	131
ANNEX 1. Section factor for unprotected and insulated steel section	131
ANNEX 2. Critical temperature $\theta_{a,cr}$ for values of the utilization factor μ_0	133
ANNEX 3. Building category	134
ANNEX 4. Safety factors for permanent and variable actions	135
ANNEX 5. Recommended values of Ψ factors for buildings.....	136
ANNEX 6. Steel cross section's classification	137
ANNEX 7. Imperfection factor and buckling curve's selection tables	139
ANNEX 8. Effective length of the T-stub.....	140
ANNEX 9. Fire extinguisher ball and intumescent coating.....	141

GENERAL INTRODUCTION

Chosen as the adequate material used for most of the constructions made in the world due to its numerous advantages, structural steel is an alloy of iron and carbon which is capable of achieving greater span lengths with smaller deflections at lower costs with a better structural performance. Steel provides unbeatable speed of construction and off-site fabrication, thereby reducing the financial risks associated with site-dependent delays. The inherent properties of steel allow much greater freedom at the conceptual design phase, thereby helping to achieve greater flexibility and quality. The various structures which comes under the edges of steel structures are used for industrial, residential, office and commercial purposes. Moreover, steel can be used for the construction of other structures like bridges, railways and transmission line towers. In Africa and in Cameroon in particular, most of the steel constructions present are industrial buildings used for production or for storage . Unfortunately, it has been observed that these structures are highly damaged by fire even though steel is non-combustible, reason why this work is made.

Fire was the first important source of power in the development process of the human civilization. However, thousands of years of human history indicate that fire has also brought massive disasters. It has caused the death of thousands of people, massive building damage, and billions of economic losses. Consequently, fire safety is still one of the most important issues for the public security of people and goods. The main objective of this work is therefore, to analyse the structural behaviour of a steel building subjected to fire and proposed some solutions in order to reduce or prevent this damage.

In order to achieve this objective, a steel building that was damaged by fire will be used for the study. This study is divided in three parts and the first part (Chapter 1) consists of a literature review on steel, steel structures, the effect of fire on steel structures and how structural analysis of fire in a structure can be made. The second chapter (Chapter 2) is the methodology. In this chapter the verification procedure of the building with the solicitations gotten with the help of the software SAP2000 and the modelling process in Abaqus/CAE will be explained. Finally, in the third chapter (Chapter 3), the results of the static verification and fire analyses of the roofing elements, global structural elements and local structural elements will be presented. Afterwards, the results obtained from the fire analysis of two protective systems will be presented and based on their conductivity, environmental impact and their aesthetic aspects one of these two materials will be chosen as the best protective material.

CHAPTER 1: LITERATURE REVIEW

Introduction

The objective of this chapter is to present an overview on steel, steel structures, the effect of fire on steel structures and how structural analysis of fire in a structure can be made. Section 1.1 will present steel, its manufacturing processes, its properties, the different types of steel, their uses, defects and prevention of defects. The historical background of steel structures until its use in modern construction, the way they are joined using connecting devices, the different type of steel buildings made from steel associated with the advantages and disadvantages of steel will be presented in section 1.2. The effect of fire on steel structures will be developed in section 1.3. This section will illustrate an overview of structural damaged events due to fire that happened in the world, the experimental large-scale fire test and numerical research that have been carried out in the past in order to understand the effect of fire on steel structures. Section 1.4 will present the structural fire analysis method of steel structures illustrating how different thermal actions can be considered on structures in order to design a fire resisting structure and the different methods to evaluate the thermal response and mechanical response of a structure subjected to fire.

1.1. Steel

Steel is a malleable iron/carbon alloy containing from 0.10% to as much as 2% carbon, which determines the level to which it can be hardened. It is sometimes further alloyed with manganese, molybdenum, chromium, nickel, etc. to improve the ease with which it can be hardened and other characteristics such as corrosion resistance. The first steel almost certainly was obtained when the other elements necessary for producing it were accidentally present when iron was heated. Proving to be harder and stronger than bronze, iron began to displace bronze in weaponry and tool. The development of steel can be traced back 4000 years to the beginning of the Iron Age.

1.1.1. Steelmaking process

Steelmaking is the process of producing steel from iron ore and/or scrap. In steelmaking, impurities such as nitrogen, silicon, phosphorus, sulphur and excess carbon (the most important impurity) are removed from the sourced iron, and alloying elements such as manganese, nickel, chromium, carbon and vanadium are added to produce different grades of steel. Limiting dissolved gases such as nitrogen and oxygen and entrained impurities in the steel is also important to ensure the quality of the products cast from the liquid steel (Deo et al., 1993).

Steelmaking has existed for millennia, but it was not commercialized on a massive scale until the late 14th century. One of the ancient process of steelmaking was the crucible process but with time, in the 1850s and 1860s, the Bessemer process and the Siemens-Martin process were discovered and they turned steelmaking into a heavy industry. Today there are two major commercial processes for making steel, namely basic oxygen steelmaking, and electric arc furnace (EAF) steelmaking (Turkdogan, 1996).

1.1.1.1. Crucible process

The crucible process is a process for melting metals and alloys in pots, or crucibles, made of refractory materials as illustrated in figure 1.1. It is the oldest known method for melting metals and it was used for producing sharp knives, strong tools, and such steel weapons as damask blades. The earliest known use of the technique occurred in India and central Asia in the early 1st millennium CE. Steel was produced by heating wrought iron with materials rich in carbon, such as charcoal in closed vessels. The crucible process was rediscovered in Europe in 1740 by the British inventor Benjamin Huntsman. The product was pure steel of uniform composition suitable for knives, razor blades, clock and watch springs, and pendulums. Most of the development work on the crucible process occurred in the first half of the 19th century. Although crucible steel was expensive and could be produced only in small quantities, it remained for long time the only material suitable for making certain critical tools and mechanical parts.



Figure 1.1. Melting metal in crucible

(<https://www.dreamstime.com/stock-photo-steel-pouring-hot-plant-image66078777>)

1.1.1.2. Bessemer process

Bulk steel production was made possible by Henry Bessemer in 1855, when he obtained British patents for a pneumatic steelmaking process. The Bessemer process was the first inexpensive industrial process for the mass production of steel from molten pig iron using the

Bessemer converter as shown in figure 1.2. Bessemer used a pear-shaped vessel lined with ganister, a refractory material containing silica, into which air was blown from the bottom through a charge of molten pig iron. Bessemer realized that the subsequent oxidation of the silicon and carbon in the iron would release heat and that, if enough vessel were used, the heat generated would more than offset the heat lost. A temperature of 1650 °C could thus be obtained in a blowing time of 15 minutes with a charge weight of about half a ton.



Figure 1.2. Bessemer Converter (<http://sab.hopcroft.name/2009-06-07/DSCN2647.JPG>)

One difficulty with Bessemer's process was that it could convert only a pig iron low in phosphorus and sulphur. In 1878 Sidney Gilchrist Thomas and Percy Gilchrist developed a basic-lined converter in which calcined dolomite was the refractory material. This enabled a lime-rich slag to be used that would hold phosphorus and sulphur in solution. World production of steel rose to about 50 million tons by 1900.

1.1.1.3. Open hearth furnace

Open-hearth furnaces (Figure 1.3) are one of several kinds of furnace in which excess carbon and other impurities are burnt out of pig iron to produce steel (Barraclough, 1990). Since steel is difficult to manufacture owing to its high melting point, normal fuels and furnaces were insufficient and the open-hearth furnace was developed to overcome this difficulty. Compared to Bessemer steel, its main advantages were that it did not expose the steel to excessive nitrogen (which would cause the steel to become brittle), was easier to control, and permitted the smelting and refining of large amounts of scrap iron and steel. This process was developed in the 1860s by William and Friedrich Siemens in Britain, and Pierre and Émile Martin in France. The open-hearth furnace was fired with air and fuel gas that were preheated by combustion gases to 800 °C. A flame temperature of about 2000 °C could be obtained, and

this was sufficient to melt the charge. Initially an acid-lined furnace was used, but later a basic process was developed that enabled phosphorus and sulphur to be removed from the charge. The great advantage of the open hearth was its flexibility: the charge could be all molten pig iron, all cold scrap, or any combination of the two.

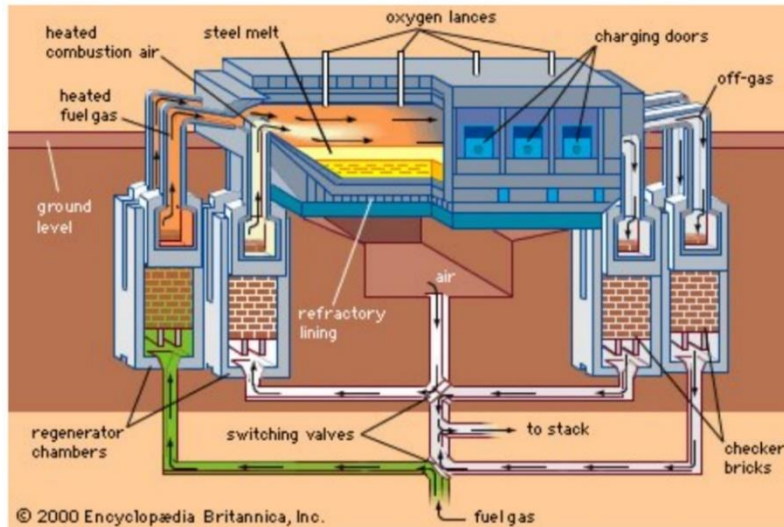


Figure 1.3. Open-hearth furnace

(<https://www.britannica.com/technology/open-hearth-furnace>)

1.1.1.4. Basic oxygen steelmaking

Basic oxygen steelmaking, also known as Linz–Donawitz-steelmaking or the oxygen converter process is a method of primary steelmaking in which carbon-rich molten pig iron is made into steel using an oxygen converter as presented in figure 1.4. The Linz-Donawitz (LD) process, developed in Austria in 1949, blew oxygen through a lance into the top of a pear-shaped vessel similar to a Bessemer converter. Since there was no cooling effect from inert nitrogen gas present in air, any heat not lost to the off-gas could be used to melt scrap added to the pig-iron charge. In addition, by adding lime to the charge, it was possible to produce a basic slag that would remove phosphorus and sulphur. With this process, which became known as the basic oxygen process (BOP), it was possible to produce 200 tons of steel from a charge consisting of up to 35 percent scrap in 60 minutes. With time, it increased to 400 tons and, with a low-silicon charge, blowing times could be reduced to 15 to 20 minutes. After the introduction of the Linz-Donawitz process, a modification was developed that involved blowing burnt lime through the lance along with the oxygen. Known as the OLP (Oxygen-lime powder) process, this led to the more effective refining of pig iron smelted from high-phosphorus European ores. Beginning about 1960, all oxygen steelmaking processes replaced the open-hearth and Bessemer processes on both sides of the Atlantic.

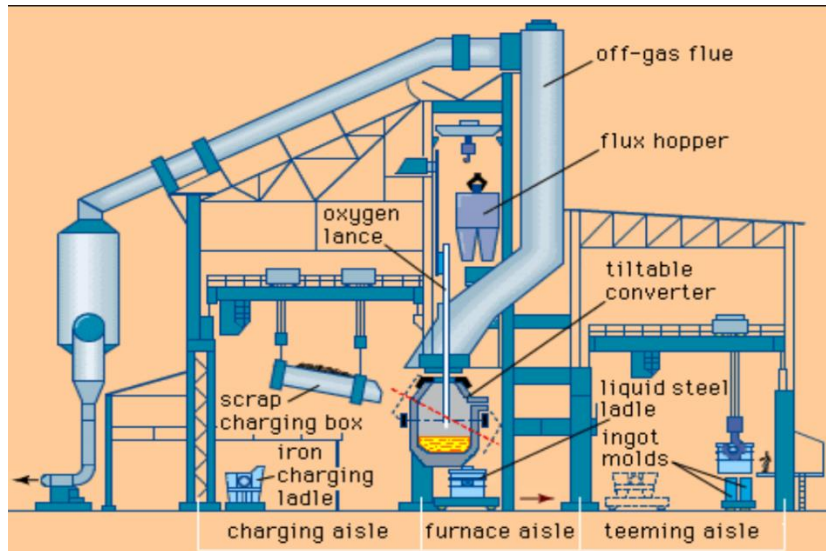


Figure 1.4. Oxygen furnace

(<https://cdn.britannica.com/43/1543-004-45F68D85/oxygen-furnace-shop.jpg>)

1.1.1.5. Electric arc furnace

With the increasing sophistication of the electric power industry toward the end of the 19th century, it became possible to contemplate the use of electricity as an energy source in steelmaking using an electric arc furnace as illustrated in figure 1.5.

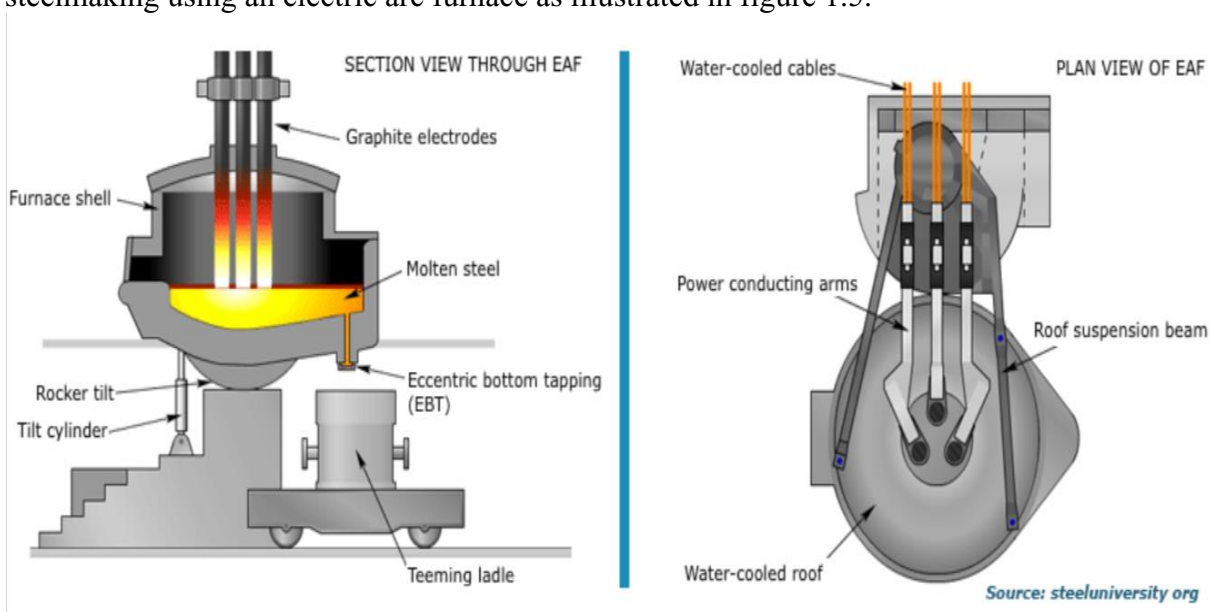


Figure 1.5. Section (a) and plan (b) view of an electric arc furnace

(<http://www.iipinetwork.org/wp-content/letd/content/electric-arc-furnace.html>)

By 1900, small electric-arc furnaces capable of melting about one ton of steel were introduced. These were used primarily to make tool steels, there by replacing crucible steelmaking. By 1920 furnace size had increased to a capacity of 30 tons. The electricity supply was three-phase 7.5 megavolt-amperes, with three graphite electrodes being fed through the

roof and the arcs forming between the electrodes and the charge in the hearth. By 1950 furnace capacity had increased to 50 tons and electric power to 20 megavolt-amperes.

1.1.2. Properties of steel

Steel is an alloy composed mainly of iron, so its density varies around that of iron (7320 to 7860 kg/m³), depending on its chemical composition and thermal treatments. According to EN 1993-1-1 (2005), steels have a modulus of elasticity of 210 000 N/mm², shear modulus of 81 000 N/mm², Poisson's ratio of 0.3 and coefficient of thermal expansion of 12*10⁻⁶ perK, regardless of their composition. The properties of steel which result from its chemical composition and method of manufacture will be discussed as follows.

1.1.2.1. Tensile strength

Tensile strength is the amount of stress that an element can take before becoming structurally deformed. The tensile strength of steel is comparatively high, making it highly resistant to fracture or breakage, which is a key point in its use in infrastructure building

1.1.2.2. Ductility

One of the useful mechanical properties of steel is its ability to change shape on the application of force to it, without resulting in a fracture. This property enables it to be used in the making of different shapes and structures ranging from thin wires or large automotive parts and panels.

1.1.2.3. Durability

Since the 1800s, steel's durability has been recognised as an upgrade to cast iron. The higher the concentration of carbon within the metal, the greater its durability. The hardness of this alloy reflect its ability to resist strain, external wear and tear. The addition of certain elements, makes some types of steel resistant to corrosion. Stainless steel for instance contains nickel, molybdenum and chromium which improve its ability to resist corrosion.

1.1.2.4. Conductivity

Steel, particularly stainless steel, is a good conductor of heat and electricity, making it a good choice for domestic cookware and electrical wiring.

1.1.2.5. Lustre

One of the physical properties of steel is its attractive outer appearance. It is silvery in colour with a shiny, lustrous outer surface.

1.1.2.6. Magnetic

Generally, steel is a magnetic material, but this depends on the type of steel in question. For example, steel cans are made up of ferromagnetic elements like iron and are attracted to magnets. However, austenitic stainless steel does not behave in a magnetic way due to its higher concentration of chromium and nickel.

1.1.3. Type of steel

Different types of steel are produced according to the mechanical and physical properties required for their application. To make different steels, manufacturers vary the type and quantity of alloy metals, the production process, and the manner in which the steels are worked to produce particular products. Based on their chemical compositions, steels can be broadly categorized into four groups which are carbon steels, alloy steels, stainless steels, and tool steels.

1.1.3.1. Carbon steels

Carbon steels are alloys made from a combination of iron and carbon. By varying the percentage of carbon, it is possible to produce steel with a variety of different qualities as shown in table 1.1. In general, the higher the carbon level the stronger and more brittle the steel.

Table 1.1. Steel classification according to their carbon content (Mbessa, 2005)

Hardness	Carbon content (%)
Extra-soft steel	< 0.15
Very soft steel	0.15 – 0.20
Soft steel	0.2 – 0.25
Semi-soft steel	0.30 – 0.35
Semi-hard steel	0.35 – 0.40
Hard steel	0.35 - 0.45
Very hard steel	0.45 – 0.55
Extra-hard steel	> 0.55

Low carbon steel is sometimes called "wrought iron". It is easy to work and may be used for decorative products such as fencing or lamp posts. Medium carbon steel is very strong and is often used for large structures such as bridges. High carbon steel is used mainly for wires. The ultra-high carbon steel also called "cast iron" is used for pots and other items. Cast iron is very hard steel, but it is also quite brittle.

1.1.3.2. Alloy steels

Alloy steels are so named because they are made with a small percentage of one or more metals besides iron. The addition of alloys changes the properties of steels. For example, steel made from iron, chromium, and nickel produces stainless steel. The addition of aluminium can make steel more uniform in appearance. Steel with added manganese becomes exceptionally hard and strong.

1.1.3.3. Stainless steels

Stainless steel is an iron/chromium alloy that contains from 10 to 30% chromium which gives the metal high resistance to corrosion. When steel contains over 11% chromium, it is about 200 times more resistant to corrosion as steels that do not contain chromium. The three groups of stainless steels are austenitic steels, ferritic steels and martensitic steels. Austenitic steels are non-magnetic steels which contains very high amount of chromium, and small amounts of nickel and carbon. These are very commonly used for food processing and piping. Concerning ferritic steels, they contain about 15% chromium but only trace amounts of carbon and metal alloys such as molybdenum, aluminium, or titanium. These steels are magnetic, very hard and strong, and can be strengthened further by cold working. And finally, martensitic steels contain moderate amounts of chromium, nickel, and carbon, They are magnetic, heat-treatable and are often used for cutting tools such as knives and surgical equipment.

1.1.3.4. Tool steels

Tool steel refers to a variety of carbon steel and alloy steel that are particularly well-suited to be made into tools. Their suitability comes from their distinctive hardness, resistance to abrasion and deformation, and their ability to hold a cutting edge at elevated temperatures. They can contain tungsten, molybdenum, cobalt, and vanadium. They are used, not surprisingly, to make tools such as drills. There are a variety of different types of tools steels, containing varying amounts of different alloy metals.

1.1.4. Uses of steel

Steel is used in every aspect of our lives. It is both the most widely used and most recycled metal material on earth. From stainless and high-temperature steels to flat carbon products, steel in its various forms and alloys offer different properties to meet a wide range of applications. For these reasons, as well as the metal's combination of high strength and relatively low production cost, steel is now used in countless product. According to the World Steel Association (2020), steel applications can be divided into seven primary market sectors which are buildings and infrastructure (52%), mechanical equipment (16%), automotive (12%),

metal products (10%), other transport (5%), domestic appliances (2%) and electrical equipment (3%).

1.1.4.1. Buildings and infrastructure

More than half of the steel produced annually is used to construct buildings and infrastructure such as bridges and underground pipes for water or natural gas. According to the WSA, most of the steel used in this sector is found in reinforcing bars (44%); sheet products, including those used in roofs, internal walls, and ceilings (31%); and structural sections (25%). In addition to those structural applications, steel is also used in buildings for HVAC systems and in items such as stairs, rails, and shelving. Besides bridges, applications for steel in transportation-related infrastructure include tunnels, rail track, fuelling stations, train stations, ports, and airports. The WSA says approximately 60% of steel use in this area is as rebar placed inside reinforced concrete.

1.1.4.2. Mechanical equipment

According to WSA, the second-greatest use of steel includes bulldozers, tractors, machinery that makes car parts, cranes, and hand tools such as hammers and shovels. It also includes the rolling mills that are used to shape steel into various shapes and thicknesses.

1.1.4.3. Automotive

On average, almost 900 kilograms of steel is used to make a car, according to the WSA. About a third of that is used in the body structure and exterior, including the doors. Another 23% is in the drive train, and 12% is in the suspension. Advanced high-strength steels, which are made using complex processes and are lighter in weight than traditional steels, account for about 60% of a modern car's body structures.

1.1.4.4. Metal products

This market sector includes various consumer products such as furniture, packaging for food and drinks, and razors.

1.1.4.5. Other transport

Steel is used in ships, trains and parts of planes. Hulls of large ships are almost all made of steel, and steel ships carry 90% of global cargo, the WSA says. Steel is important for sea transportation since almost all of the world's approximately 17 million shipping containers are made of steel. Besides the cars, steel shows up in trains in the wheels, axels, bearings, and motors. In airplanes, steel is crucial for engines and landing gear.

1.1.4.6. Domestic appliances

Clothes washers and dryers, microwave ovens, dishwashers, and refrigerators all contain steel in varying amounts, including the motors, when applicable.

1.1.4.7. Electrical equipment

The last major steel market sector involves applications in the production and distribution of electricity. That means transformers, which have a magnetic steel core; generators; electric motors; pylons; and steel-reinforced cables.

1.1.5. Defects of steel

Metal defects are imperfections in the structure of metals and alloys which affects the properties of such materials like electrical conductivity, magnetic permeability, strength, density, and plasticity. Steel is not spared by defects and it is been observed that it is vulnerable to corrosion (Mbessa, 2005).

Corrosion of steel is an electrochemical process that requires the simultaneous presence of moisture and oxygen. Essentially, the iron in the steel is oxidised to produce rust, which occupies approximately six times the volume of the original material. The rate at which the corrosion process progresses depends on a number of factors, but principally the micro-climate immediately surrounding the structure. Corrosion can have a variety of negative effects on metals and some of its effect include a significant deterioration of important infrastructures as well as increase in the risk of catastrophic equipment failures. It was noted that the degree of corrosion strongly affected the mechanical properties of steel, particularly the ultimate stress and strain.

1.1.6. Prevention of defects

Prevention of corrosion can be done by selecting the right metal type, protective coating, environmental measures, metallic coatings, corrosion inhibitors and design modification.

1.1.6.1. Metal type

Whenever possible, it is advisable to use steel that is not subjected to corrosion. Metals like aluminium and stainless steel could be used as alternative materials. The cost factor and the strength of the material need to consider when these alternatives are selected.

1.1.6.2. Protective coating

The mainly two types of protective coatings that can be used for corrosion prevention are paint and powder coatings. Painting acts as a protective barrier to the steel and it avoids the

steel exposing to the environment. Depending on the nature of the structure and where it is to be constructed, the specification for painting is made. On the other way, powder coating is a membrane created on the steel surface. In order to apply powder coating, the metal surface should be cleaned, a dry powder is applied, then the metal is heated and powder fuses into a smooth continuous film.

1.1.6.3. Environmental measures

Corrosion is caused by a chemical reaction between the metal and gases in the surrounding environment. By taking measures to control the environment, these unwanted reactions can be minimized. This can be as simple as reducing exposure to rain or seawater, or more complex measures, such as controlling the amounts of sulphur, chlorine, or oxygen in the surrounding environment.

1.1.6.4. Metallic coatings

This coating involves coating the metal with an additional metal type that is more likely to oxidize. There two main techniques for achieving this coating are cathodic and anodic protection. The most common example of cathodic protection is the coating iron alloy steel with zinc, a process known as galvanizing. Zinc is a more active metal than steel, and when it starts to corrode it oxides which inhibits the corrosion of the steel. On the other hand, anodic protection involves coating the iron alloy steel with a less active metal, such as tin. Tin will not corrode, so the steel will be protected as long as tin coating is in place.

1.1.6.5. Corrosion inhibitors

Corrosion inhibitors are chemicals that react with the surface of the metal or the surrounding gases to suppress the electrochemical reactions leading to corrosion. They work by being applied to the surface of a metal where they form a protective film. Inhibitors can be applied as a solution or as a protective coating using dispersion techniques. Corrosion inhibitors are commonly applied via a process known as passivation. In passivation, a light coat of a protective material, such as metal oxide, creates a protective layer over the metal which acts as a barrier against corrosion.

1.1.6.6. Design modifications

Design modifications can help reduce corrosion and improve the durability of any existing protective anti-corrosive coatings. Ideally, designs should avoid trapping dust and water, encourage movement of air, and avoid open crevices. Ensuring the metal is accessible for regular maintenance will also increase longevity.

1.2. Steel structures

Steel structures are metal buildings made of structural steels which are alloys of iron, with carefully controlled amounts of carbon and various other metals such as manganese, chromium, aluminium, vanadium, niobium and copper. The carbon content is less than 0.25%, manganese is less than 1.5% and the other elements are in trace amounts (T.J.MacGinley, 1998). The inclusion of copper gives the corrosion resistant steel Cor-ten. The production processes such as cooling rates, quenching and tempering, rolling and forming also have an important effect on the micro structure, giving small grain size which improves steel properties.

1.2.1. Historical background

Although the first metal used by human beings was probably some type of copper alloy such as bronze, the most important metal developments throughout history have occurred in the manufacture and use of iron and its famous alloy called steel (Jack C. McCormac and al., 2012).

One of the first major uses of steel for construction purposes was in train stations but with time it evolved and was used in the construction of steel-framed buildings, skyscrapers and bridges. The 10-storey Home Insurance Building in Chicago was the first skyscraper in the world to be constructed with steel frame and it was completed in 1885. Steel structures became popular in the early 20th century and became widespread around the world, during which most iconic landmarks like the Chrysler Building and the Empire State Building (Figure 1.6), were erected with steel as a main construction element.



Figure 1.6. Empire State Building (<https://urbansplatter.com>)

Nowadays steel is one of the principal modern materials used for constructions all over the world. As steel has higher scale of tensile strength, it allows development of new structural systems such as cantilevers and offers unwavering support to build far-reaching aesthetic possibilities such as gravity-defying skyscrapers. It is a versatile material which has led to its inclusion in nearly every stage of the construction process from framing and floor joists, to

roofing materials. There are many structural steel products used in modern construction such as steel beams, pipes, and cables. This steel is put to use in the construction of buildings, garages, railroad construction across the world, transmission line towers and manufacturing sheds. Figure 1.7 shows the picture of the Seattle Amazon spheres made of steel and glass materials.



Figure 1.7. Amazon spheres (<https://www.aisc.org>)

1.2.2. Steel connecting devices

A steel structure is an assemblage of different members which are joined to one another with the help of connecting devices so that they become a single composite unit. There are two common ways to connect structural steel members – using bolts or welds. Rivets, while still available, are not currently used for new structures and will not be considered here. These two ways of connections can be accompanied by either connecting plates or connecting angles (Tamboli, 2017). Steel connections are classified according to a variety of criteria.

1.2.2.1. Classification based on the connecting medium

Based on the connecting medium there are bolted, welded and bolted-welded connections. Bolted joints have as principal components cap screw (bolt) with completely or partially threaded stem (Figure 1.8), nut usually with hexagonal form, and washer usually with circular form. The two kind of bolts that exist are bearing type bolts (common bolts) and high strength structural bolts. The common bolt can be subjected to forces that are perpendicular (shear) or parallel (tensile) to the longitudinal axis, or by a combination of both. On the other hand, high strength structural bolts are used when the common bolts slip under shear.

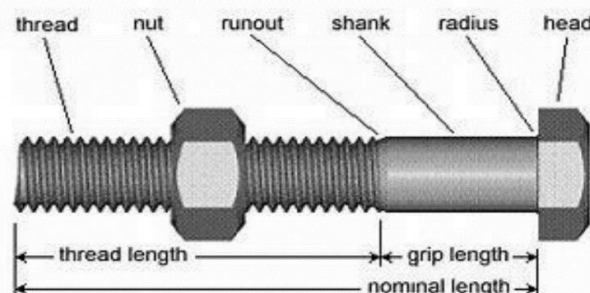


Figure 1.8. Parts of a bolt (<https://www.hbjinyong.com/fastener/hex-bolt-and-nut/>)

When designing bolts for connections, the characteristic value should be adopted from the values of table 1.2 given in EN 1993-1-8, (2005).

Table 1.2. Nominal values of the yield strength and the ultimate tensile strength for bolts

Bolt class	4.6	4.8	5.6	5.8	6.8	8.8	10.9
f_{yb} (N/mm ²)	240	320	300	400	480	640	900
f_{ub} (N/mm ²)	400	400	500	500	600	800	1000

In welded joints the components are connected together by welds. Welding is a process of union of various elements with the aim of obtaining continuity of material through fusion. They have a rigidity that can be advantageous if properly accounted for design even though they are negatively affected by shrinkage. The main types of welds used for steel connections are fillet, butt and plug welds (Tamboli, 2017).

Fillet weld which is the most commonly used weld, has the general shape of an isosceles right angle and its strength is determined by the throat thickness. While, butt welds are used to connect two pieces of material together along a single edge in a single plane as shown in figure 1.9. Plug welds are used to connect steel components together by a series of small circular welds.

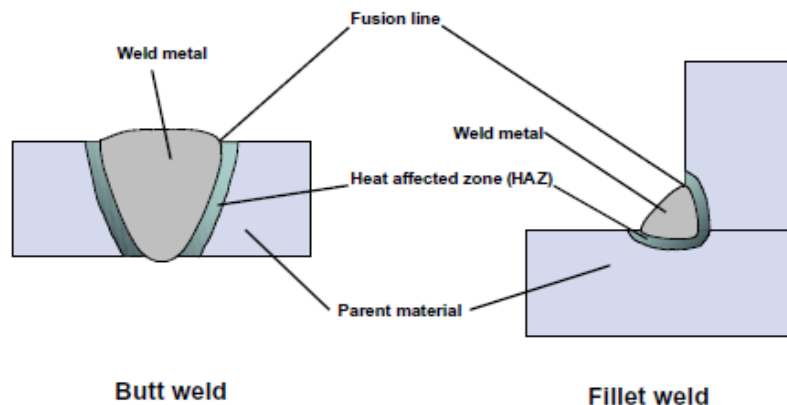


Figure 1.9. Butt and fillet weld (<https://www.steelconstruction.info/Welding>)

Bolted-welded connection is a mixture of bolts and welds which give access to the strength of a connection made with welds and mechanical fasteners. Due to the difference in rigidity and ductility of its various components, its design should be done with extreme care and attention.

1.2.2.2. Classification based on the type of internal force

There are three basic forces to which connections are subjected. These are axial force, shear force, and moment. Many connections are subject to two or more of these simultaneously.

Connections are usually classified according to the major load type to be carried, such as shear connections, which carry primarily shear; moment connections, which carry primarily moment; and axial force connections, which carry primarily axial force (Tamboli, 2017).

Shear connections (Figure 1.10) are the most common type of steel connections, and are referred to as “simple” or “semi-rigid” connections because no bending moment is considered. Common shear connections include plates, web angles and seat angles.



Figure 1.10. Shear connection

(<https://skyciv.com/technical/types-of-steel-connections-and-their-classification>)

Moment connections (Figure 1.11) primarily carry moment loading, however are usually designed to resist shear and axial loading as well. For this reason, they are referred to as “rigid” or “fully restrained” connections and are used to create a frame. Common moment connections include directly welded members, flange plates, and end plate connections.



Figure 1.11. Moment connection

(<https://skyciv.com/technical/types-of-steel-connections-and-their-classification>)

Axial connections (Figure 1.12) primarily carry axial loads and include splices, bracing, truss connections, and hangers. They are typically used to connect columns to columns, or beams to beams sometimes with different section sizes.



Figure 1.12. Axial connection

(<https://skyciv.com/technical/types-of-steel-connections-and-their-classification>)

1.2.2.3. Classification based on the type of members joining

When undertaking steel connection design, one of the primary considerations are the type of members that the steel connection is to join. The common configurations include beam to beam, column to column, beam to column and column base plate connections.

Concerning beam to beam connections, there are generally two types, depending on the beam geometry. The first type is a primary beam connected to an adjacent secondary beam and the other type is through the use of a beam splice for linearly aligned members.

Column to column connections are usually done with the use of a column splice which is capable of connecting columns of different cross-sectional area. These splices are designed for both moment and shear resistances unless intended to be used as internal hinges.

Beam to column connections are the most common type of member configuration, with the column acting as the supporting member and the beam acting as the supported member in an adjacent orientation. They can be connected using end plates, web or flange cleats and haunched connections.

Column base plate connection consider the connection made between a column and a concrete pedestal as represented in figure 1.13. Steel plates are placed at the bottom of columns and above the concrete base. Anchor bolts are usually installed into the concrete pedestal, connecting the base plate so that uplift can be resisted during construction.



Figure 1.13. Column base plate connection

(<https://civil-engg-world.blogspot.com/2011/05/base-plate-for-steel-column.html?m=1>)

1.2.3. Type of steel structures

Structural steel frame is a key option when it comes to construct a variety of building projects. There exist a wide range of steel structures types in buildings, each with its own specific purpose and level of complexity.

1.2.3.1. Single storey buildings

These buildings are typically used for workshops, factories, industrial and distribution warehouses, retail and leisure. Referred colloquially as ‘sheds’, sizes vary from small workshops of just a few hundred square metres up to massive distribution warehouses covering over one hundred thousand square metres. These buildings are usually required to provide large open floor areas, with few internal structural columns, thus offering freedom for activities that involve moving plant and equipment inside the building. The essentially three layers of a single storey building are the primary steel frame, consisting of columns, rafters and bracing; the secondary steelwork, consisting of side rails and purlins for the walls and roof; and cladding for the roof and the walls. The schematic arrangement of a typical single storey building showing both the structural frame and the building is shown in figure 1.14.

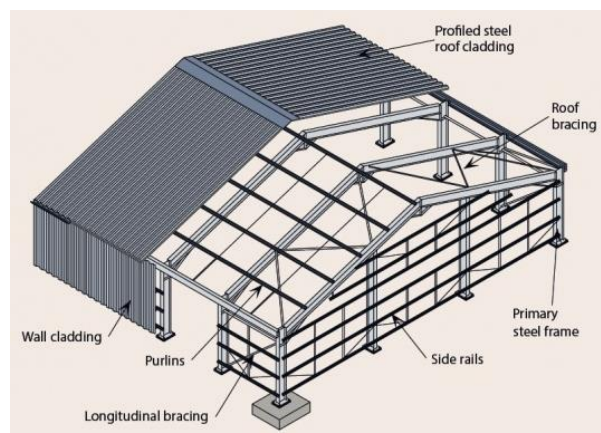


Figure 1.14. Single-storey building

(https://www.steelconstruction.info/Single_storey_industrial_buildings)

The two main framing options for single-storey industrial buildings are portal frames and lattice trusses. Portal frames are statically indeterminate structure, comprising columns and horizontal or pitched rafters, connected by moment-resisting connections as shown in figure 1.15. Portal frames come in a variety of different shapes and sizes, with flat and pitched roofs.

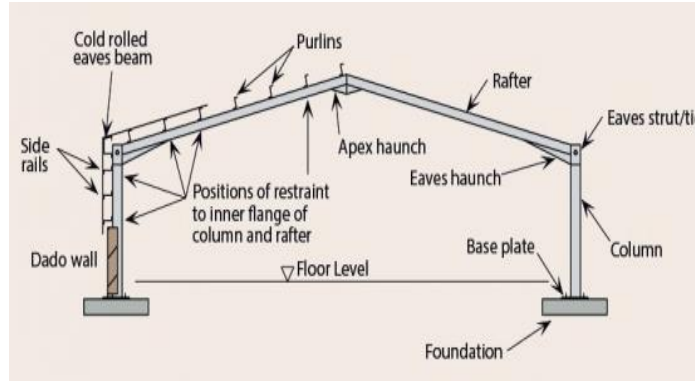


Figure 1.15. Single span symmetric portal frame (https://www.steelconstruction.info/Portal_frame)

On the other hand, lattice trusses are frames with trussed roof which are used for very large spans (greater than 50 m), for production facilities needing heavy plant suspended from the roof area or where deflection criteria are particularly critical. Trusses are triangulated assembly of members usually either rolled or structural hollow sections as shown in figure 1.16.



Figure 1.16. Lattice truss structure (<https://www.steelconstruction.info>).

1.2.3.2. Multi-storey buildings

These buildings are used in the construction of commercial buildings such as offices, shops and mixed residential-commercial buildings. The flooring systems are commonly made of either composite slabs or precast concrete slabs. The higher the building, the lower its resistance to horizontal actions and the greater the need to use stabilising systems on the building. The negative effects of horizontal forces like wind actions and, in some regions, seismic actions can be counteracted by using stabilising systems as bracing systems or concrete core systems as shown in figure 1.17. Bracing may be in various generic forms, such as X, V and K forms.

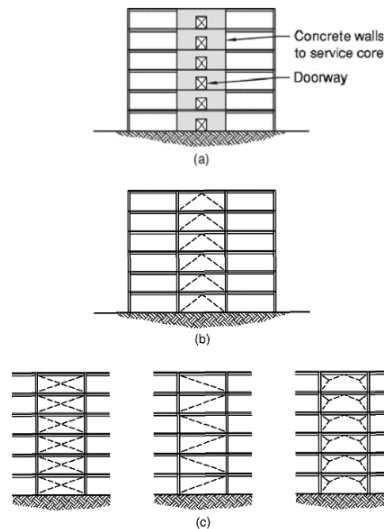


Figure 1.17. Types of braced frame: (a) Concrete core, (b) inverted V bracing, (c) alternative types of triangulated bracing (Davison et al., 2012).

Concrete cores are normally placed in the centre of tall buildings as shown in figure 1.17 and are constructed in advance of the installation of the surrounding steelwork. The core area typically represents about 5-7% of the plan area for medium rise buildings and can increase to 12-20% for high rise buildings (Davison et al., 2012).

1.2.3.3. Special steelwork

These structures are not the baseline ‘beam and stick’ or common portal frame structures which form much of the volume of structures industries are constructed with. They are generally those with complex 3D load paths or non-regular geometry, or those that are required to have a longer than normal span or have a lower than normal self-weight (Davison et al., 2012). Typical modern special structures include 3-dimensional grids based on regular solids (space frames), curved forms such as domes and vaults, and surface-stressed tension structures and cable nets. A typical example of special steel structure is a stadium (Figure 1.18).



Figure 1.18. Japoma stadium

1.2.4. Advantages and disadvantages of steel structures

From skyscrapers and bridges to beautiful contemporary houses and industrial structures, steel is used in almost every type of structure. Due to its high popularity, it is important to know its advantages and disadvantages while using it.

1.2.4.1. Advantages of steel structures

Steel construction combines a number of unique features that make it a good solution for many applications in the construction industry.

One of the most evident advantage of using steel in construction is its ability to span long distances without the need of supporting interior columns. A clear span interior space provides more floor-plan flexibility and it also allows greater freedom for later renovations and changes.

Structural steel components are stronger and lighter than the components made of weight-bearing concrete. This makes steel structures to be stronger and more durable since they can withstand extreme forces or harsh weather conditions, such as earthquakes, strong winds, hurricanes and heavy snow to a great extent.

Steel is incredibly versatile as it can be moulded into almost any shape and sizes. It is also a very ductile material which permits steel buildings to deform without failure under high tensile stresses, thus giving warning to inhabitants to evacuate before collapse (Jack et al., 2012).

Furthermore, steel structures are easily installed and are constructed rapidly due to the fact that steel parts are pre-manufactured to a specific design inside the manufacturing plant and are shipped out in ready-to-be erected conditions.

Moreover, structural steel components are termite proof, environmentally friendly and cost-effective due to the fact that they are easier to transport and there is no waste of waste of material on the site. Steel is environmentally friendly because it is made from recycled materials and can be recycled at the end of its lifespan.

1.2 .4.2. Disadvantages of steel structures

Every material has some benefits as well as flaws and steel structures are not spared. They are susceptible to different environmental conditions.

When steel structures are exposed to severe or aggressive weather conditions, it may get corroded due to the action of steel with atmospheric oxygen or aggressive environment. For

preventing such problems, expensive applications of paints are required making the maintenance cost of steel to be very high.

Due to high strength/weight ratio, steel products are in general slenderer and consequently more susceptible to buckling than reinforced concrete members. They are also quite susceptible to fatigue and are responsive to brittle fracture when they loss their ductility.

Although steel elements are incombustible up to a temperature, the strength of steel gets highly compromised at the exposure of high temperatures due to fire or when other materials within a building burn, making them susceptible to buckling.

1.3. Fire effect on steel structures

Fire was the first important source of power in the development process of the human civilization. However, thousands of years of human history indicate that fire has also brought massive disasters. Until now, fire is still the most common cause of severe disasters (Wang et al., 2019). It has caused the death of thousands of people, massive building damage, and billions of economic losses. Consequently, fire safety is still one of the most important issues for the security of people. Modern building structures are mainly constructed with steel, and it is well known that fire greatly affects this material. Steel loses most of its strength and stiffness when it is exposed to fire reaching a temperature greater than 600 °C. At 600 °C the yielding strength of structural steel represents only 40% of its initial value, while the young's modulus falls down to 30% (Georgeta et al., 2017). Consequently, owing to the degradation of the material mechanical performance, a structure constructed with steel materials easily fails and collapses under the fire condition.

1.3.1. Overview of structural damaged events due to fire

Damage and collapse of steel structures due to fire is been observed all around the world and even our country suffers from these disasters. Some cases of steel buildings that have been subjected to fire are mentioned in this section.

1.3.1.1. Damaged structures due to fire in the world

An example of one of the structures that have been damaged by fire is the McCormick Center. The McCormick Place was an exhibition centre on Chicago's Lake Shore Drive that opened in November 1960. The centre included a theatre, several restaurants and banquet rooms, and over 46 000 m² of exhibition space. In January 1967, it hosted the National Housewares Manufacturers Association Show but on Monday, 16 January, 1976 at around 02:00 a.m., the janitors noticed smoke rising from a small fire at the back of an exhibition booth which

ended into a huge fire that was out of control which killed a person. The fire fighters arrived by 02:30 a.m. and extinguished the fire by 10:00 a.m. but the centre was essentially destroyed as the shown in figure 1.19.



Figure 1.19. Destroyed McCormick Center (<https://guides.library.illinois.edu/>)

Another structure was the AMA industry. On Tuesday, 11 December, 2018, a black cloud and a pungent smell quickly spread over Rome, due to the fire that broke out in a 2000 m² shed belonging to AMA (Figure 1.20), the municipal waste management company of the Italian capital. The fire broke out at around 05:00 a.m. and about 40 firefighters were mobilised to extinguish it. It caused great material damage to the company.



Figure 1.20. AMA industry in fire (<https://www.francetvinfo.fr>)

1.3.1.2. Damaged structures due to fire in Africa

Early on Monday, 11 May 2020, morning, in the Yopougon industrial zone in Ivory Coast, a huge fire broke out in the chemical company Industrap/Carocol (Figure 1.21). This fire, which was followed by strong explosions, broke out at around 05:58 a.m. The six-fire service equipment deployed at the scene were successful after several difficulties in containing the flames at approximately 10:50 a.m. Unfortunately, one of the workers lost his life and the property damage was very significant.



Figure 1.21. Yopougon industrial zone in fire (<https://www.koaci.com>)

Another case of fire disaster that happened in Africa was in Morocco precisely in Casablanca. A huge fire broke out at 04:30 a.m. on Tuesday, 22 September, 2020, in the industrial area of Sidi Bernoussi as shown in figure 1.22, causing panic among residents of nearby neighbourhoods. The depot, which is owned by an international logistics company, was used by companies marketing paint products, communications equipment, clothing and diapers, among others. No human loss happened due to the disaster but extensive property damage was observed.



Figure 1.22. Industrial area of Sidi Bernoussi (<https://www.challenge.ma>)

1.3.1.3. Damaged structures due to fire in Cameroon

In French-speaking Africa, Cameroon situated on the Gulf of Guinea has a great amount of companies that shine in the national triangle producing various products that are useful to the population. However, for some time now, events have been taking place which are likely to weaken the economic fabric of Cameroon. After the fires in markets and houses, today it is some huge Cameroonian industries that are suffering the damage of flames.

In 2019, a massive explosion rocked one of the giant storage tanks at the National Refining Company (SONARA) in Limbola, Limbe, Southwest region of Cameroon, on Friday 31 May, 2019, at 11:30 p.m. (Figure 1.23). “Flames consumed four of the 13 production units and partially blew up three others, stopping all the SONARA refining process” the Minister of Water Resources and Energy, Gaston Eloundou Essomba said (Cameroon Tribune, 2019). Few

days later on the 3rd of June 2019, one of the tanks of the refinery, which is used to store crude oil, was licked by fire. This company, which is almost entirely state owned apart from a 4% stake held by Total, has a capacity of 2.1 million tonnes of crude a year. It serves the whole country, so the delayed caused by the fire caused important damages to the country. It had a significant impact on the revenue collected by the General Tax Directorate (DGI) of the Ministry of Finance. According to the state's 2019 budget execution report, the fire, which affected SONARA, cost the public treasury billions of FCFA in tax collection losses. The rehabilitation work was estimated at 250 billion FCFA (Sylvain, 2020).



Figure 1.23. Damaged SONARA structure
(<https://thesuncameroon.cm/huge-explosion-fire-ravage-sonara>)

On the 1st of January 2018, a huge fire broke out at the Cameroonian Fermentation company (FERMENCAM), leader of Cameroon's sachet whiskey market, burning its main warehouses located in the quarter named Bonaberi of the city of Douala which is the economic capital of Cameroon. The numerous flammable products in the warehouses of this firm have caused the spread of the fire to eight neighbouring houses and a school. The disaster having occurred on the new-year's day in the absence of employees which were at home, only important property damages were sustained as shown in figure 1.24.



Figure 1.24. Damaged structure of FERMENCAM warehouses
(<https://www.cameroun24.net/blog/?pg=actu&ppg=1&pp=&id=4359>)

On Thursday, 3rd of November 2018, a fire broke out around 11:40 p.m., in the premises of Annex 2 of the cosmetics company Biopharma in Douala the economical capital of Cameroon (Cameroon Tribune, 2018). The employees who were on duty at that time immediately alerted the neighbouring companies to try to fight the flames. As the flames became increasingly violent, the elements of the Ter brigade from Logbaba were the first to arrive at the site with their riot control trucks to rescue the company. The elements of the city's fire fighters also arrived at the site and literally put themselves in the thick of the action. For several hours, the battle against the flames was fierce until the early hours of the morning and it was at 7:00 a.m. that the fire was completely brought under control. This caused serious damaged to the structure of the building (Figure 1.25).



Figure 1.25. Damaged structure of Biopharma's warehouse
(<https://www.cameroon-tribune.cm/article.html/21978/fr.html/incendie-biopharma>)

1.3.2. Experimental research on the fire performance of structures

Over the years many isolated member tests and full-scale tests under fire have been carried out in several institutions (Wald et al., 2006). The current review is interested in modern era large-scale, structural fire resistance testing, with a particular emphasis on experiments aimed at better understanding the full-structure response of real buildings in real fires.

1.3.2.1. AISI and NBS test

The renaissance of large-scale structural fire testing started with tests performed by the American Iron and Steel Institute (AISI) and the National Building Standards (NBS) in the early 1980s with the objective of assessing the global behaviour of steel-concrete composite frame structures and validating a computer model, FASBUS II, for structural response to fire (Bisby et al., 2013). A large scale non-standard structural fire test was executed in 1982, on a two storey, four bay (4.9 m × 6.1 m each in plan), composite steel-framed building. The test structure was meant to represent a corner section of a typical mid-rise office building. According to Gales et al. (2012), a fire compartment was built into the corner bay of the structure. A fire load was supplied by propane burners which 'reproduced' 100 minutes of the

ASTM E119 (ASTM, 1980) standard time temperature curve. Water tanks were used to simulate the design live loads. This test highlighted a number of differences in response between the performance of a real structure and the performance of an isolated structural element, albeit in both cases under a standard fire heating scenario. Most importantly, secondary load paths, structural interactions, membrane actions, and discrete cracking in the concrete slabs, were all identified as playing roles in the structure's response (Bisby et al., 2013).

1.3.2.2. BHP William Street fire test

In the early 1990s a series of four fire tests was performed by steel company BHP (Broken Hill Proprietary) to investigate the structural fire performance of a specific steel-framed office building in Melbourne, Australia. The existing 41 storey building (140 William Street) was undergoing renovation and refurbishment after an extensive asbestos removal program. The test was intended to show that with the installation of a light hazard sprinkler system and a non-fire rated suspended ceiling, the passive fire protection could be removed from the structural steelwork of the beams and the underside of the steel deck floors (British Steel, 1999; Thomas et al., 1992). A test building was constructed to simulate a typical single storey corner bay of the William Street building, that is an isolated 12 m × 12 m bay. The fuel load consisted of typical office furnishings amounting to a fuel load of about 53.5 kg/m². Gravity loads were applied using water tanks (Bisby et al., 2013).

The first two tests were concerned primarily with the effectiveness of the proposed sprinkler system, and as such the fires were not significant for the structure. The third test examined the structural and thermal performance of the composite slab. In this test the beams had 'partial fire protection' and the entire floor assembly was protected (to unknown extent) by a suspended ceiling system which 'remained largely in place' during the fire exposure. Peak gas phase temperatures were about 1254 °C, but the composite slab supported the imposed service load. The fourth test used unprotected steel beams and composite slab, although still with a suspended ceiling, and had a peak gas phase temperature of 1228 °C. The maximum beam temperatures in this test were 632 °C, and the maximum beam deflection was 120 mm (with no 'obvious signs' of impending collapse). Most of the beam deflection was recovered on cooling.

1.3.2.3. Cardington fire test

Between 1995 and 1996, British Steel (now Corus) and Building Research Establishment (BRE) conducted six fire tests on an eight story steel building with composite floor system (Agarwal et al., 2014). Few years later the Czech Technical University (CVUT)

performed a subsequent Cardington test in 2003 (Wald et al., 2006). The building was 21 m × 45 m and had a total height of 33 m. All beams were designed as simply supported acting compositely with a 130 mm thick concrete slab on steel decking. Beam-to-beam connections were made using fin-plate connections and beam-to-column connections using flexible end plates. Sandbags were used to simulate gravity loads for a typical office occupancy (Bisby et al., 2013). A plan view of the test structure is given in figure 1.26 which shows the approximate locations and compartment sizes for the various fire tests performed.

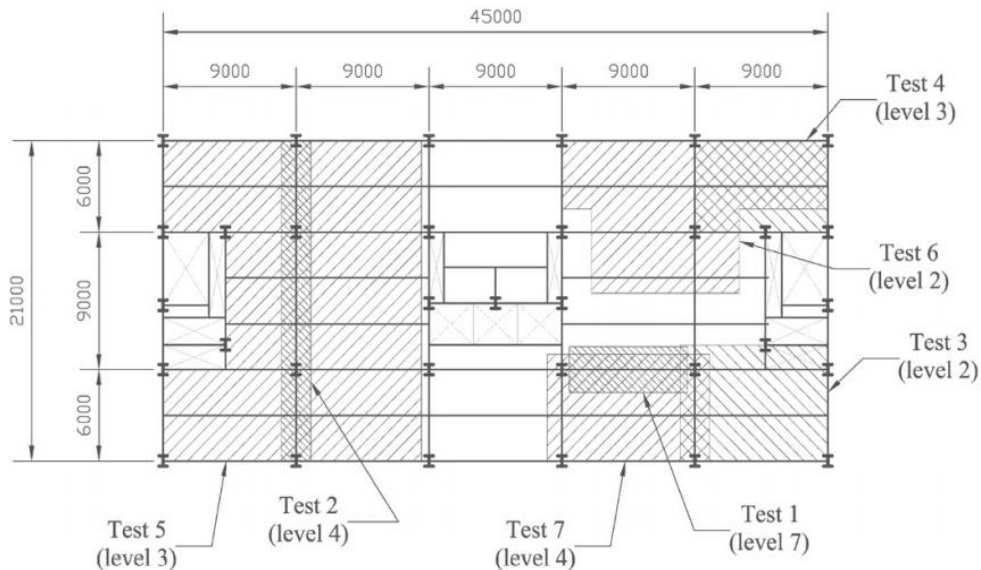


Figure 1.26. The Cardington fire tests (Bisby et al., 2013)

According to British Steel (1999), the first test performed in Cardington was a restrained beam test involving a single 305 x 165 x 40UB composite beam section supporting the seventh floor of the building. A gas-fired furnace was used to heat the beam to approximately 900 °C. Maximum sagging of 232 mm was reported in the beam. Yielding and local buckling at the ends of the heated portion of the beam were observed. Restraining forces against thermal expansion and the rotational demands for accommodating thermal gradient through the depth of the beam had caused buckling of the web and lower flange at the beam ends.

The second test, a plane frame test involved heating a series of beams and columns across the full width of the building. Again, a gas-fired furnace was used to heat the steelwork to approximately 800 °C. Maximum air temperature of approximately 750 °C was achieved. The unprotected portions of the columns squashed at steel temperature of about 670 °C. In shear connections, top bolts or shear plates were observed to have failed.

The third test, the British Steel corner compartment test was the first natural fire carried out in the Cardington Laboratory, representing a typical office fire (timber cribs were used to

provide a fire load of 45 kg/m²). In this test, both the perimeter beams and the columns were fire protected with the internal beam unprotected. Load bearing concrete blocks were used for the compartment walls. Large sagging and retraction of the secondary beam inside the compartment were reported in the heating and cooling phases, respectively. Buckling of the bottom flanges and webs near the ends were also reported.

The fourth test, the BRE corner compartment test also used timber cribs to provide a fire load of 40 kg/m². The compartment walls were constructed using fire-resistant board and the northern boundary was formed by constructing double-glazed aluminium screens. All columns were protected up to and including the connections. Maximum steel temperature was recorded to be about 903 °C. During the fire event, maximum vertical deflection at the centre of the compartment was about 270 mm. About 40% of this deflection was recovered during cooling. Local buckling in the bottom flanges of the beams was reported.

The fifth test was the largest compartment test in the world. The compartment was designed to represent a modern open-plan office (18 m x 21 m). The compartment was bounded by fire resistant walls. The main aim of this test was to investigate the ability of a large area of composite slab to support the applied load once the main beams had failed. Consequently, all the beams had no fire protection and all columns were fire protected. Again, the ventilation conditions governed the fire severity. Owing to the longer spans, the maximum deflection was about 557 mm, which recovered to 480 mm after cooling. Many of the connections were found fractured or sheared after cooling. Almost all the beams underwent local buckling and distortion at the ends.

In the demonstration test (sixth test), unlike in the previous tests, real furniture (desks, chairs, filing cabinets, computer terminals, etc.) were used to provide the fire load. The ventilation was provided by windows and blank openings. The beams were unprotected while the columns were protected. This test was characterized by a rapid rise in temperature representing a severe fire scenario. The unprotected beams were reported to have reached temperature of 1150 °C and maximum deflections of 640 mm. Like all the previous tests, the bottom flanges and the webs of the beams buckled at both ends, and there were signs of tension yielding in the top flange.

Test seven is reported in detail by Wald et al. (2006) which studied the global behaviour of the structure in an 11 m × 7 m, side-compartment of the building. This test was concerned primarily with issues around tensile membrane action and the robustness of steel connections

during fire. Two primary beams (unprotected), two columns (protected), and three secondary beams (unprotected) were exposed to fire with a fire load consisting of 40 kg/m² of wood cribs. The maximum recorded gas phase temperature was 1108 °C, with a maximum steel temperature of 1088 °C. No collapse was observed despite maximum deflections up to 1200 mm which recovered by about 925 mm on cooling, buckling of the beams occurred adjacent to the joints during the heating phase resulting from restraint to thermal expansion provided by the surrounding structure and as in test six, cracking of the concrete slab occurred at the column heads due to non-lapped steel mesh in the concrete slab (Bisby et al., 2013).

Taken together, these seven tests demonstrated many important aspects of the full-structure response of composite steel-framed buildings during fire. The principal results of these tests are summarised in table 1.3.

Table 1.3. Summary of results of the Cardington fire tests (Wald et al., 2006)

Test	Sponsor	Description	Floor area (m ²)	Location	Time (min) to maximum atmosphere temp.	Maximum temperature (°C)		Measured deformations (mm)	
						Gas	Steel	Maximal	Residual
1	BS	Restrained beam	8 x 3	Level 7	170	913	875	232	113
2	BS	Plane frame	21 x 2.5	Level 4	125	820	800	445	265
3	BS	1st Corner	9 x 6	Level 2	114	1000	903	269	160
4	BRE	2nd Corner	10 x 7	Level 3	75	1020	950	325	425
5	BRE	Large compartment	21 x 18	Level 3	70	-	691	557	481
6	BS	Large compartment (office)	18 x 9	Level 2	40	1150	1060	610	-
7	CVUT	Structural integrity	11 x 7	Level 4	55	1108	1088	>1000	925

1.3.3. Numerical research on the Cardington test (PiT Project)

In 1995, the Edinburgh University in collaboration with Corus and Imperial College proposed a project to model the four British Steel fire tests on the Cardington frame. It was funded by the UK DETR PiT (Partners in Technology) scheme. The title of the project was “The behaviour of steel framed structures under fire conditions” and the main objective was to understand and exploit the results of the large scale fire tests at Cardington so that rational design can be developed for composite steel frameworks at the fire limit state (PiT Project, 2000). The PiT project started in March 1996 running for four years ending in March 2000. Although the main research team consisted of the Edinburgh University, Corus and Imperial College, the BRE and Steel Construction Institute (SCI) also provided valuable input.

The methodology proposed to achieve the stated objective was to develop rigorous models of the British Steel fire tests using a finite element software. The numerical models of the tests ranged in complexity from very simple grillage models to detailed shell representations of the beams and slab. The University of Edinburgh and Corus used the commercial code ABAQUS whilst Imperial College made use of their in-house finite element code ADAPTIC.

The basic finite elements used in for modelling the Cardington structures were the shell elements for the composite slab; the beam elements for the columns and beams; and the spring elements for the joints because they represent the strength and stiffness between two points which are assumed to be nearly coincident.

Concerning material modelling, steel is modelled using an elasto-plastic model. Full degradation of the stress-strain curves with temperature is allowed. The steel material properties were taken directly from the material definition in EN 1993-1-2 (2005) and include the enhanced strain hardening effect above 400 °C. On the other hand, concrete modelling poses considerable numerical challenges. This is primarily due to the nature of concrete's low tensile (cracking) strength and brittle behaviour. Full degradation of concrete material properties with temperature was included. Reinforced concrete properties are included by modelling the rebars with a steel material model. This allows for the specification of layers or individual rebars of reinforcing steel to be included within concrete elements. The reinforcement layers are assumed to be one-dimensional, acting purely in tension or compression. Some approximations to the transfer of load from cracking concrete to reinforcement is allowed within the concrete cracking model itself. The concrete material properties were taken directly from the material definition in EN 1992-1-1 (2004).

As the predominant response of the structure is restraint to thermal expansion, it is important that close attention is paid to applying the correct boundary conditions to the model. The bases of the columns in the floor structure are fully restrained in all directions and the tops of the columns are translationally restrained in the horizontal directions.

Concerning the loading of the structure, there were two types of load that needed to be applied to heated structures. The first type was gravity loading, which is normally straightforward to apply. The second type consisted of the temperatures of the main structural elements. And for the analysis procedure, the only technique the analysis package had available is the standard Newton-Raphson solution method. Using this technique, it is necessary to reduce the solution increment size when instabilities occur, leading to quite lengthy solution times. The most important part of the analytical technique for heated structures is accounting for geometric nonlinearity. High axial forces due to restraint to thermal expansion, coupled with large deflections due to thermal strains, mean that geometric nonlinearity is extremely important.

The output from all the models were comparable and agreed with the measured test data. It was concluded that, the Cardington composite steel framed building exhibited very stable

behaviour under the various fire scenarios tested because of the nature of its highly redundant structural form and that the thermo-mechanical phenomena observed (a combination of restrained thermal expansion and thermal bowing) defines the structural behaviour and depends upon the frame layout and the thermal regime of the fire compartment (PiT Project, 2000).

1.4. Structural fire analysis

The design of steel member nowadays involves much more than a calculation of the properties required to support loads and the selection of the lightest section providing these properties. The fire resistance aspect should also be taken into account. Steel is, indeed, less flammable than other construction materials like wood, and more flammable than concrete if exposed to fire for long but its strength and endurance can be reduced if exposed to high temperature due to fire. The strength and stiffness of typical steel structures degrade rapidly under elevated temperatures (Shi et al., 2020). Steel doesn't need to melt for the building to collapse, it simply has to be heated to temperatures where the section of the building on fire can no longer support its load.

1.4.1. Thermal analysis

The first stage in a structural fire engineering design is to define the appropriate fire design scenario. The choice of the design fire scenario will dictate the choice of design fire to be used. From these parameters, it is possible to calculate the atmosphere temperatures and the evolution of temperature in the members of the structure.

1.4.1.1. Atmosphere temperatures

A determination of the thermal actions to be used in subsequent structural analysis can be achieved either through a prescriptive approach, which relies on data from standard test methods, or from performance-based approach which is a consideration of the physical parameters specific to a particular building (Lennon et al., 2007).

a. Nominal temperature-time curves

Temperature-time curves are analytical functions of time that give a temperature. They have to be considered as conventional, or arbitrary, functions. Their temperatures is of the same order of magnitude as temperatures observed in fires. Because they are conventional, such relationships are thus to be used in a prescriptive regulatory environment. EN 1991-1-2 (2002) proposes three different nominal temperature-time curves which are standard temperature-time curve, external fire curve and hydrocarbon curve.

The standard temperature-time curve is the one that has been historically used, and it is still used today, in standard fire tests to rate structural elements. It is used to represent a fully developed fire in a compartment. It is often referred to as the ISO curve because the expression was taken from the ISO 834 standard. This standard curve is given by equation (1.1).

$$\theta_g(t) = 20 + 345 * \log_{10} (8t + 1) \quad (1.1)$$

Where :

θ_g is the gas temperature [°C]; and

t is the time [min].

The external time-temperature curve is used for the outside surface of separating external walls of a building which are exposed to a fire that develops outside the building or to the flames coming through the windows of a compartment situated below or adjacent to the external wall. The external curve is given by equation (1.2).

$$\theta_g(t) = 20 + 660 * (1 - 0.687e^{-0.32t} - 0.313e^{-3.8t}) \quad (1.2)$$

The hydrocarbon time-temperature curve is used for representing the effects of a hydrocarbon type fire. In situations where petrochemicals or plastics form a significant part of the overall fire load, the temperature rise is very rapid due to the much higher calorific values of these materials. Therefore, for such situations, an alternative temperature-time curve has been developed of the form of equation (1.3).

$$\theta_g(t) = 20 + 1080 * (1 - 0.325e^{-0.167t} - 0.675e^{-2.5t}) \quad (1.3)$$

b. Equivalent time of fire exposure

EN 1991-1-2 (2002) includes a method for determining the appropriate fire resistance period for design based on a consideration of the physical characteristics of the fire compartment. The formulation of this method is shown in equation (1.4).

$$t_{e,d} = (q_{f,d} * k_b * w_f) * k_c \quad (1.4)$$

Where :

$t_{e,d}$ is the equivalent time of fire exposure for design [min];

$q_{f,d}$ is the design fire load density [MJ/m²];

k_b is a conversion factor that dependent on thermal properties of linings;

w_f is the ventilation factor; and

k_c is a correction factor dependent on material.

It is noted that for protected steel and reinforced concrete, k_c equals to 1.0 and where no detailed assessment of the thermal properties is made the factor k_b equals to 0.09.

In the absence of horizontal openings in the compartment, the ventilation factor is represented as in equation (1.5).

$$w_f^{1/4} = (6/H)^{0.3} * [0.62 + 90 * (0.4 - \alpha_v)^4] \quad (1.5)$$

Where :

H is the height of the fire compartment [m]; and

$\alpha_v = A_v/A_f$ where A_v and A_f are the ventilation and floor area respectively [m²].

The verification is that the fire resistance of the member should be greater than the time equivalent value.

c. Parametric temperature-time curves

Along with the time equivalent approach, parametric fires are an example of the simple calculation methods for determining the compartment internal atmosphere time– temperature relationship. According to EN 1991-1-2 (2002), parametric temperature-time curves are valid for fire compartments up to 500 m² of floor area, without openings in the roof and for a maximum compartment height of 4 meters. It applies only to the post-flashover phase, which is of primary concern when considering structural issues and assumes a uniform temperature within the compartment. The basic formulation in annex A of EN 1991-1-1 (2002) is as represented in equation (1.6).

$$\theta_g(t) = 20 + 1325 * (1 - 0.324e^{-0.2t^*} - 0.204e^{-1.7t^*} - 0.472e^{-19t^*}) \quad (1.6)$$

Where :

θ_g is the temperature in the fire compartment [°C];

$t^* = t\Gamma$ [h];

t is time [h];

$\Gamma = [O/b]^2 / (0,04/1160)^2$;

$$b = \sqrt{(\rho c \lambda)} \text{ [J/m}^2 \text{ s}^{1/2} \text{ K]};$$

O is the opening factor ($A_v \sqrt{h} / A_t$) [$\text{m}^{1/2}$];

A_v is the area of vertical openings [m^2];

h is the height of vertical openings [m];

A_t is the total area of enclosure [m^2];

ρ is the density of boundary enclosure [kg/m^3];

c is the specific heat of boundary of enclosure [J/kgK]; and

λ is the thermal conductivity of boundary [W/mK].

The values 0.04 and 1160 refer to the opening factor and thermal properties of the compartment used in the development of the approach.

In order to estimate the duration of fire, the relationship between the fire load and the opening must be considered. The maximum temperature in the heating phase occurs at a time t_{max} given by equation (1.7).

$$t_{max} = \max[0.2 * 10^{-3} * q_{t,d} / O; t_{lim}] \quad (1.7)$$

Where :

$q_{t,d}$ is the design value of the fire load density related to the total surface area of the enclosure (values of $q_{t,d}$ should be in the range 50 –1000 MJ/m²);

t_{lim} is a minimum value for the duration of the fire based on slow, medium or fast fire growth rates.

For office accommodation a medium fire growth rate should be assumed corresponding to a value of t_{lim} equal to 20 min. The temperature–time curves for the cooling phase are then given by equation (1.8), (1.9) and (1.10).

$$\theta_g(t) = \theta_{max} - 625(t^* - t_{max}^*) \quad \text{for } t_{max}^* \leq 0.5 \quad (1.8)$$

$$\theta_g(t) = \theta_{max} - 250(t^* - t_{max}^*) (t^* - t_{max}^*) \quad \text{for } t_{max}^* < 2 \quad (1.9)$$

$$\theta_g(t) = \theta_{max} - 250(t^* - t_{max}^*) \quad \text{for } t_{max}^* \geq 2 \quad (1.10)$$

d. Thermal actions for external members

External structural members may be exposed to fire by flames and radiated heat emanating from openings in the building. Annex B of EN 1991-1-2 provides a calculation approach for determining thermal actions for external members. This method considers steady-state conditions for the various parameters and it is valid only for fire loads $q_{f,d}$ higher than 200 MJ/m².

e. Advanced fire models

In certain circumstances it may be necessary to go beyond a reliance on nominal fire exposures or simple calculation methods. Advanced methods, including zone models based on a solution of the equations for conservation of mass and energy or more complex computational fluid dynamics (CFD) models, as described in annex D of EN 1991-1-2 may be used to provide information based on a solution of the thermodynamic and aerodynamic variables at various points within the control zone. Such models have been used effectively for many years to model the movement of smoke and toxic gases and are now being extended to model the thermal environment for particular post-flashover fire scenarios (Lennon et al., 2007).

1.4.1.2. Member temperatures

After the calculation of the atmosphere temperatures, the next step is to determine the temperature distribution within the structural elements. This is done through the calculation of the section factor. The section factor A/V is a convenient parameter to measure the thermal response of a steel member. Basically, the rate at which a steel element will increase in temperature is proportional to the surface area (A) of steel exposed to the fire and inversely proportional to the mass or volume (V) of the section. In a fire, a member with low section factor will heat up at a slower rate than one with high section factor. Calculation of the section factor for unprotected and insulated steel section is shown in annex 1.

EN 1993-1-2 (2005) provides a simple design approach for calculating the thermal response of unprotected steel members. Assuming an equivalent uniform temperature distribution in a cross-section, the increase of temperature $\Delta\theta_{a,t}$ [K] in an unprotected steel member during a time interval Δt is given by equation (1.11).

$$\Delta\theta_{a,t} = k_{sh} \frac{A_m/V}{c_a \rho_a} \dot{h}_{net,d} \Delta t \quad \text{for } \Delta t \leq 5s \quad (1.11)$$

Where :

ρ_a is the unit mass of steel [kg/m³];

A_m is the surface area of the member per unit length [m^2];

A_m/V is the section factor for unprotected steel members [m^{-1}];

c_a is the specific heat of steel [J/kgK];

$\dot{h}_{net,d}$ is the net heat flux per unit area [W/m^2];

k_{sh} is the correction factor for the shadow effect ($k_{sh} = 1.0$ if the shadow effect is ignored);

Δt is the time interval (s); and

V is the volume of the member per unit length [m^3].

The correction factor for the shadow effect k_{sh} is given by:

$$k_{sh} = \begin{cases} \frac{0.9 [A_m/V]_b}{A_m/V} & \text{for I – sections under nominal fire actions} \\ \frac{[A_m/V]_b}{A_m/V} & \text{for other cases} \end{cases}$$

Where :

$A_m/V \geq 10 m^{-1}$; and

$[A_m/V]_b$ is the box value of the section factor.

Concerning insulated steel members, EN 1993-1-2 (2005) provides a simple design approach with non-reactive fire protection materials. The insulating materials can be in the form of profiled or boxed systems, but do not include intumescent coatings. Assuming uniform temperature distribution, the temperature increase $\Delta\theta_{a,t}$ of an insulated steel member during a time interval Δt (≤ 30 s) is calculated using equation (1.12).

$$\Delta\theta_{a,t} = \frac{\lambda_p A_p / V}{d_p c_a \rho_a} \frac{(\theta_{g,t} - \theta_{a,t})}{(1 + \Phi/3)} \Delta t (e^{\Phi/10} - 1) \Delta\theta_{g,t} \quad \text{but } \Delta\theta_{a,t} \geq 0 \text{ if } \Delta\theta_{g,t} > 0 \quad (1.12)$$

$$\text{with } \Phi = \frac{c_p \rho_p}{c_a \rho_a} d_p A_p / V$$

Where :

λ_p is the thermal conductivity of fire protection material [W/mK];

$\theta_{a,t}$ is the steel temperature at time t [$^{\circ}C$];

$\theta_{g,t}$ is the ambient gas temperature at time t [$^{\circ}\text{C}$];

$\Delta\theta_{g,t}$ is the increase of ambient gas temperature during time interval Δt [K];

ρ_a is the unit mass of steel [kg/m^3];

ρ_p is the unit mass of fire protection material [kg/m^3];

A_p/V is the section factor for members insulated by fire protection material [m^{-1}];

A_p is the appropriate area of fire protection material per unit length [m^2];

c_a is the temperature-dependent specific heat of steel [J/kgK];

c_p is the temperature-independent specific heat of fire protection material [J/kgK];

d_p is the thickness of fire protection material [m];

Δt is the time interval [s]; and

V is the volume of the steel member per unit length [m^3].

This analysis can also be performed using a finite element software which conducts non-linear heat transfer analysis in order to obtain the thermal response and the nodal temperature histories ($T-t$ responses) of the structure (Agarwal et al., 2014). The heat transfer analysis accounts for the effects of radiation heat transfer from the fire to the exposed surface, convection heat transfer from the gas to the exposed surface, and conduction heat transfer within the cross-section. The temperature profiles developed from the heat transfer analysis are used in structural analysis.

1.4.2. Structural analysis

According to EN 1991-1-2 (2002), imposed and constrained expansions and deformations caused by temperature changes due to fire exposure result in effects of actions (forces and moments) which shall be considered and accounted by the chosen support models and boundary conditions, and/or implicitly considered by conservatively specified fire safety requirements. The analysis may be undertaken for a single member, a part of the structure or a global analysis of the entire structure using different available methods.

1.4.2.1. Critical temperature method

The critical temperature method is a tabulated method where, the critical temperature, $\theta_{a,cr}$, for a steel member at time, t , with a uniform temperature distribution is the temperature at

which the capacity of the member is reduced to the applied load. In EN 1993-1-2, the critical temperature may be determined for any degree of utilization from equation (1.13).

$$\theta_{a,cr} = 39.19 \ln \left[\frac{1}{0.9674\mu_0^{3.833}} - 1 \right] + 482 \quad (1.13)$$

Where μ_0 is the degree of utilization in the member and must not be taken less than 0,013. Examples of values of $\theta_{a,cr}$ for values of μ_0 from 0.22 to 0.80 are given in annex 2.

For members with class 1, class 2 or class 3 cross-sections and for all tension members, the degree of utilization μ_0 at time $t = 0$ may be obtained from equation (1.14).

$$\mu_0 = E_{fi,d} / R_{fi,d,0} \quad (1.14)$$

Where :

$E_{fi,d}$ is the applied load at the fire limit state;

$R_{fi,d,0}$ is the resistance capacity of the member under normal conditions.

Alternatively for tension members, and for beams where lateral-torsional buckling is not a potential failure mode, μ_0 may conservatively be obtained from equation (1.15).

$$\mu_0 = \eta_{fi} [\gamma_{M,fi} / \gamma_{M0}] \quad (1.15)$$

Where η_{fi} is the reduction factor of the design load level for fire situation

1.4.2.2. Resistance method

Resistance method is a simple calculation method based on load bearing of the structure. According to EN 1993-1-2 (2005), the load-bearing function of a steel member shall be assumed to be maintained after a time, t , in a given fire equation (1.16).

$$E_{fi,d} \leq R_{fi,d,t} \quad (1.16)$$

Where :

$E_{fi,d}$ is the design effect of actions for the fire design situation, according to EN 1991-1-2 (2002);

$R_{fi,d,t}$ is the corresponding design resistance of the steel member, for the fire design situation, at time t .

The design resistance $R_{fi,d,t}$ at time t should be determined, usually in the hypothesis of a uniform temperature in the cross-section, by modifying the design resistance for normal

temperature design in EN 1993-1-2 (2005), to take account of the mechanical properties of steel at elevated temperatures.

1.4.2.3. Advanced calculation method

Advanced calculation model is a finite element (FE) model able to solve numerically, with reliable approximation, the partial differential equations describing member's response for assumed fire conditions. Due to high cost of experimental studies addressing to fire design, extensive research has been carried out in recent years based on the numerical simulation of steel structures subjected to fire conditions, especially with finite element method (FEM) developments (Landesmann et al., 2005). According to EN 1993-1-2 (2005), these calculation methods should include separate calculation models for the determination of the development and distribution of the temperature within structural members (thermal response model); and the mechanical behaviour of the structure or of any part of it (mechanical response model). This method may be used in association with any heating curve, provided that the material properties are known for the relevant temperature range. The calculation results may refer to temperatures, deformations and fire resistance times.

Conclusion

A general overview of steel, steel structures, the effect of fire on steel structures and structural fire analysis were discussed in this chapter. The first part illustrated steel, its manufacturing processes, its properties, the different types of steel that exist, their uses, defects and prevention of defects. The second part presented the historical background of steel, how it is used in modern construction today and how its different members can be joint to form a structure using connecting devices. The different types of structures that can be constructed using structural steel and a brief overview of the advantages and disadvantages of using steel structures were discussed. In the third part, focus was made on the effect of fire on steel structures. This part mentioned the different fire damaged events that happened all over the world, the different experimental and numerical research that were done on steel structures subjected fire. And the last part dealt with the structural fire analysis of steel structures showing how different thermal actions can be considered on structures in order to design a fire resisting structure and a description of the different methods used to thermally and structurally analyse a structure subjected to fire. The two following chapters (chapters 2 and 3) focus on the analysis of a steel structure that was subjected to fire using a computer aided program and the possible solutions that can be proposed in order to reduce the fire damages of such structures.

CHAPTER 2: METHODOLOGY

Introduction

The previous chapter enabled us to know more about the material called steel, have an overview of steel structures, observed the damaged caused by fire on steel structures and understand how structural fire analysis is made. This chapter will focus on the description of the methodology of the work. The methodology is the part of the study that establishes the research procedure after the definition of the problem, so as to achieve the set of objectives. It is partitioned in different sections, the first being a general recognition of the site done by a documentary research. This is followed by data collection that will enable the modelling and analysis of the industrial store building. The objective of this chapter is to show the static verification procedure of an existing building in compliance with Eurocode 3, the modelling and fire analysis procedure used in the software Abaqus/CAE and finally, analysing two fire protective systems.

2.1. General site recognition

The recognition of the site will be based on documentary researched on the study site. It allows the knowledge of the physical parameters like the geographical location, the climate, and the hydrology and on the other hand the socio-economic parameters.

2.2. Site visit

The site visit is the phase that consists in going down to the study site in order to discover it. The site visit will be done in two phases, the first phase for direct observation of the site and the second for surveys.

2.3. Data collection

The data collected are the structural plans and the data concerning the different properties of the materials used on the site.

2.3.1. Structural data

Structural data contains the structural plan that shows the disposition of the different structural elements of the building and their geometrical dimensions. They are collected using AutoCAD. These data are composed of structural details and they contain the sections of the different elements used in the construction of the building.

2.3.2. Characteristics of materials

This is the data that characterises the materials that were used for the implementation of the structure. Knowing the material properties will help to obtain the resisting forces and moments. The material properties will be divided in two parts, one for the steel members, and the other for the concrete used as foundation.

2.4. Codes and loads conditions

The codes used and the different types of loads acting on steel industrial building will be presented in this section. This study will focus on three main types of actions which acts on steel buildings. These actions are permanent, variable and accidental loads.

2.4.1. Codes

The building will be described according to EN1991-1-1 (2002), clause 6.3.2 as a been part of Category E1 as shown in annex 3 since it is used for storage. Depending on the location of the building and government accepted standards, design codes are used for the definition of loads and calculations. European codes will be used in this study and the Eurocodes used are reported in table 2.1.

Table 2.1. Codes

Codes	Abbreviation
Eurocode 0: Basis of structures	EN1990_E_2002
Eurocode 1 : Actions on structures	EN1991_E_2002
Eurocode 2 : Design of concrete structures	EN1992_E_2004
Eurocode 3: Design of steel structures	EN1993_E_2005
Eurocode 5 : Design of timber structures	EN1995_E_2004
Eurocode 9 : Design of aluminium structures	EN1999_E_2007

2.4.2. Permanent loads

Also known as static or dead loads, these are actions that act on the whole nominal life of the structure with a negligible variation of their intensity in time. These include the self-weight of the structural elements and the self-weight of the non-structural elements present in the nominal life of the structure but which do not take part in the load bearing mechanism.

2.4.3. Variable loads

These are actions on structures for which their variation in magnitude with time is not negligible. These actions include imposed loads and wind loads.

2.4.3.1. Imposed loads

These are loads other than the weight of the structure like loads of people, objects, vehicles etc. They depend on building occupancy and maintenance (roof elements). According to Eurocode 1, the appropriate load with respect to the building occupancy is selected. The metallic hangar belongs to building category E1, since it is an area for storage as shown in annex 3. Concerning the maintenance load, it shall be considered for the roof of the hangar for the static analysis of the structure.

2.4.3.2. Wind loads

Wind actions fluctuate with time and act directly as pressures on the external surfaces of enclosed structures and, because of porosity of the external surface, also act indirectly on the internal surfaces. They may also act directly on the internal surface of open structures. The pressures created inside a building due to access of wind through openings could be suction (negative) or pressure (positive) of the same order of intensity while those outside may also vary in magnitude with possible reversals. Thus the design value shall be taken as the algebraic sum of the two in appropriate or concerned direction. The response of a building to high wind pressures depends not only upon the geographical location and proximity of other obstructions to airflow but also upon the characteristics of the structure like the size, shape and dynamic properties of the structure.

a. Basic wind velocity

EN 1991-1-4 (2002) specifies that the fundamental value of the basic wind velocity, $v_{b,0}$ is the characteristic 10 minutes mean wind velocity, irrespective of wind direction and time of year, at 10 m above ground level in open country terrain with low vegetation such as grass and isolated obstacles with separations of at least 20 obstacle heights. This basic wind velocity will be calculated from equation (2.1).

$$v_b = C_{dir} \times C_{season} \times v_{b,0} \quad (2.1)$$

Where C_{dir} and C_{season} are respectively the directional and seasonal factor. EN 1991-1-4 (2005) recommend this value to be taken as 1.

b. Basic and peak velocity pressure

The basic velocity will be calculated as shown in equation (2.2).

$$q_b = \frac{1}{2} \times \rho_{air} \times v_b^2 \quad (2.2)$$

Where $\rho_{air} = 1.25 \text{ kg/m}^3$ (air density).

The peak velocity pressure $q_p(z)$ at height z , which includes mean and short-term velocity fluctuations, shall be determined as presented on equation (2.3).

$$q_p(z) = [1 + 7I_v(z) + 12 \times \rho \times v_m(z)^2] \quad (2.3)$$

Where :

I_v is the turbulence intensity;

ρ is density;

$v_m(z)$ is the mean wind velocity as shown in equation (2.4).

$$v_m(z) = c_r(z) \times c_o(z) \times v_b \quad (2.4)$$

Where :

$c_o(z)$ is the orography factor;

$c_r(z)$ is the roughness factor as calculated in equation (2.5) or (2.6).

$$c_r(z) = k_T \times \ln\left(\frac{z}{z_0}\right) \quad \text{for } z_{\min} \leq z \leq z_{\max} \quad (2.5)$$

$$c_r(z) = c_r(z_{\min}) \quad \text{for } z \leq z_{\min} \quad (2.6)$$

Where :

z_0 is the roughness length;

k_T is the terrain factor, depending on the roughness length z_0 as shown in equation (2.7).

$$k_T = 0.019 * \left(\frac{z_0}{z_{0,II}} \right) * 0.07 \quad (2.7)$$

Where :

$z_{0,II} = 0.05$ (terrain category IV, taken from table 2.2);

z_{\min} is the minimum height;

z_{\max} is to be taken as 200 m.

Table 2.2. Terrain categories and terrain parameters

Terrain category	z_0 m	z_{min} m
0 Sea or coastal area exposed to the open sea	0,003	1
I Lakes or flat and horizontal area with negligible vegetation and without obstacles	0,01	1
II Area with low vegetation such as grass and isolated obstacles (trees, buildings) with separations of at least 20 obstacle heights	0,05	2
III Area with regular cover of vegetation or buildings or with isolated obstacles with separations of maximum 20 obstacle heights (such as villages, suburban terrain, permanent forest)	0,3	5
IV Area in which at least 15 % of the surface is covered with buildings and their average height exceeds 15 m	1,0	10
NOTE: The terrain categories are illustrated in A.1.		

The turbulence intensity $I_v(z)$ at height z is defined as the standard deviation of the turbulence divided by the mean wind velocity. It is calculated as represented in equation (2.8) and (2.9).

$$I_v = k_1 c_0(z) * \ln\left(\frac{z}{z_0}\right) \quad \text{for } z_{min} \leq z \leq z_{max} \quad (2.8)$$

$$I_v = I_v(z_{min}) \quad \text{for } z < z_{min} \quad (2.9)$$

Where k_1 is the turbulence factor and the recommended value for k_1 is 1,0.

The peak velocity pressure $q_p(z)$ can also be calculated as shown in equation (2.10).

$$q_p(z) = c_e(z) * q_b \quad (2.10)$$

Where $c_e(z)$ is the exposure factor illustrated in figure 2.1 as a function of height above terrain and the terrain category.

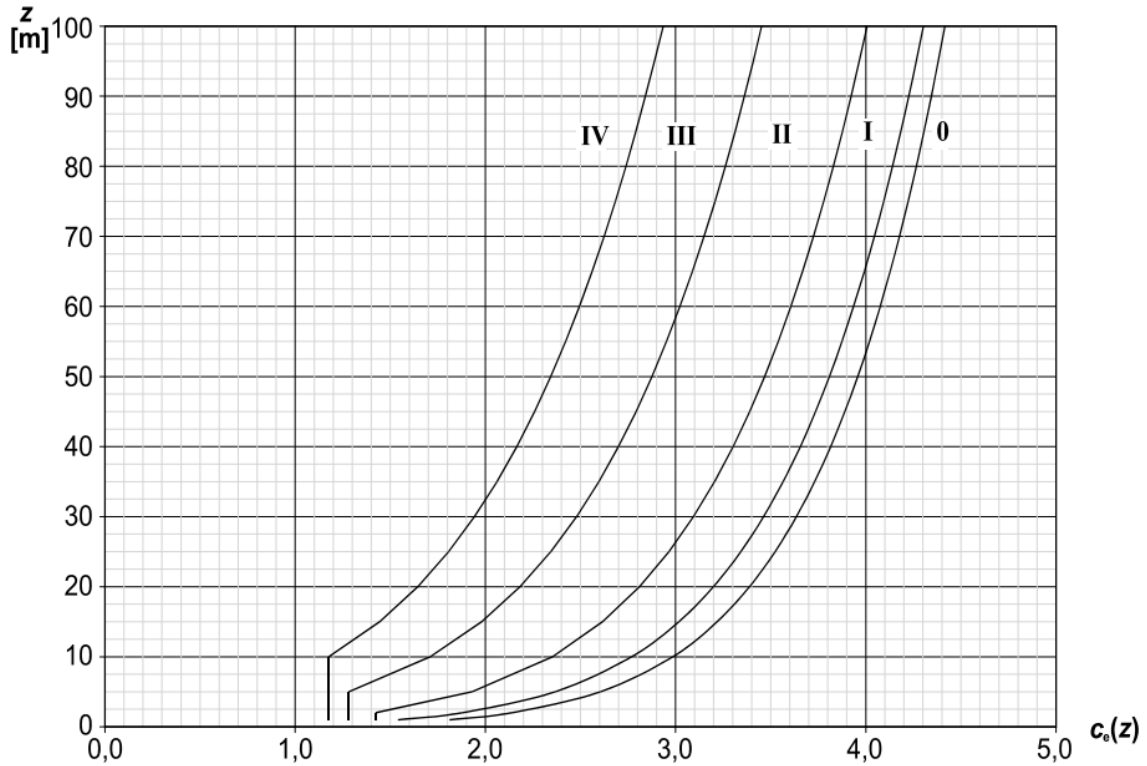


Figure 2.1. Illustrations of the exposure factor $c_e(z)$ for $c_0=1,0$, $k_1=1,0$ (BS EN1991-1-4)

c. Wind pressure on surfaces

The effect of wind on the structure as a whole is determined by the combined action of external and internal pressures acting upon it. A positive wind load stands for pressure whereas a negative wind load indicates suction on the surface. This definition applies for the external wind action as well as for the internal wind action. The pressure distribution is shown in figure 2.2.

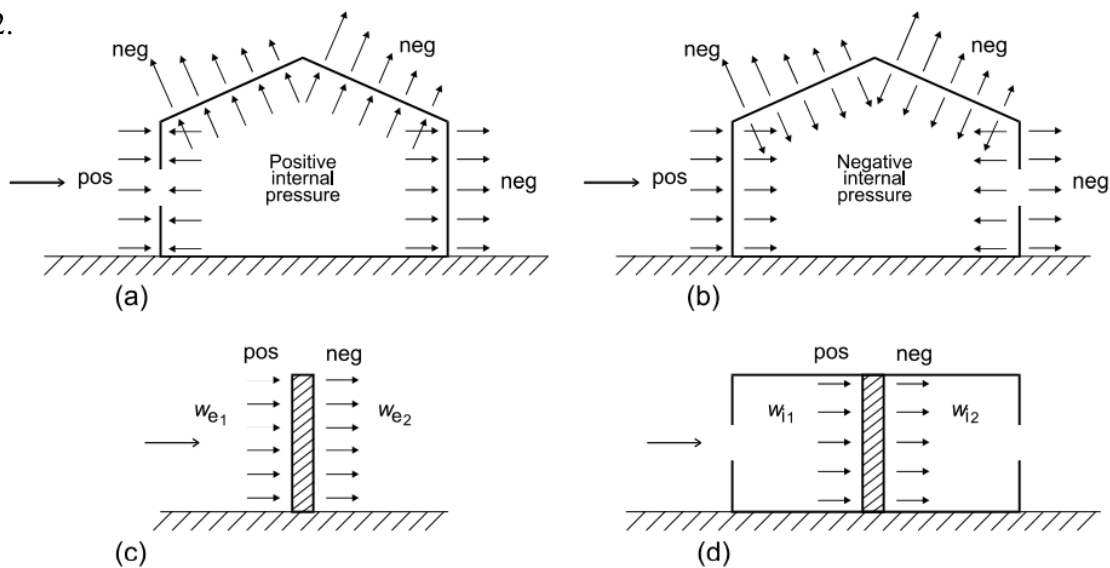


Figure 2.2. Pressure on surfaces

d. External wind pressure

The wind pressure acting on the external surfaces, w_e , should be obtained from equation (2.11).

$$w_e = q_p(z_e) * c_{pe} \quad (2.11)$$

Where :

$q_p(z_e)$ is the peak velocity pressure;

z_e is the reference height for the external pressure;

c_{pe} is the pressure coefficient for the external pressure depending on the size of the loaded area.

e. Internal wind pressure

The internal pressure coefficient depends on the size and distribution of the openings in the building envelope. The wind pressure acting on the internal surfaces of a structure, w_i , will be obtained from equation (2.12).

$$w_i = q_p(z_i) * c_{pi} \quad (2.12)$$

Where :

z_i is the reference height for the internal pressure;

c_{pi} is the pressure coefficient for the internal pressure.

The net pressure on a wall, roof or element is the difference between the pressures on the opposite surfaces taking due account of their signs. The wind loadings per unit length, w , for an internal frame are calculated using the influence width (spacing between the columns) i_s , as presented in equation (2.13). The worst combination of external and internal pressures are to be considered for every combination for the analysis.

$$w = (c_{pe} - c_{pi}) * q_p * i_s \quad (2.13)$$

2.4.4. Accidental loads

These loads are usually of short duration but of significant magnitude, that are unlikely to occur on a given structure during the design working life. An accidental action can be expected in many cases to cause severe consequences unless appropriate measures are taken. These loads include fire, explosions, impact from vehicles etc. In this work, the accidental load that will be taking into consideration is the fire load.

2.4.5. Limit states

A structure is designed according to the corresponding limit states in such a way to sustain all actions acting upon it during its intended life. This implies it will be designed having adequate structural stability (ultimate limit states) and remain fit for the use it is required (serviceability limit states).

2.4.5.1. Ultimate limit states

According to EN 1990 (2002), ultimate limit states (ULS) corresponds to the loss of structural capacity of the whole structure or one of its fundamental element (for example structural collapse). It concerns the safety of people and/or the safety of the structure. The loss of structural capacity includes :

- Loss of equilibrium of the whole structure or one of its fundamental parts;
- Excessive displacements or deformations;
- Reaching of the maximum strength capacity of parts of structures, joints, foundations;
- Reaching of the maximum strength capacity of the entire structure;
- Reaching of failure mechanisms in the soils.

2.4.5.2. Serviceability limit states

Serviceability limit state (SLS) is the inability of the structure to meet the specify service requirement. This include mainly :

- Functioning of the structure or structural members under normal use;
- Comfort of people;
- The appearance of the construction works.

2.4.6. Load combinations

A combination of actions defines a set of values used for the verification of the structural reliability for a limit state under the simultaneous influence of different actions. For the verification of the structure at ultimate limit state (ULS), the load combinations used were given by equation (2.14) and (2.15).

$$\text{ULS1} : \gamma_{G,1} G_1 + \gamma_{G,2} G_2 + \gamma_{Q,m} Q_m + \gamma_{Q,w} \Psi_{0,w} Q_w \quad (2.14)$$

$$\text{ULS2} : \gamma_{G,1} G_1 + \gamma_{G,2} G_2 + \gamma_{Q,w} Q_w + \gamma_{Q,m} \Psi_{0,m} Q_m \quad (2.15)$$

Where :

Q_m is the maintenance load on the roof;

Q_w are the wind loads acting on the roof, windward and leeward side;

G_1 are the self-weight of the structural components;

G_2 is the self-weight of the aluminium roof;

$\gamma_{i,j}$ is the safety factor for permanent and variable loads and its values are obtained from annex 4.

$\Psi_{i,j}$ are the combination coefficients and their values are given in annex 5.

A load envelope is obtained from ULS combinations to have the most unfavourable condition for an element. This will be used for the design verification.

For the verification of the structure at serviceability limit state (SLS), the load combination used is given in equation (2.16), (2.17) and (2.18).

$$\text{SLS1 (characteristic combination)} : G_1 + G_2 + Q_m + \Psi_{0,w} Q_w \quad (2.16)$$

$$\text{SLS2 (frequent combination)} : G_1 + G_2 + \Psi_{1,w} Q_w + \Psi_{2,m} Q_m \quad (2.17)$$

$$\text{SLS3 (quasi-permanent combination)} : G_1 + G_2 + \Psi_{2,m} Q_m + \Psi_{2,w} Q_w \quad (2.18)$$

2.5. Structural design method of steel structures

The structural design process encompasses the static analysis of the steel structure and the verification of members at ULS and SLS. It is done firstly by creating a numerical model of the structure in order to have the solicitations, then verifying the cross section of the different elements and the design verifications will be done with respect to EN1993-1-1 (2005) on different members after classifying each cross sections.

2.5.1. Numerical static analysis tool

Numerical modelling in civil engineering is used as a tool that facilitates engineers to evaluate the behaviour of structures. The software used for the static analysis of the structure is SAP2000.

2.5.1.1. Presentation of the numerical software SAP2000

SAP (System Application Product) 2000 is a software of calculation and design of engineering structures particularly adapted to the buildings and civil engineering works. It offers many possibilities of analysis of the static and dynamic effects with complements of design and verification of the structures in reinforced concrete, metallic frame and others types

of structures. The software allows to carry out the modelling steps (definition of geometry, boundary conditions, loading of the structure and more) in a totally graphic, numerical or combined way, using the countless tools available. The program offers many analysis possibilities as linear static analysis, p-delta analysis, non-linear static analysis and dynamic analysis. The software considerably facilitates the analysis of the results by offering the possibility to visualise the distortion of system, the diagrams of the forces and curves envelopes, the fields of constraints, the Eigen modes of vibration and more.

2.5.1.2. Analysis steps

Modelling will consist of creating the appropriate material, section properties, loads and loads combinations. The steel elements shall be drawn according to the plans and the supports conditions assigned to be pinned. The structure shall be loaded with respect to specific load patterns discussed in section 2.4. The load combinations will be defined prior to the analyses to satisfy the ULS and SLS conditions discussed in sections 2.4.5.1 and 2.4.5.2. The case study presented in section 3.3 will be loaded and a static linear analysis will be done to obtain the solicitations and verify the different elements in compliance with Eurocode 3 norms. Before any element is verified, it needs to be classified according to its capacity to develop plastic hinges and rotation deformations.

2.5.2. Classification of the sections

The classification of a section depends on geometric characteristics. The sections of the members to be design are going to be classified as class 1, 2, 3, or 4. Eurocode defines these classes as follows :

- Class 1 cross-sections are those which can form a plastic hinge with the rotation capacity required from plastic analysis without reduction of the resistance.
- Class 2 cross-sections are those which can develop their plastic moment resistance, but have limited rotation capacity because of local buckling.
- Class 3 cross-sections are those in which the stress in the extreme compression fibre of the steel member assuming an elastic distribution of stresses can reach the yield strength, but local buckling is liable to prevent development of the plastic moment resistance.
- Class 4 cross-sections are those in which local buckling will occur before the attainment of yield stress in one or more parts of the cross-section.

The sections are going to be classified according to annex 6.

2.5.3. Members in bending

The ULS design verification procedure of the members in bending will take into considerations uniaxial bending, shear resistance and lateral torsional buckling.

2.5.3.1. Uniaxial bending

The design value of the bending moment M_{Ed} at each cross-section shall satisfy equation (2.19).

$$\frac{M_{Ed}}{M_{c,Rd}} \leq 1 \quad (2.19)$$

Where M_{Ed} is the design moment and $M_{c,Rd}$ is the resisting moment.

The design resistance for bending about one principal axis of a cross-section is determined as described by equation (2.20), (2.21) and (2.22).

$$M_{c,Rd} = M_{pl,Rd} = \frac{W_{pl}f_y}{\gamma_{M0}} \quad \text{for class 1 or 2 cross sections} \quad (2.20)$$

$$M_{c,Rd} = M_{el,Rd} = \frac{W_{el,min}f_y}{\gamma_{M0}} \quad \text{for class 3 cross sections} \quad (2.21)$$

$$M_{c,Rd} = \frac{W_{eff,min}f_y}{\gamma_{M0}} \quad \text{for class 4 cross sections} \quad (2.22)$$

Where :

f_y is the yielding strength;

W_{pl} is the plastic section modulus;

W_{elmin} is the elastic section modulus;

$W_{eff,min}$ is the effective section modulus.

2.5.3.2. Shear resistance

The design value of the shear force V_{Ed} at each cross section shall satisfy equation (2.23).

$$\frac{V_{Ed}}{V_{c,Rd}} \leq 1.0 \quad (2.23)$$

Where $V_{c,Rd}$ is the design shear resistance.

For plastic design $V_{c,Rd}$ is the design plastic shear resistance $V_{pl,Rd}$ as given in equation (2.24).

$$V_{pl,Rd} = \frac{A_v(f_y/\sqrt{3})}{\gamma_{M0}} \quad (2.24)$$

Where A_v is the shear area as illustrated in figure 2.3.

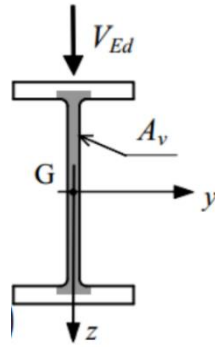


Figure 2.3. Beam shear resisting area

For rolled I and H sections with load parallel to web, the shear area A_v may be taken as showed in equation (2.25).

$$A_v = A - 2bt_f + (t_w + 2r) \quad \text{but not less than } \eta h_w t_w \quad (2.25)$$

In addition the shear buckling resistance for webs without intermediate stiffeners should be verified according to section 5 of EN 1993-1-5 (2006), if equation (2.26) is true.

$$\frac{h_w}{t_w} > 72 \frac{\varepsilon}{\eta} \quad (2.26)$$

Where :

h_w is the height of the web;

t_w is the thickness of the web.

$$\varepsilon = \sqrt{\frac{235}{f_y}}$$

According to EN 1993-1-5 (2006), the value $\eta = 1,20$ is recommended for steel grades up to and including S460. For higher steel grades $\eta = 1,00$ is recommended.

Shear and bending moment may interact if present at the same time on the member due to the loading condition. Provided that the design value of shear force does not exceed 50% of $V_{pl,Rd}$, no reduction of the resistances defined for the bending and axial force need to be made. If V_{Ed} exceeds 50% of $V_{pl,Rd}$, the reduced plastic shear resistance is calculated using a reduced yield strength given by equation (2.27).

$$f'_y = (1 - \rho)f_y \quad (2.27)$$

$$\text{Where } \rho = \left(\frac{2V_{Ed}}{V_{pl,Rd}} - 1 \right)^2$$

2.5.3.3. Lateral torsional buckling

A laterally unrestrained member subject to major axis bending should be verified against lateral-torsional buckling using equation (2.28).

$$\frac{M_{Ed}}{M_{b,Rd}} \leq 1.0 \quad (2.28)$$

Where:

M_{Ed} is the design value of the moment;

$M_{b,Rd}$ is the design buckling resistance moment.

The design buckling resistance moment of a laterally unrestrained beam is calculated using equation (2.29).

$$M_{b,Rd} = \chi_{LT} W_y \frac{f_y}{\gamma_{M1}} \quad (2.29)$$

Where :

W_y is the appropriate section modulus as follows:

- $W_y = W_{pl,y}$ for class 1 or 2 cross-sections
- $W_y = W_{el,y}$ for class 3 cross-sections
- $W_y = W_{eff,y}$ for class 4 cross-sections

χ_{LT} is the reduction factor for lateral-torsional buckling, which will be calculated as shown in equation (2.30).

$$\chi_{LT} = \frac{1}{\Phi_{LT} + \sqrt{\Phi_{LT}^2 - \bar{\lambda}_{LT}^2}} \quad \text{But } \chi_{LT} \leq 1.0 \quad (2.30)$$

Where :

$$\Phi_{LT} = 0.5 \left[1 + \alpha_{LT} (\bar{\lambda}_{LT} - 0.2) + \bar{\lambda}_{LT}^2 \right]$$

α_{LT} is an imperfection factor

$$\bar{\lambda}_{LT} = \sqrt{\frac{W_y f_y}{M_{cr}}}$$

M_{cr} is the elastic critical moment for lateral-torsional buckling.

Beams with sufficient restraint to the compression flange are not susceptible to lateral-torsional buckling. In addition, beams with certain types of cross-sections, such as square or circular hollow sections are not susceptible to lateral-torsional buckling.

2.5.4. Members in tension

For members in axial tension, at ULS the design resisting value of the tensile force $N_{t,Rd}$ at each cross-section shall satisfy equation (2.31).

$$\frac{N_{Ed}}{N_{t,Rd}} \leq 1.0 \quad (2.31)$$

Where, N_{Ed} is the design tension load and $N_{t,Rd}$ is the resisting tensile force of the element and it is the minimum between $N_{pl,Rd}$ and $N_{u,Rd}$ given in equations (2.32) and (2.33).

$$N_{pl,Rd} = \frac{Af_y}{\gamma_{M0}} \quad (2.32)$$

$$N_{u,Rd} = \frac{0.9A_{net}f_u}{\gamma_{M2}} \quad (2.33)$$

Where :

$N_{pl,Rd}$ is the design plastic resistance of the gross cross-section;

$N_{u,Rd}$ is the design ultimate resistance of the net cross-section at holes for fasteners;

f_y is the yield strength of steel;

A_{net} is the net cross section area;

γ_{M2} is the safety coefficient with value 1.25.

2.5.5. Members in compression

For members in compression, the element is verified at ULS for pure compression and buckling resistance.

2.5.5.1. Pure compression

For pure compression, the design resisting value of the compressive force $N_{c,Rd}$ at each cross-section shall satisfy equation (2.34).

$$\frac{N_{Ed}}{N_{c,Rd}} \leq 1.0 \quad (2.34)$$

Where $N_{c,Rd}$ should be determined by equation (2.35) and (2.36).

$$N_{c,Rd} = \frac{Af_y}{\gamma_{M0}} \quad \text{for class 1,2 or 3 cross-section} \quad (2.35)$$

$$N_{c,Rd} = \frac{A_{eff}f_y}{\gamma_{M0}} \quad \text{for class 1,2 or 3 cross-section} \quad (2.36)$$

2.5.5.2. Buckling resistance

A compression member should be verified against buckling using equation (2.37).

$$\frac{N_{Ed}}{N_{b,Rd}} \leq 1.0 \quad (2.37)$$

Where :

N_{Ed} is the design value of the compression force;

$N_{b,Rd}$ is the buckling resistance force and is given by equation (2.38) and (2.39).

$$N_{b,Rd} = \frac{\chi Af_y}{\gamma_{M1}} \quad \text{for class 1, 2 and 3 cross-sections} \quad (2.38)$$

$$N_{b,Rd} = \frac{\chi A_{eff}f_y}{\gamma_{M1}} \quad \text{for class 4 cross-sections} \quad (2.39)$$

Where χ is the reduction factor for the relevant buckling mode. The value of χ for the appropriate non-dimensional slenderness, $\bar{\lambda}$, should be determined from figure 2.4 or from equation (2.40).

$$\chi = \frac{1}{\Phi + \sqrt{\Phi^2 - \bar{\lambda}^2}} \quad \text{but } \chi \leq 1.0 \quad (2.40)$$

Where $\Phi = 0.5 \left[1 + \alpha_{LT}(\bar{\lambda}_{LT} - 0.2) + \bar{\lambda}_{LT}^2 \right]$

With α the imperfection factor obtained from annex 7.

The non-dimensional slenderness $\bar{\lambda}$ is given by equation (2.41) and (2.42)

$$\bar{\lambda} = \sqrt{\frac{Af_y}{N_{cr}}} = \frac{L_{cr}}{i} \frac{1}{\lambda_1} \quad \text{for class 1,2 and 3 cross-sections} \quad (2.41)$$

$$\bar{\lambda} = \sqrt{\frac{A_{eff}f_y}{N_{cr}}} = \frac{L_{cr}}{i} \frac{\sqrt{\frac{A_{eff}}{A}}}{\lambda_1} \quad \text{for class 4 cross-section} \quad (2.42)$$

Where :

L_{cr} is the buckling length in the buckling plane considered;

i is the radius of gyration about the relevant axis, determined using the properties of the gross cross-section;

$$\lambda_1 = \pi \sqrt{\frac{E}{f_y}} = 93.9\varepsilon ;$$

$$\varepsilon = \sqrt{\frac{235}{f_y}} \quad (f_y \text{ in N/mm}^2).$$

N_{cr} is the elastic critical force for the relevant buckling mode based on the gross cross sectional properties.

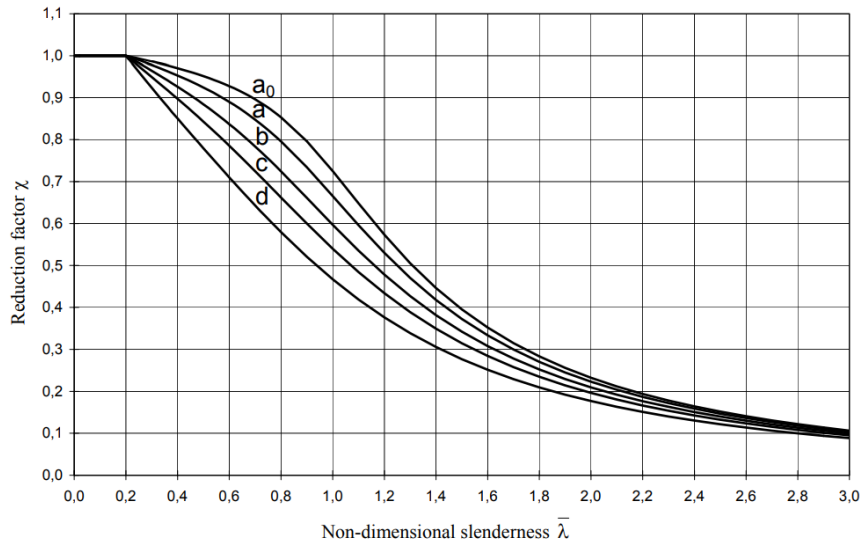


Figure 2.4. Buckling curves

When an element is subjected to axial and flexural load, equation (2.43) should be verified.

$$\frac{N_{Ed}}{N_{c,Rd}} + \frac{M_{Ed}}{M_{c,Rd}} \leq 1.0 \quad (2.43)$$

In which N_{Ed} is the design axial force and M_{Ed} the design moment acting on the element at the cross-section under consideration, $N_{c,Rd}$ is the cross-section axial resistance, and $M_{c,Rd}$ is the cross-section moment resistance.

For doubly symmetrical I- and H-sections or other flanges sections, allowance need not be made for the effect of the axial force on the plastic resistance moment about the y-y axis when both the criteria of equation (2.44) and (2.45) are satisfied.

$$N_{Ed} \leq 0.25N_{pl,Rd} \quad (2.44)$$

$$N_{Ed} \leq \frac{0.5h_w t_w f_y}{\gamma_{M0}} \quad (2.45)$$

Where :

h_w is the height of the web;

t_w is the thickness of the web;

f_y is the yield strength of steel;

γ_{M0} is the safety coefficient with value 1.25.

2.5.6. Connection design

The connection between the structural members are done using bolted connections and they are going to be analysed at ULS based on EN1993-1-8 (2005). The connection is a bearing type bolted connection using non-preloaded bolts.

2.5.6.1 Beam-column connection

The beam to column connection present in this work is an eave moment connection connecting a rafter with a column since the building is made of a portal frame with eaves haunches.

a. Shear resistance of the bolts

The shear resistance of the bolts are going to be verified according to equations (2.46) and (2.47).

$$F_{v,Rd} = 0.6 f_{ub} \frac{A_b}{\gamma_{M2}} \quad \text{for class 4.6, 5.6 and 8.8} \quad (2.46)$$

$$F_{v,Rd} = 0.5 f_{ub} \frac{A_b}{\gamma_{M2}} \quad \text{for class 4.8, 5.8, 6.8 and 10.9} \quad (2.47)$$

Where:

A_b is the cross sectional area of the bolt at the shear plane determined by equation (2.48);

f_{ub} is the ultimate strength of the bolt;

γ_{M2} is a safety factor which value is recommended as 1.25.

$$A_b = \frac{\pi d^2}{4} \quad (2.48)$$

b. Bearing resistance

The bearing resistance of the bolt on the plate is going to be verified according to equations (2.49).

$$F_{b,Rd} = \frac{k_1 a_b f_u d t}{\gamma_{M2}} \quad (2.49)$$

Where :

d is the diameter of the bolts;

f_u is the yielding strength of the plate;

a_b is the smallest of α_b ; $\frac{f_{ub}}{f_u}$ or 1;

α_b equals $\frac{e_1}{3d_0}$ for end bolts and $\frac{p_1}{3d_0} - \frac{1}{4}$ for inner bolts;

k_1 is the smallest of $2.8 \frac{e_2}{d_0} - 1.7$ or 2.5 for edge bolts;

k_1 is the smallest of $1.4 \frac{p_2}{d_0} - 1.7$ or 2.5 for inner bolts;

d_0 is the diameter of the bolts holes on the plate;

e_1 , e_2 , p_1 , p_2 are the dispositions on the plate and are represented in figure 2.5.

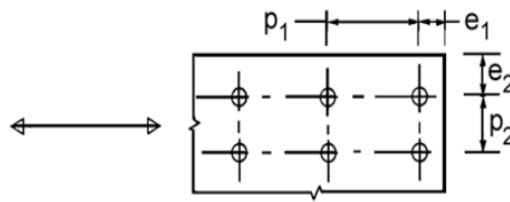


Figure 2.5. Spacing of the holes on the plate (EN 1993-1-8, 2005)

c. Traction resistance

The resistance to traction of each bolt is given by equation (2.50).

$$F_{t,Rd} = \frac{k_2 f_{ub} A_s}{\gamma_{M2}} \quad (2.50)$$

Where :

A_s is the tensile stress area of the bolt;

k_2 is the equal to 0.9.

d. Simultaneous traction and shear

Simultaneous traction and shear will be verified as shown in equation (2.51).

$$\frac{F_{v,Ed}}{F_{v,Rd}} + \frac{F_{t,Ed}}{1.4F_{t,Rd}} \leq 1.0 \quad (2.51)$$

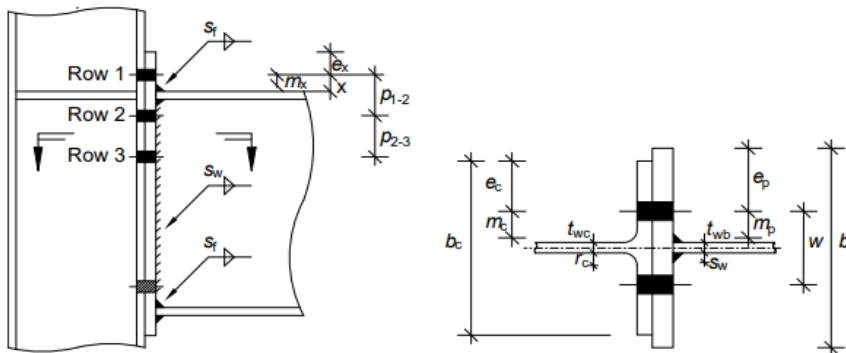
Where $F_{v,Ed}$ and $F_{t,Ed}$ are respectively the shear and traction forces.

e. Resistances of bolt rows in the tension zone

The effective design tension resistance for each row of bolts in the tension zone is limited by the least resistance of bending in the column flange, tension in the column web, bending in the end plate and tension in the rafter web. In bolted connections an equivalent T-stub in tension may be used to model the design resistances for the end plate and the column flange separately.

i. Column flange in bending

The connection geometry for an end plate connection is shown in figure 2.6. The geometry for a haunched connection in a portal frame would be similar although the beam would usually be at a slope and there will be more bolts rows as shown in figure 2.7 which provides information to identify its basic joint components.



For the end plate:

$$m_p = \frac{w}{2} - \frac{t_{wb}}{2} - 0.8s$$

$$e_p = \frac{b_p}{2} - \frac{w}{2}$$

For the column flange:

$$m_c = \frac{w}{2} - \frac{t_{wc}}{2} - 0.8r_c$$

$$e_c = \frac{b_c}{2} - \frac{w}{2}$$

For the end plate extension only:

$$m_x = x - 0.8s_f$$

Adjacent to a flange or stiffener:

m_2 is calculated in a similar way to m_x , above. m_2 is the distance to the face of the flange or stiffener, less 0.8 of the weld leg length.

Note: dimensions m and e , used without subscripts, will commonly differ between column and beam sides

where:

- w is the horizontal distance between bolt centrelines (gauge)
- b_p is the end plate width
- b_c is the column flange width
- t_{wb} is the beam web thickness
- t_{wc} is the column web thickness
- s is the weld leg length ($s = \sqrt{2}a$, where a is the weld throat) (subscripts f and w refer to the flange and the web welds respectively)
- r_c is the fillet radius of the rolled section (for a welded column section use s , the weld leg length)

Figure 2.6. Connection geometry (SCI P398)

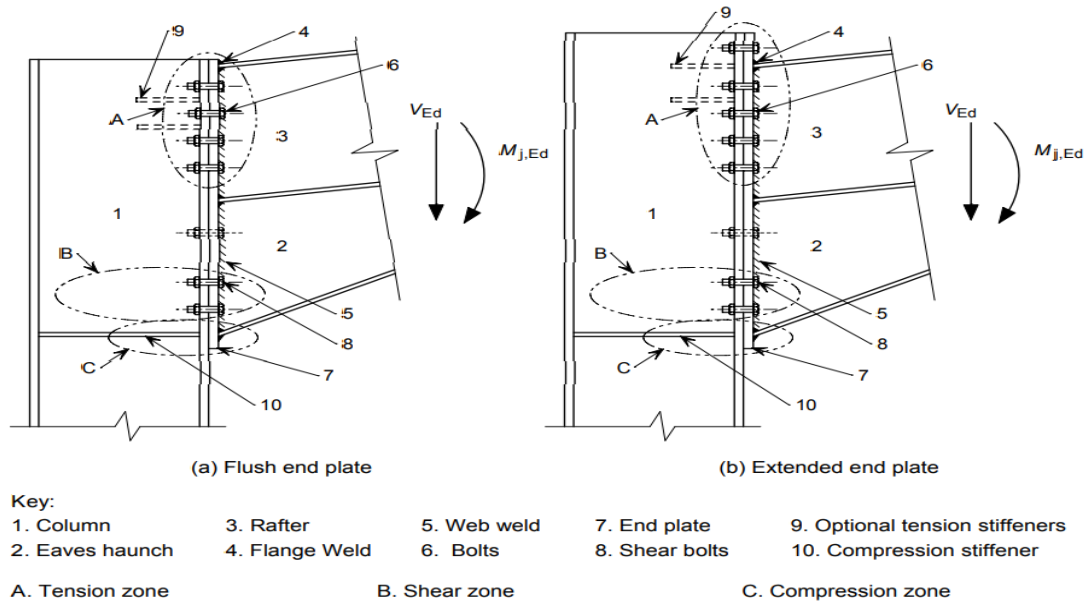


Figure 2.7. Portal frame eaves connections with bolted end plate (NCCI, 2008)

The resistances are calculated for three possible modes of failure and the least value is taken as shown in equation (2.52).

$$F_{t,fc,Rd} = \min (F_{T,1,Rd}; F_{T,2,Rd}; F_{T,3,Rd}) \quad (2.52)$$

- *Mode 1*

For the failure mode 1, the failure is due to the plate as shown in figure 2.8.

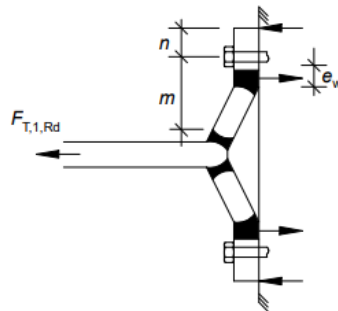


Figure 2.8. Complete flange yielding (SCI P398)

Using ‘Method 2’ in Table 6.2 of EN 1993-1-8 (2005), the design resistance of the T-stub flange is calculated as shown in equation (2.53).

$$F_{T,1,Rd} = \frac{(8n - 2e_w)M_{pl,1,Rd}}{2mn - e_w(m + n)} \quad (2.53)$$

Where :

$M_{pl,1,Rd}$ is the plastic resistance moment of the equivalent T-stub for mode 1 as calculated in equation (2.54).

$$M_{pl,1,Rd} = \frac{0.25 \sum l_{eff,1} t_p^2 f_y}{\gamma_{M0}} \quad (2.54)$$

m is defined in figure 2.6;

$$e_w = \frac{d_w}{4};$$

d_w is the diameter of the washer or the width across points of the bolt head, as relevant.

Washers are not necessarily provided and it is conservative to assume washers are not used;

$\sum l_{eff,1}$ is the effective length of the equivalent T-stub for mode 1 (see annex 8);

$t_{w,b}$ is the web thickness of the beam;

n is the $\min \{ e_c ; e_p ; 1.25m \}$

e_c is the edge distance of the column flange;

e_p is the edge distance of the end plate.

- *Mode 2*

For the failure mode 2, the failure is due to the local yielding of the plate and bolts failure as show in figure 2.9.

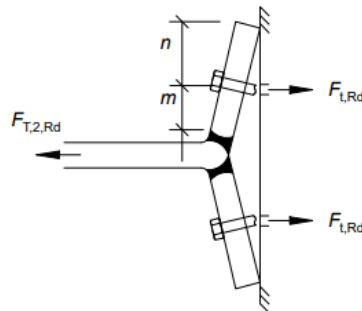


Figure 2.9. Bolt failure with flange yielding (SCI P398)

The design resistance of the T-stub flange is calculated as shown in equation (2.55).

$$F_{T,2,Rd} = \frac{2M_{pl,2,Rd} + n \sum F_{t,Rd}}{m + n} \quad (2.55)$$

Where:

$\sum F_{t,Rd}$ is the total tension resistance for the bolts in the T-stub (is equal to $2 * F_{t,Rd}$ for a single row);

$M_{pl,2,Rd}$ is the plastic resistance moment of the equivalent T-stub for mode 2 as calculated in equation (2.56);

$$M_{pl,2,Rd} = \frac{0.25 \sum l_{eff,2} t_p^2 f_y}{\gamma_{M0}} \quad (2.56)$$

$\sum l_{eff,2}$ is the effective length of the equivalent T-stub for mode 2 (annex 8).

- **Mode 3**

In mode 3, the failure is due to the bolts as shown in figure 2.10.

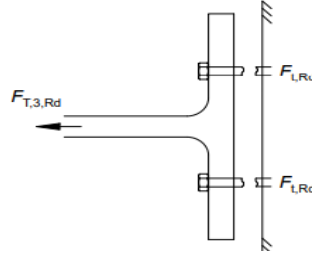


Figure 2.10. Bolt failure (SCI P398)

The design resistance of the T-stub flange is given by equation (2.57).

$$F_{T,3,Rd} = \sum F_{t,Rd,u} \quad (2.57)$$

- ii. **Column web in transverse tension**

The transverse tension resistance for a column web is given in equation (2.58).

$$F_{t,wc,Rd} = \frac{\omega b_{eff,t,wc} t_{wc} f_{y,wc}}{\gamma_{M0}} \quad (2.58)$$

Where :

ω is the reduction factor to allow for the interaction with shear in the column web panel as calculated in equation (2.59).

$$\omega = \frac{1}{\sqrt{1 + 1.3 (b_{eff,c,wc} t_{wc} / A_{vc})^2}} \quad (2.59)$$

A_{vc} is the shear area of the column. For rolled I and H sections it can be conservatively taken as $h_w t_w$;

$b_{eff,t,wc}$ is equal to l_{eff} .

iii. End-plate in bending

The design resistance and failure mode of an end-plate in bending, together with the associated bolts in tension, can be determined following the methodology used for column flange and using equation (2.60).

$$F_{t,ep,Rd} = \min(F_{T,1,Rd}; F_{T,2,Rd}; F_{T,3,Rd}) \quad (2.60)$$

iv. Rafter web in tension

The resistance of the rafter web in tension can be calculated as shown in equation (2.61).

$$F_{t,wb,Rd} = \frac{b_{eff,wb} t_{wb} f_{y,wb}}{\gamma_{M0}} \quad (2.61)$$

Where $b_{eff,t,wb}$ is equal to l_{eff}

f. Total resisting moment

The total resisting moment is obtained from the sum of the products of the traction resistance in each bolt row in the tension zone times their respective distances d_i from the centre of resistance of the compression zone (neutral axis of the compression flange) as shown in equation (2.62).

$$M_{Rd} = \sum F_{t,Rd,i} * d_i \quad (2.62)$$

2.5.6.2. Beam-beam connection

This connection is done between the two rafters of the portal frame as shown in figure 2.11. The verification procedure will be done as for the beam to column connection.

The shear resistance per bolt is computed using equation (2.46) or equation (2.47) depending of the bolt grade. Bearing resistance per bolt, traction resistance per bolt and total moment resistance will be verified using equation (2.49), (2.50) and (2.62) respectively.

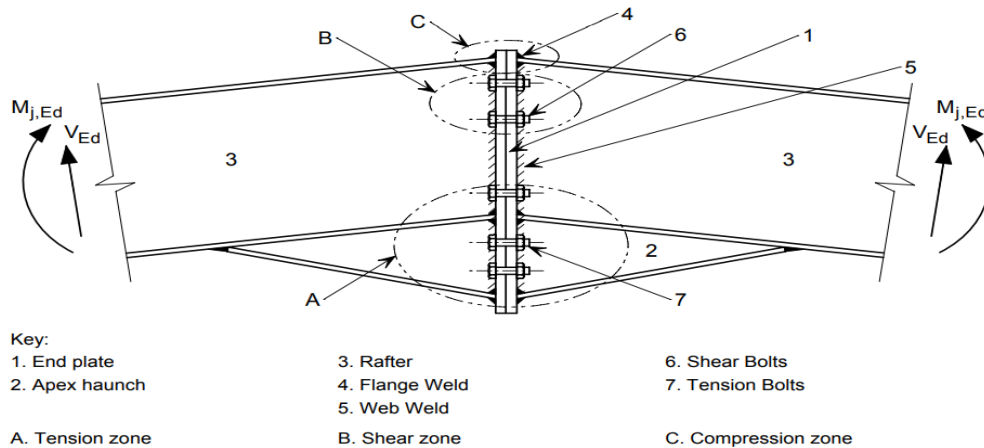


Figure 2.11. Portal frame apex connection with bolted extended end plate (NCCI, 2008)

2.5.6.3. Brace connection

The presence of the brace is mainly to take horizontal loads and this loads transit through the brace connections. This connection will be a simple connection that is no moment.

The shear resistance per bolt is computed using equation (2.46) or equation (2.47) depending of the bolt grade and the bearing resistance will be verified using equation (2.49).

2.5.6.4. Column base connection

The verification of the column base connection is done by verifying the concrete footing and the thickness of the plate.

a. Concrete footing

Firstly the bearing capacity is verified using equation (2.63).

$$\sigma_{sol} \leq \sigma_{adm} \quad (2.63)$$

Where σ_{sol} is the pressure exerted by the footing on the ground and it is calculated using equation (2.64).

$$\sigma_{sol} = \frac{N_{SLS} + \gamma * A * B * H}{A * B} \quad (2.64)$$

Where :

N_{SLS} is the SLS axial force solicitation at the level of the column base connection;

A and B are the dimensions of the section of the concrete footing;

H is the height of the concrete footing;

γ is the unit weight of concrete.

Afterwards, the compressive resistance of the concrete block is verified with the help of equation (2.65).

$$\sigma < f_{ck} \quad (2.65)$$

Where :

f_{ck} is the characteristic compressive cylinder strength of concrete;

σ is the compression constraint exerted on the concrete bloc calculated using equation (2.66).

$$\sigma = \frac{N}{ab} \quad (2.66)$$

With a and b being the length and width of the steel plate.

b. Plate

Admitting that part of the plate at the edge of the columns will be subjected to an uplift due to the reactions from the foundations, it will bend according to the tangent lines 1 and 2 shown in figure 2.12.

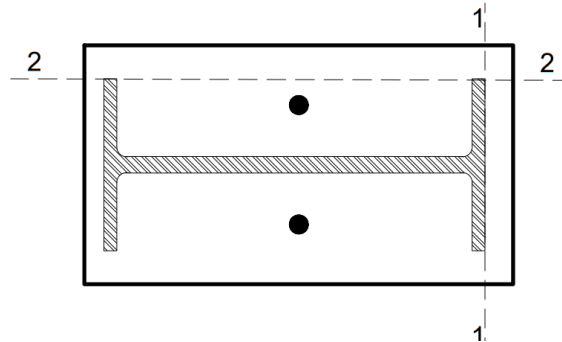


Figure 2.12. Tangent lines on the base plate which determine uplift (Morel, 2005)

The thickness of the plate is verified using equation (2.67).

$$t \geq u \sqrt{\frac{3\sigma}{f_y}} \tag{2.67}$$

Where :

u is the perpendicular distance from the edge of the beam flange to the edge of the column (lever arm).

Afterwards the shear resistance, bearing resistance and traction resistance of the anchors will be verified using equation (2.46) or (2.47), (2.49) and (2.50) respectively.

2.5.7. Serviceability limit states check for steel members

For the structure, it shall be verified that the maximum deflection of each elements is less than its maximum value according to Eurocodes. For beam elements, the maximum vertical deflection should be less than $l/200$, where l is the length of the beam in millimetres. For columns, the maximum horizontal deflection should be less than $h/300$, where h is the height of the column.

2.6. Numerical fire analysis tool

A numerical model is a model that reflect more or less what will happen in the reality if the same designing procedure is applied. In civil engineering it is used as a tool that facilitates engineers to evaluate the behaviour of structures. The numerical methods are convenient and

less time-consuming for analysis. Abaqus is the software that will be used in order to analyse the impact of fire globally and locally on the case study building

2.6.1. Presentation of the numerical software ABAQUS

Abaqus is a finite element calculation software package developed by ABAQUS, Inc (Dassault Systems). The Abaqus suite of software for Finite Element Analysis (FEA) is known for its high performance, quality and ability to solve all kind of challenging simulations more than any other software. It consists of three products which are ABAQUS/Standard, ABAQUS/Explicit and ABAQUS/CAE. It is the latter product that is used in this work.

Abaqus/CAE has a complete Abaqus environment that provides a simple, consistent interface for creating, submitting, monitoring, and evaluating results from Abaqus/Standard and Abaqus/Explicit simulations. It is a unitless software so the dimensions used needs to be coherent. Abaqus/CAE is divided into modules, where each module defines a logical aspect of the modelling process. Moving from module to module, the model is built and Abaqus/CAE generates an input file that is submitted to the Abaqus/Standard or Abaqus/Explicit analysis product. The analysis product performs the analysis, sends information to Abaqus/CAE in order for the job to be monitored by the user and it generates an output database. Finally, the visualization module of Abaqus/CAE can be used to read the output database and view the results of the analysis.

2.6.2. Analysis step

The units used in all the models were millimetres (mm) for length, tonne (t) for mass, newton (N) for force, megapascals (N/mm²) for pressure, millijoules (mJ) for energy, seconds (s) for time, degree Celsius (°C) for temperature and t/mm³ for density. The absolute zero temperature, -237.15 °C, and the Stefan-Boltzmann constant, $5.67 \cdot 10^{-11}$ mW/mm² K⁴, were introduced in the model attribute of each analysis. The fire analysis made with Abaqus is a sequentially coupled heat transfer analysis since the elevated temperature generated in the structure due to fire effects has a strong influence on the mechanical behaviour of the structure while the mechanical behaviour of the structural elements does not really influences the thermal response. This analysis is performed by first conducting an uncoupled heat transfer analysis and then a stress/deformation analysis.

2.6.2.1. Local analysis on roofing elements

The analysis of the structure started with a local analysis on the roofing elements, made of metal sheet which recovers the structure, in order to observed its behaviour when affected

by fire. The metal sheet in question is ribbed sheet aluminium 7/10th and it relies on steel purlins. To analyse an element on Abaqus/CAE, the first step consists to create a part representing the element (aluminium sheet and purlin). The different parts created for this analysis in this work are 3D deformable solid elements and they are shown in figure 2.13 and figure 2.14.

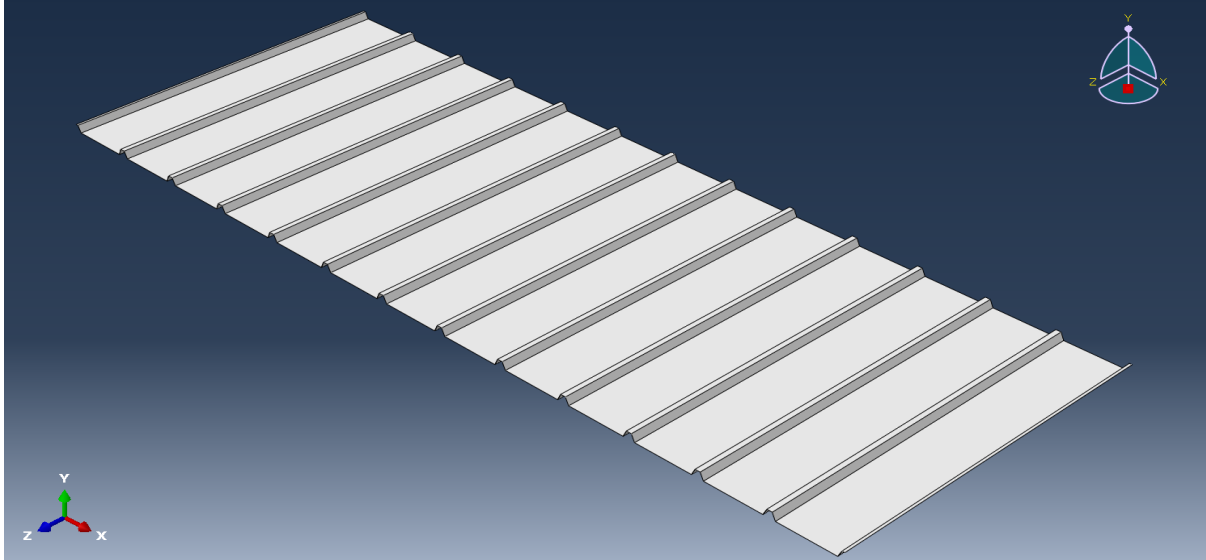


Figure 2.13. Modelling of aluminium sheet

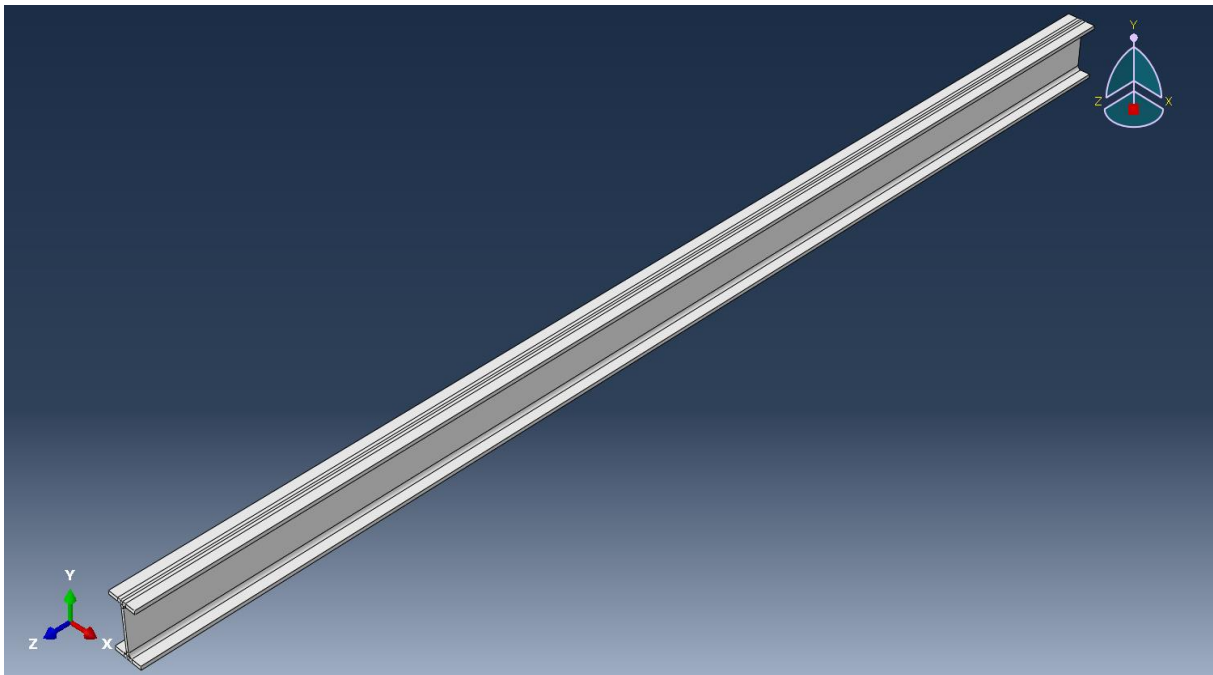


Figure 2.14. Modelling of purlin IPE80

The second step consists to define materials properties of the different part created. Aluminium zinc is the material used for the roofing, its density is $2.70 \cdot 10^{-9} \text{ t/mm}^3$, coefficient of linear thermal expansion is $23 \cdot 10^{-5} \text{ }^\circ\text{C}^{-1}$ and its other properties are shown from table 2.3 to table 2.5.

Table 2.3. Elastic properties of aluminium zinc (EN 1999-1-2)

Young's modulus	Poisson's ratio	Temperature
70000	0.3	20
69300	0.3	50
67900	0.3	100
65100	0.3	150
60200	0.3	200
54600	0.3	250
47600	0.3	300
37800	0.3	350
2800	0.3	400
0.1	0.3	550

Table 2.4. Plastic properties of aluminium zinc

Yield stress	Plastic strain	Temperature
205.6003571	0	20
280.56	0.002	20
185.0013292	0	100
252.504	0.002	100
154.1131192	0	150
210.42	0.002	150
102.6745224	0	200
140.28	0.002	200
47.19071653	0	250
64.5288	0.002	250
22.56068283	0	300
30.8616	0.002	300
12.30400238	0	350
16.8336	0.002	350
0.11	0	550
0.2002	0.002	550

Table 2.5. Thermal properties of aluminium zinc (EN 1999-1-2)

Conductivity	Specific heat	Temperature
140	903000000	0
145	923500000	50
150	944000000	100
155	964500000	150
160	985000000	200
165	1005500000	250
170	1026000000	300
175	1046500000	350
180	1067000000	400
185	1087500000	450
190	1108000000	500

Concerning the purlin, steel S235 is the material used. Its density is $7.85 \cdot 10^{-9} \text{ t/mm}^3$, coefficient of linear thermal expansion is $12 \cdot 10^{-6} \text{ K}^{-1}$ and its other properties are shown from table 2.6 to table 2.8.

Table 2.6. Elastic properties of steel S235 (EN 1993-1-2)

Young's modulus	Poisson's ratio	Temperature
210000	0.3	20
210000	0.3	100
189000	0.3	200
168000	0.3	300
147000	0.3	400
126000	0.3	500
65100	0.3	600
27300	0.3	700
18900	0.3	800
14175	0.3	900
9450	0.3	1000
4725	0.3	1100
0.1	0.3	1200

Table 2.7. Plastic properties of steel S235 (Ramberg-Osgood)

True stress	Plastic strain	Temperature
235.7329762	0	20
432	0.179207363	20
235.7329762	0.0009984	100
432	0.180205763	100
190.2365118	0.0023184	200
432	0.181525763	200
144.5043144	0.0037184	300
432	0.182925763	300
99.00785	0.0051984	400
432	0.184405763	400
84.86387143	0.0067584	500
336.96	0.185965763	500
42.43193571	0.0083984	600
203.04	0.187605763	600
17.67997321	0.0101184	700
99.36	0.189325763	700
11.78664881	0.011	800
47.52	0.190207363	800
8.839986607	0.0118	900
25.92	0.191007363	900
5.893324405	0.0138	1000
17.28	0.193007363	1000
2.946662202	0.0158	1100
8.64	0.197007363	1100
0.1	0.197007363	1200

Table 2.8. Thermal properties of steel S235 (EN 1993-1-2)

Conductivity	Specific heat	Temperature
54	439801760	20
53.334	487620000	100
50.67	529760000	200
47.34	564740000	300
44.01	605880000	400
40.68	666500000	500
37.35	760217391.3	600
34.02	1008157895	700
30.69	5000000000	735
27.3	803260869.6	800
27.3	650000000	900
27.3	650000000	1000
27.3	650000000	1100
27.3	650000000	1200

Materials properties are inserted and assigned to each element in the property module. The next module used is the assembly module which is used to assemble the aluminium sheet and the purlin created in the part module are shown in figure 2.15.

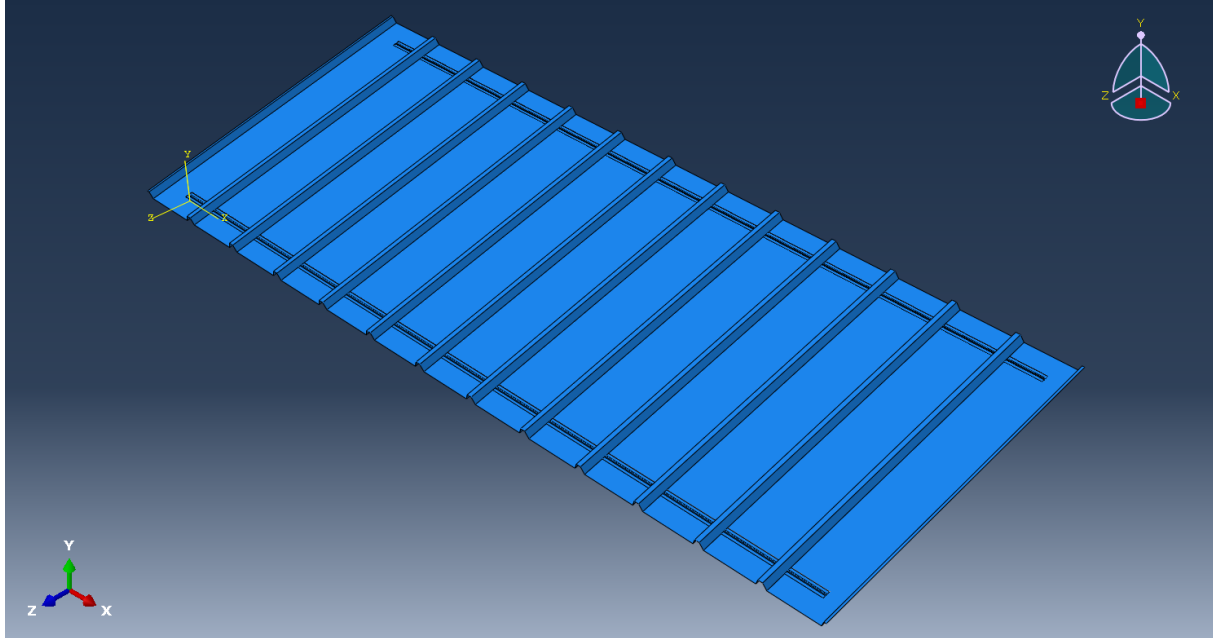


Figure 2.15. Assembly model of the roofing elements

Then, the next module used is the interaction module which is used to create the interaction between the parts created. For the different parts touching themselves, surface-to-surface contacts were created in which conduction information were attributed. A film interaction property was also created in order to create convection and radiation interaction because of the heat analysis that will be done. The value of the film coefficient used was $0.0025 \text{ mW/mm}^2 \text{ K}$. The amplitude describing convection and radiation is the time history describing the evolution of temperature with time of the standard temperature-time curve given in EN 1991-1-2 (2002) expressed by equation (2.68) and represented by figure 2.16 was applied on the lower part of the roofing elements in order to represent fire burning inside the building.

$$\theta_g(t) = 20 + 345 \cdot \log_{10}(8t + 1) \quad (2.68)$$

Where :

θ_g is the gas temperature [$^{\circ}\text{C}$]; and

t is the time [min].

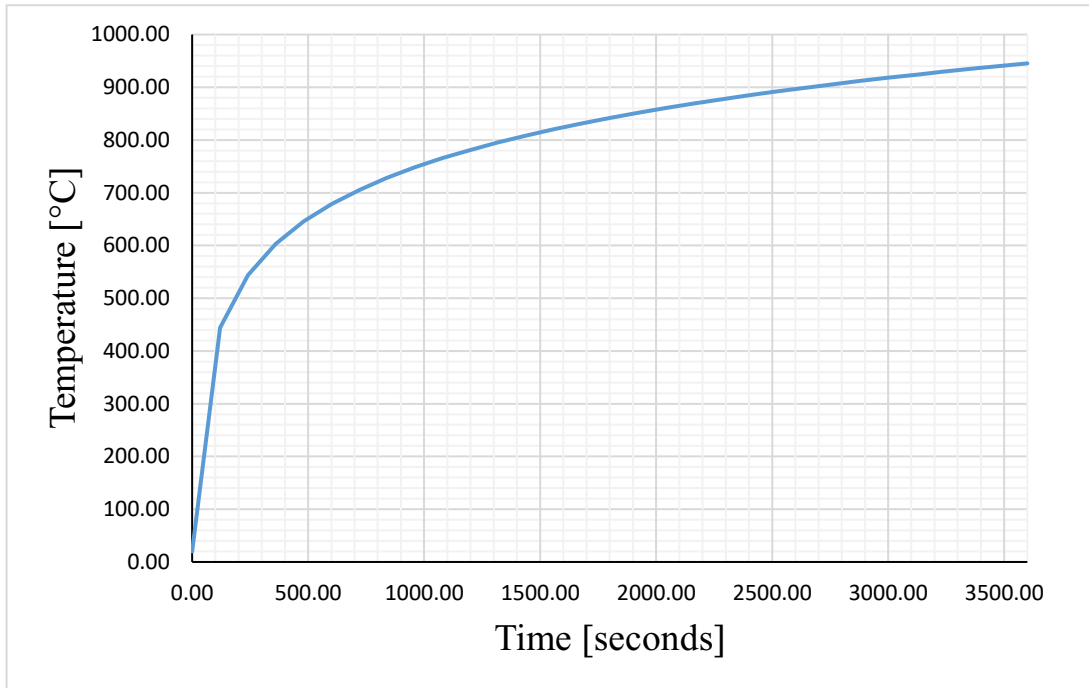


Figure 2.16. Standard nominal temperature curve

Afterwards, a step is created in the step module. Since the analysis is a sequentially coupled heat transfer analysis, the first part of the analysis is done using the heat transfer step with no load applied on the structure but with a predefined temperature load that gives the structure an initial temperature of 20 °C and well defined boundary conditions in the load module as illustrated in figure 2.17. This boundary conditions consisted of pinned connections at the level of the purlins.

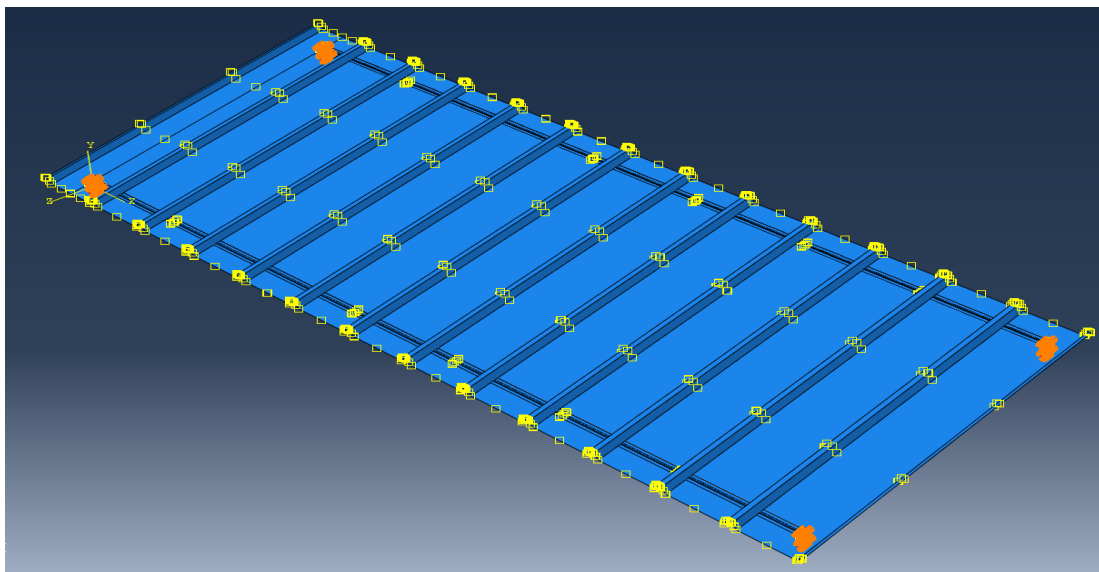


Figure 2.17. Predefined ambient temperature and boundary conditions on the roof

Afterwards, the different part of the structure are meshed, assigned heat transfer as element mesh type in function of the step used and verified that there is no meshing error in the mesh module. At the end of this first part, a job is created and the thermal results are gotten.

After having the results of the thermal analysis, the previous model is copied and some modifications are done in other to analyse the mechanical behaviour of the model after the thermal impact. The modifications consist of replacing the heat transfer step into a general static step, applying the gravity loads of the various elements and a pressure load of 0.00061 N/mm^2 representing the variable loads present on the roof on the top of the aluminium zinc panel, importing the result of the previous thermal analysis as a new predefined load on the structure, assigning 3D Stress as the mesh element type in function of the step and then running a newly created job.

Due to the fact that the aluminium sheet used for roofing is a non-structural elements and that it doesn't affects the other structural elements, a global analysis of the structure is made without modelling it but by taking into consideration all the structural elements present in the building.

2.6.2.2. Global analysis on structural elements

To globally analyse the structure, it has to be modelled and then analysed using the required steps, loads, boundary conditions and mesh type. To model the structural elements, the first step consists to create the different part of the buildings (columns, rafters, purlins, vertical bracing and horizontal bracings). The created model represents only the macro parts of the building and these different parts are 3D deformable shell elements with their respective thicknesses. The second step consists to define materials property in the property module. Steel S235 is the material used in the structure, its density is $7.85 \cdot 10^{-9} \text{ t/mm}^3$, expansion coefficient is $12 \cdot 10^{-6} \text{ K}^{-1}$ and its other properties are shown from table 2.8 to table 2.10. Materials properties are inserted and assigned in function of each element in the property module. The next module used is the assembly module which is used to assemble all the parts created in the part module. Only part of the structure was assembled in order to ease computation and since the building is symmetrical. The assembly model can be seen in the figure 2.18.

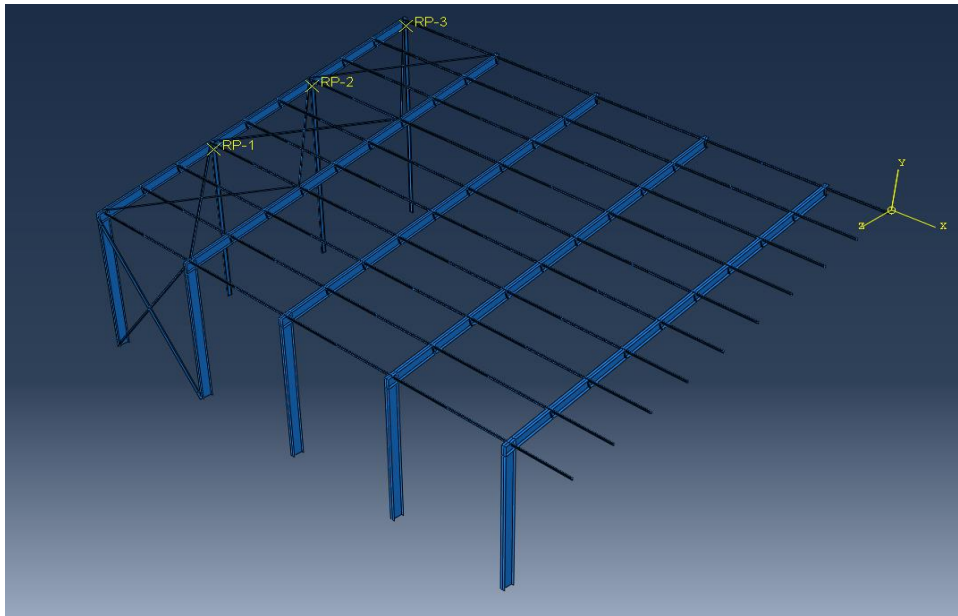


Figure 2.18. Assembly model of the building

Element assembled, the next module used is the interaction module where interactions are created between the existing parts. For the different parts touching themselves, a surface-to-surface contact was created in which conduction information were attributed. A film interaction property was created in order to create convection and radiation interaction due to heat analysis that will be done. The value of the film coefficient used was $0.0025 \text{ mW/mm}^2 \text{ K}$. The amplitude describing convection and radiation is the time history of the standard temperature-time curve given in EN 1991-1-2 (2002) expressed by equation (2.68) and represented by figure 2.16. This curve was applied on all the inner surface of the building.

Afterwards, a step is created in the step module. Since the analysis is a sequentially coupled heat transfer analysis, the first part of the analysis is done using the heat transfer step with no load applied on the structure but with a predefined temperature load that gives the structure an initial temperature of $20 \text{ }^\circ\text{C}$ and well defined boundary conditions. This boundary conditions consisted of pinned connections at the base of each column, XSYMM and ZSYMM as illustrated in figure 2.19. Later, the different part of the structure are meshed, assigned adequate element type in function of the step used and verified that there is no meshing error in the mesh module. At the end of this first part, a job is created and the thermal results are gotten.

The previous model is copied and some modifications are done in order to analyse the mechanical behaviour of the structure after the thermal impact. The modifications consist of replacing the heat transfer step into a general static step, applying the different present loads, importing the results of the previous thermal analysis as a new predefined load on the structure,

assigning the adequate mesh element type in function of the step and then running a newly created job. The different loads applied on the structure as illustrated in figure 2.19 are gravity loads on the whole structure, pressure loads of 0.00605 N/mm^2 for the external purlins, 0.0121 N/mm^2 for the internal purlins, 0.0047 N/mm^2 for the external column and 0.0095 N/mm^2 for the internal columns.

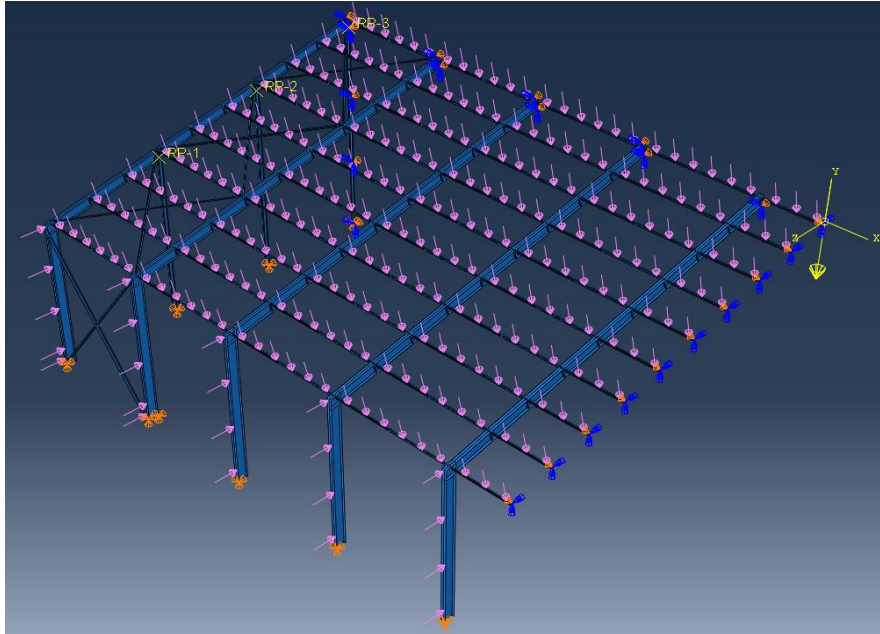


Figure 2.19. Loading and boundary conditions on the building

2.6.2.3. Local analysis on structural elements

To analyse an element, the first step is to create a part representing the structural element (purlin and column). The different parts created for the local analysis in this work are 3D deformable solid elements and they are shown in figure 2.20.

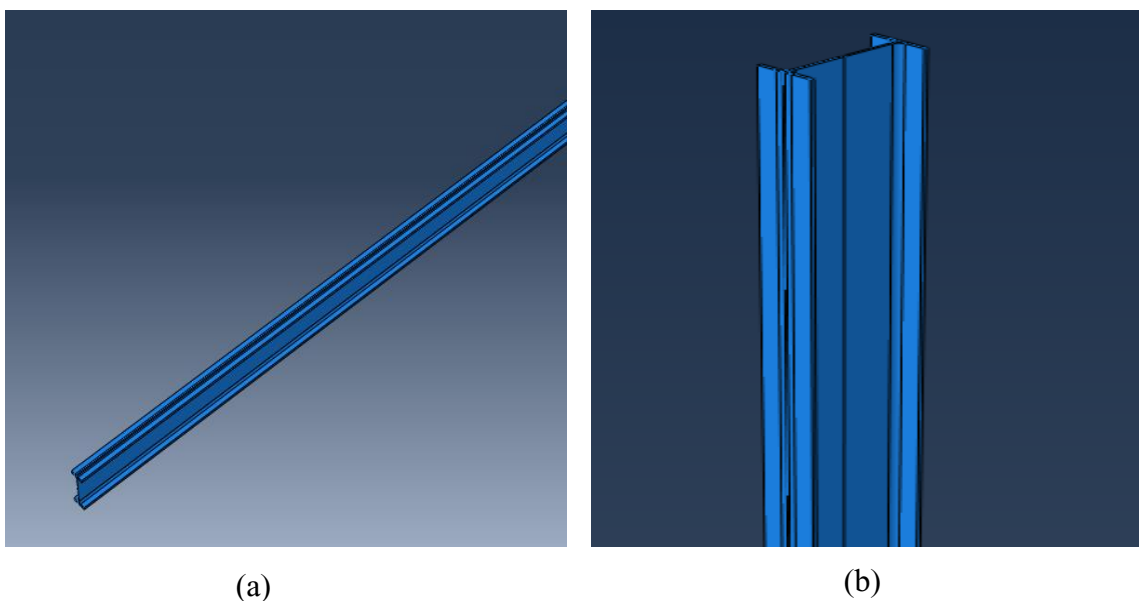


Figure 2.20. Modelling of (a) purlin IPE80 and (b) column IPE400

It is supposed that the connections have less utilisation factor than the adjacent members under fire condition, like any steel elements, due to the rapid increase of the temperature, the strength of the connection reduces, but there is something particular with the connections. Because of the added materials (plate and bolts), the quantity of material per unit of volume at the connections is greater than along the linked members, which means that the temperature at the connection increase slowly than the temperature inside the adjacent members; consequently, the strength of the connections decrease slowly compared to the strength of the elements. Therefore, in this work, the connection were not considered because according to clause 4.2.1(6) of BS EN 1993-1-2 the fire resistance of the joints may be assumed sufficient.

Steel S235 is the material used in the structure, its density is $7.85 \cdot 10^{-9} \text{ t/mm}^3$, expansion coefficient is $12 \cdot 10^{-6} \text{ K}^{-1}$ and its other properties are shown from table 2.8 to table 2.10. The second step consists to define materials property which can be elastic, plastic and thermal. The materials properties are inserted and assigned in function of each element in the property module. The next module is the assembly module which is only used to create the instance of the element and rotate it if necessary.

Then, the next step is done in the interaction module where a film interaction property is created in order to link convection and radiation interaction to it because a heat analysis will be done. The value of the film coefficient used was $0.0025 \text{ mW/mm}^2 \text{ K}$. The amplitude describing convection and radiation is the time history describing the evolution of temperature with time for one hour of the standard temperature-time curve given in EN 1991-1-2 (2002) expressed by equation (2.68) and represented by figure 2.16. These interactions were applied on one face (bottom flange) of the purlin and on three faces (inside flange and two halves of the web sides) of the column as shown in figure 2.21. Fire was applied in that way because half of the web was protected by masonry blocks, so only half of the other parts of the web were in direct contact with thermal load.

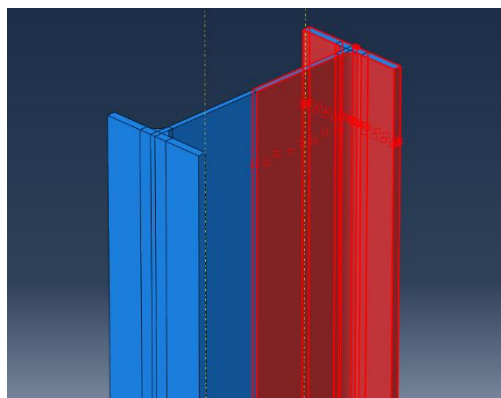


Figure 2.21. Faces of the IPE400 column where fire was applied

Afterwards, a step is created in the step module. Since it is a fire analysis, the first part of it is done using the heat transfer step with no load applied on the element but with a predefined temperature load that gives the structure an initial temperature of 20 °C and well defined boundary conditions. Pinned connections are used at the ends of the purlins and at the base of the column. Then the created part is meshed, assigned adequate element type in function of the step used and verified that there is no meshing error in the mesh module. At the end of this first part a job is created and the thermal results are gotten.

The previous model is copied and some modifications are done in other to analyse the mechanical behaviour of the structure after the thermal impact. The modifications consist of replacing the heat transfer step into a general static step, applying the different present loads, importing the result of the previous thermal analysis as a new predefined load on the structure, assigning the adequate mesh element type in function of the step and then running a newly creating job. The loads applied to the IPE80 purlin are its self-weight and a pressure load of 0.012N/mm² applied on the top flange, while the loads applied on the IPE400 column are its self-weight, a vertical pressure load of 10.13 N/mm² applied on the top of the column, and a wind pressure load of 0.000343 N/mm² applied on the outside flange.

After the fire analysis of the purlin and column was made, a particular attention was pointed on the column in order to study the effect of high temperature on different type of cross sections that can be used for columns in such buildings. There exist various types of steel cross-sectional shapes in the world but for our study, only two different cross sectional shapes were chosen in order to investigate the effect of fire on them and compare it to the IPE cross section used in the case study. The cross sections chosen are SHS 260/16 and CHS 323.9/14.2. These cross sections with their different characteristics were chosen in order to simulate their used as columns in a similar building as the case study. The IPE columns were replaced by each of these cross sections in the SAP2000 software and the different new columns were statically verified. Afterwards these different new columns were modelised in Abaqus in order to analyse them under similar fire action as the IPE400 column of the case study. The different created part of these various cross sections modelled in Abaqus/CAE showing the places where thermal loads are applied are illustrated in figure 2.22 and figure 2.23.

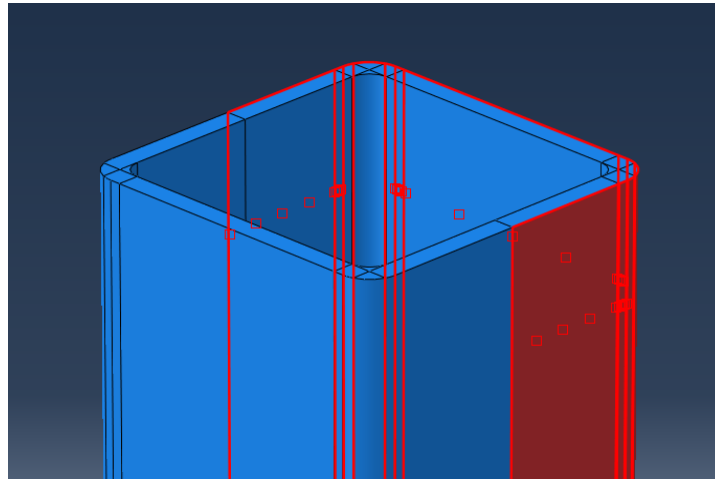


Figure 2.22. Faces of the SHS 260/16 column where fire was applied

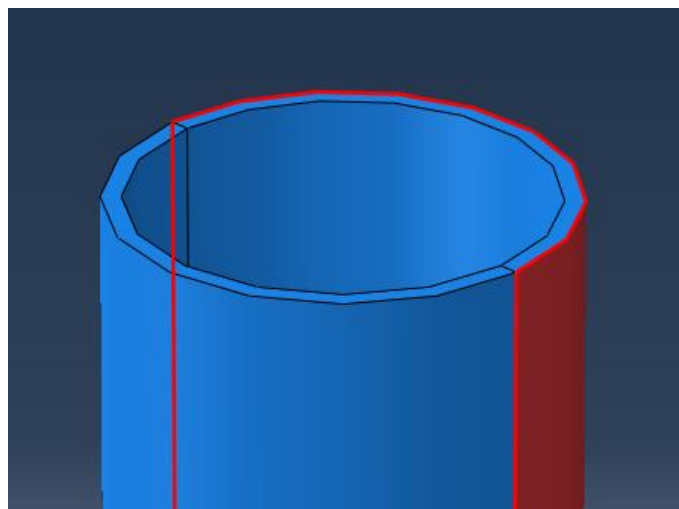


Figure 2.23. Faces of the CHS 323.9/14.2 column where fire was applied

After the heat transfer analysis made on those new cross section columns, a stress analysis was made with loads applied on the them. The loads applied on the SHS 260/16 column are its self-weight, a vertical pressure load of 5.94 N/mm^2 applied on the top of the column, and a wind pressure load of 0.000343 N/mm^2 applied on the outside flange while the loads applied on the CHS 323.9/14.2 column are its self-weight, a vertical pressure load of 6.51 N/mm^2 applied on the top of the column, and a wind pressure load of 0.000343 N/mm^2 applied on the outside flange.

2.7. Analysis of two fire protective systems

After studied the impact of fire on the structural elements of the case study, analysis will be made on the use of timber and concrete as protective materials for steel columns. The aim is to evaluate and compare timber material and concrete as passive fire protection for steel elements.

2.7.1. Hybrid steel-timber elements

This study evaluates the possibility to use timber members as a complete or partial fire protection for steel columns and it focuses on the thermal performances of steel-timber cross-sections to obtain the evolution of temperature on steel element during fire exposure. The hybrid elements considered are composed by I-shaped steel profiles partially or fully encased into timber members. The thermal behaviour is analysed by using numerical simulation in Abaqus. The timber used in this study is Iroko which density is $6.50 \cdot 10^{-10} \text{ t/mm}^3$ at ambient temperature and its properties in function of temperature are presented in table 2.9 and table 2.10.

Table 2.9. Density of timber (EN 1995-1-2)

Density	Temperature
$6.50 \cdot 10^{-10}$	20
$6.50 \cdot 10^{-10}$	100
$6.50 \cdot 10^{-10}$	200
$4.55 \cdot 10^{-10}$	300
$2.60 \cdot 10^{-10}$	400
$1.95 \cdot 10^{-10}$	500
$1.63 \cdot 10^{-10}$	600
$1.46 \cdot 10^{-10}$	700
$1.37 \cdot 10^{-10}$	800
$1.30 \cdot 10^{-10}$	900
$9.75 \cdot 10^{-11}$	1000
$6.50 \cdot 10^{-11}$	1100
$6.50 \cdot 10^{-11}$	1200

Table 2.10. Thermal properties of timber (EN 1995-1-2)

Conductivity	Specific heat	Temperature
0.12	1530000000	20
0.14	1770000000	100
0.15	2000000000	200
0.1	710000000	300
0.08	1000000000	400
0.09	1200000000	500
0.18	1400000000	600
0.25	1525000000	700
0.35	1650000000	800
0.45	1650000000	900
0.55	1650000000	1000
1	1650000000	1100
1.5	1650000000	1200

The partially protected steel-wood member is modelled as shown in figure 2.24 and the application of the thermal loads on it are illustrated in figure 2.25.

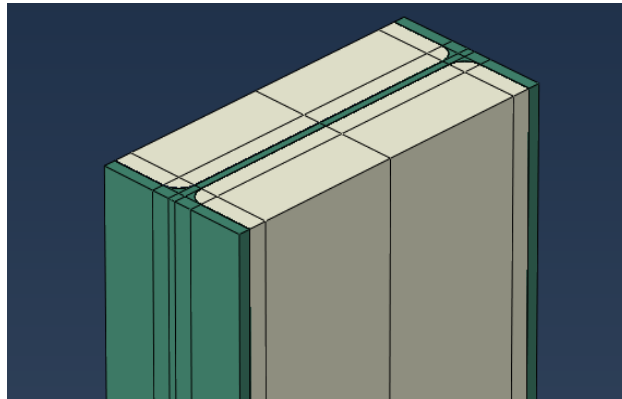


Figure 2.24. Partial hybrid steel-timber column

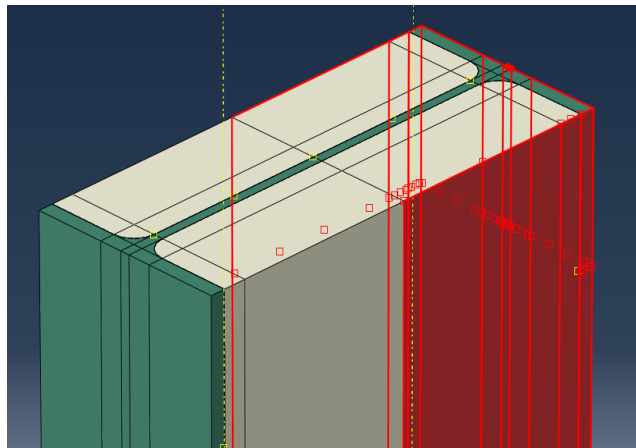


Figure 2.25. Faces of the partial hybrid steel-timber column where fire was applied

On the other side, the totally protected steel-wood member is modelled as shown in figure 2.26 and the application of the thermal loads are illustrated in figure 2.27. The dimensions of the protection are 43 cm for the height and 21 cm for the base of the section.

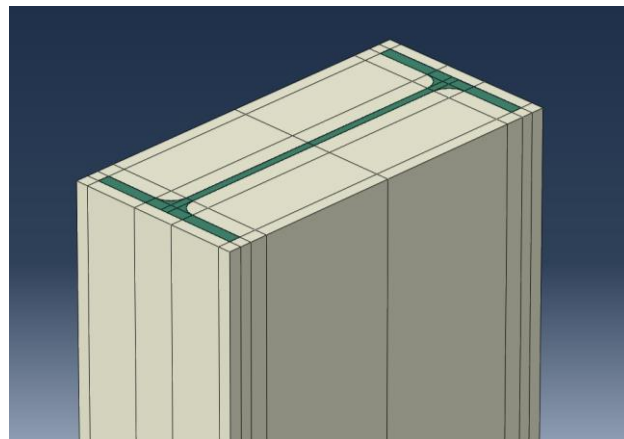


Figure 2.26. Totally protected steel-timber column

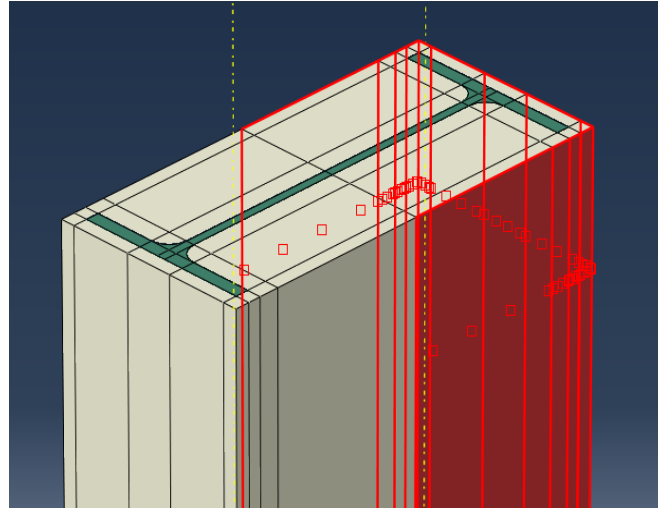


Figure 2.27. Faces of the total hybrid steel-timber column where fire was applied

2.7.2. Hybrid steel-concrete elements

This study evaluates the possibility to use concrete as a complete or partial fire protection for steel columns and it focuses on the thermal performances of steel-concrete cross-sections to obtain the evolution of temperature on steel element during fire exposure. The hybrid elements considered are composed by I-shaped steel profiles partially or fully encased in concrete. The thermal behaviour is analysed by using numerical simulation in Abaqus. The concrete used in this study is C25/30 which density is $2.40 \cdot 10^{-9} \text{ t/mm}^3$ and its other properties are presented in table 2.11.

Table 2.11. Thermal properties of concrete (EN 1992-1-2)

Conductivity	Specific heat	Temperature
1.333028	900000000	20
1.2297	900000000	100
1.1108	1000000000	200
1.0033	1050000000	300
0.9072	1100000000	400
0.8225	1100000000	500
0.7492	1100000000	600
0.6873	1100000000	700
0.6368	1100000000	800
0.5977	1100000000	900
0.57	1100000000	1000
0.5537	1100000000	1100
0.5488	1100000000	1200

The partially protected steel-concrete member is modelled as shown in figure 2.28 while the totally protected steel-concrete member is modelled as shown in figure 2.29 and the application of thermal loads on these different elements are done in the same manner as for timber elements as illustrated in figure 2.25 and 2.27.

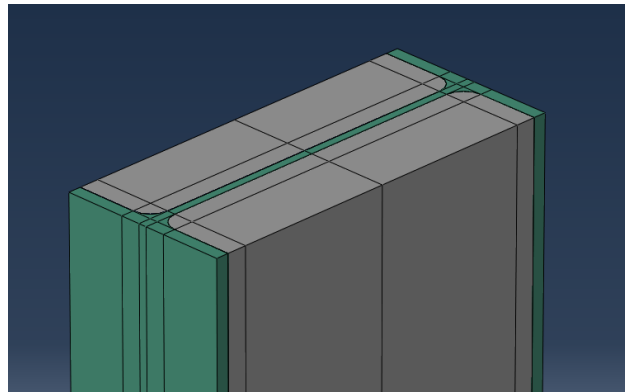


Figure 2.28. Partially protected steel-concrete column

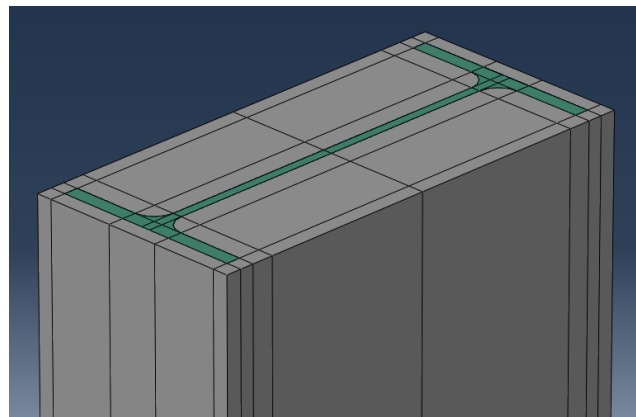


Figure 2.29. Totally protected steel-concrete column

Conclusion

This chapter was aimed on the presentation of the procedure that was followed to make this study. To summarise it, the chapter started by establishing the procedure of collecting data from the field, talked about the codes used in this study, the different loads and load combinations that will be used in the structural verification of the case study and presented the different analysis tools that were used for the work. After that, the different analysis steps made using those tools in order to statically verify the structure, analyse the behaviour of steel under fire impact and even analyse the two different fire protective materials that can be used in order to propose a protective system against such thermal impact were presented. The next chapter will show the results gotten from the design verifications, from the fire analyses of the members of the case study and the hybrid members.

CHAPTER 3 : RESULTS AND INTERPRETATIONS

Introduction

This third chapter presents the results of the procedure described in chapter two. It consists in presenting the results of the research on the site where the case study is found, the data collected and the results of the static verification of the elements of the structure. Afterwards, it presents the results of the fire analyses on the different elements of the case study, on the different column cross sections that were used in comparism with the IPE column of the case study and on the hybrid members proposed as fire protective elements.

3.1. General presentation of the site

The case study is found in the economical capital of Cameroon named Douala. In this section, a general presentation of Douala will be done, showing its physical and socio-economical parameters.

3.1.1. Physical parameters

Douala is physically presented in this section by its geographical location, climate, and hydrology.

3.1.1.1. Location

The city of Douala which coordinates are $4^{\circ} 3' 41.5296''$ N and $9^{\circ} 47' 9.8592''$ E, is found in the Littoral region of the country. The case study is located at Tractafric, in the industrial zone of the Bassa district situated in the city of Douala as shown in figure 3.1



Figure 3.1. Map of Douala showing the location of the case study (Google maps)

3.1.1.2. Climate

Douala features a tropical monsoon climate, with relatively consistent temperatures throughout the course of the year, though the city experiences somewhat cooler temperatures in July and August. Douala typically features warm and humid conditions with an average annual temperature of 27.0 °C and an average humidity of 83%. Douala sees quite plentiful rainfall during the course of the year, experiencing on average roughly 3600 mm of precipitation per year. Its driest month is December, when on average 28 mm of precipitation falls, while its wettest month is August, when on average nearly 700 mm of rain falls. These data can be gotten in Douala from the weather measuring station or from the airport.

3.1.1.3. Hydrology

The coastal city, Douala, found in the southwest of Cameroun is located on the banks of the Wouri river, whose two sides are linked by the Bonaberi Bridge. The Douala basin is predominantly an offshore basin extending from the Cameroon volcanic line in the north to the Corisco arch in the south near the Equatorial Guinea-Gabon border. The basin lies wholly within the territorial borders of Cameroon and Equatorial Guinea.

3.1.2. Socio-economical parameters

The socio-economical parameters that characterise Douala described in this section include population, transport and economic activities carried out there.

3.1.2.1. Population

Douala's 2021 population is now estimated at 3 793 363 while in 1950, the population of Douala was 94 769. Douala has grown by 130 136 since 2015, which represents a 3.55% annual change. These population estimates and projections come from the latest revision of the UN World Urbanization Prospects. These estimates represent the urban agglomeration of Douala, which typically includes Douala's population in addition to adjacent suburban areas.

3.1.2.2. Economy

Douala is a city with a modest oil resource in Africa, but is in good agricultural condition, therefore it has one of best economies in Africa. However, it also faces some problems like other underdeveloped countries such as heavy civil service and bad climate (flood and storm) to business.

Even though Douala is the economic centre of Cameroon, a large percentage of its inhabitants live below the poverty line. Recent data shows that about thirty percent of the population lives in poverty. While the aforementioned percentage is doubled for rural regions,

poverty is a growing problem for Douala due to its steadily increasing population. Unlike the rural populations of Cameroon that can grow their own foods to lessen their expenses, Douala locals are disadvantaged by living in the port city where there are not many opportunities for monetary gain.

3.1.2.3. Transport

Douala contains many transportation options like no other cities in Cameroon. Douala is linked by rail to Yaoundé, Ngaoundéré, Kumba and Nkongsamba. It has a fairly developed road network compared to other cities in the country where the population can be transported by means of cars, buses and mottos-taxis. Efforts have recently been made to renovate the city's roads, especially in the most deprived neighbourhoods but they mainly remain in deplorable state. Douala also contains an airport which is located in the eastern part of the city. Douala International Airport have direct flights to several American cities, European cities, and continental destinations like Lomé, Abidjan, Johannesburg, Kinshasa, Lagos, and other ones. The airport is the busiest in the CEMAC area and is the hub for Cameroon's national carrier, CamairCo. Another transportation option is by the sea and its seaport has 8.5 m of draft.

3.2. Physical description of the site

The case study is located at Tractafric, in the industrial zone of the Bassa district situated in the 3rd district of Douala, which has been ravaged by flames as shown in figure 3.2. The industrial zone of Bassa contains a great percent of the industrial production of the city of Douala with its 89 industrial units and these companies are active in the sectors of metal processing, carpentry, painting, printing, water and energy, and more.



Figure 3.2. Panzani's warehouse directly after fire damage

After asking some questions to the people guarding the site during site visit, it was noted that it was around 1: 00 a.m. on the night of Friday 16 to Saturday 17 November 2018 that a fire broke out in the warehouse. The employees who were on duty at the time quickly alerted the fire brigade and the police who rushed to the scene and engaged in a fierce struggle against the flames which were becoming increasingly violent. Although there was no loss of life, there was a lot of material damage.

While visiting the site, it was realised that more than half of the structure had been destroyed by the owners due to all the damages caused by fire as illustrated by figure 3.3.



Figure 3.3. Panzani's warehouse today

3.3. Presentation of the project

The project is a warehouse of the Panzani company which served as a storage of ready-to-eat products and at the same time as a central distribution point to the various product flow poles. The store was built on an area of approximately 2000 m². The interior area of the store is 30x45 m² (1350 m²). It is 45 m long, 30 m large and 10 m high.

3.3.1. Presentation of the structural data

The project is a metal-framed store, with masonry blocks and covered with a ribbed sheet roof. Figure 3.4 materialises the building, specifies its boundaries and the external environment while on the other hand figure 3.5 shows the floor plan of the disposition of the columns in the structure.

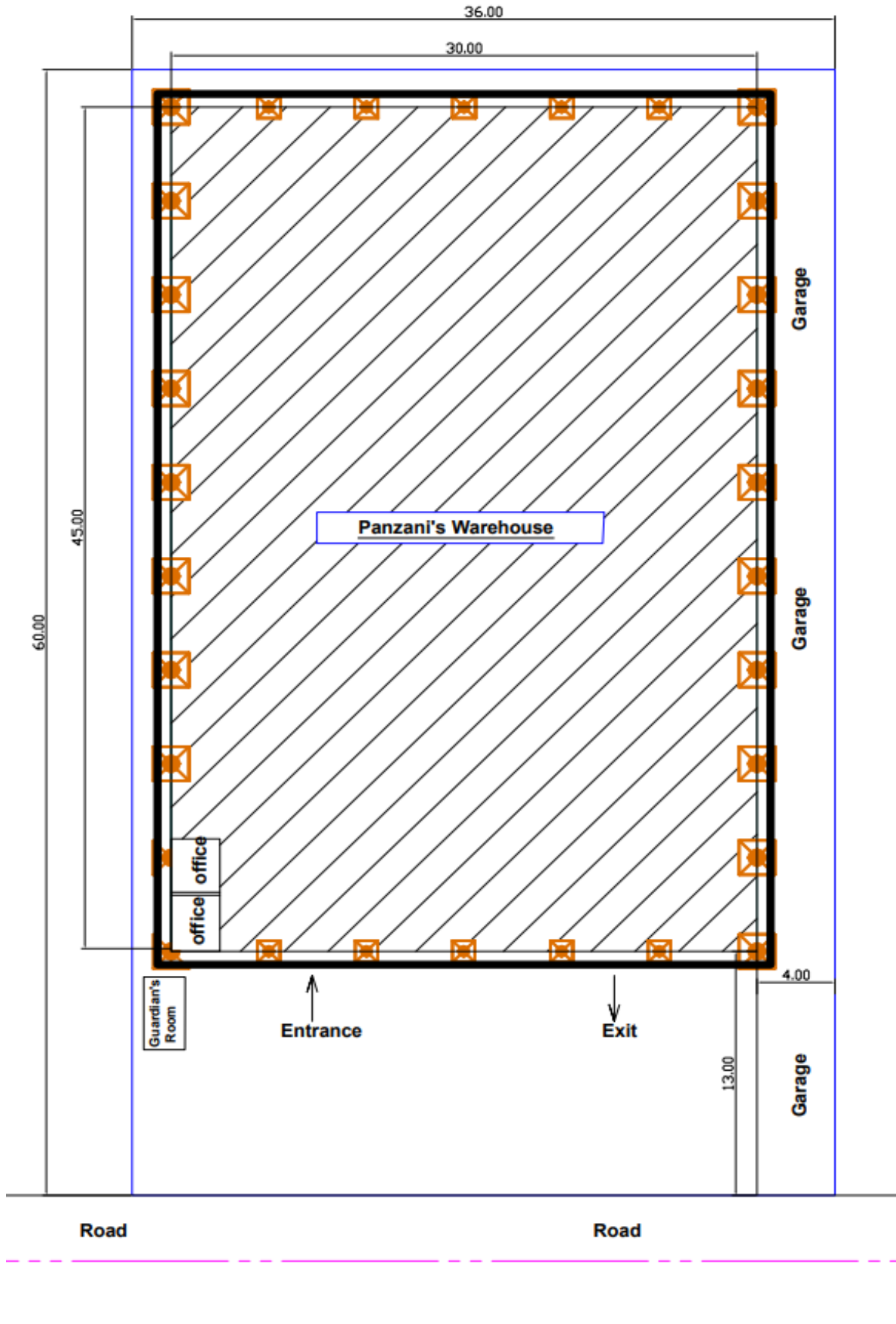


Figure 3.4. Site plan showing the store

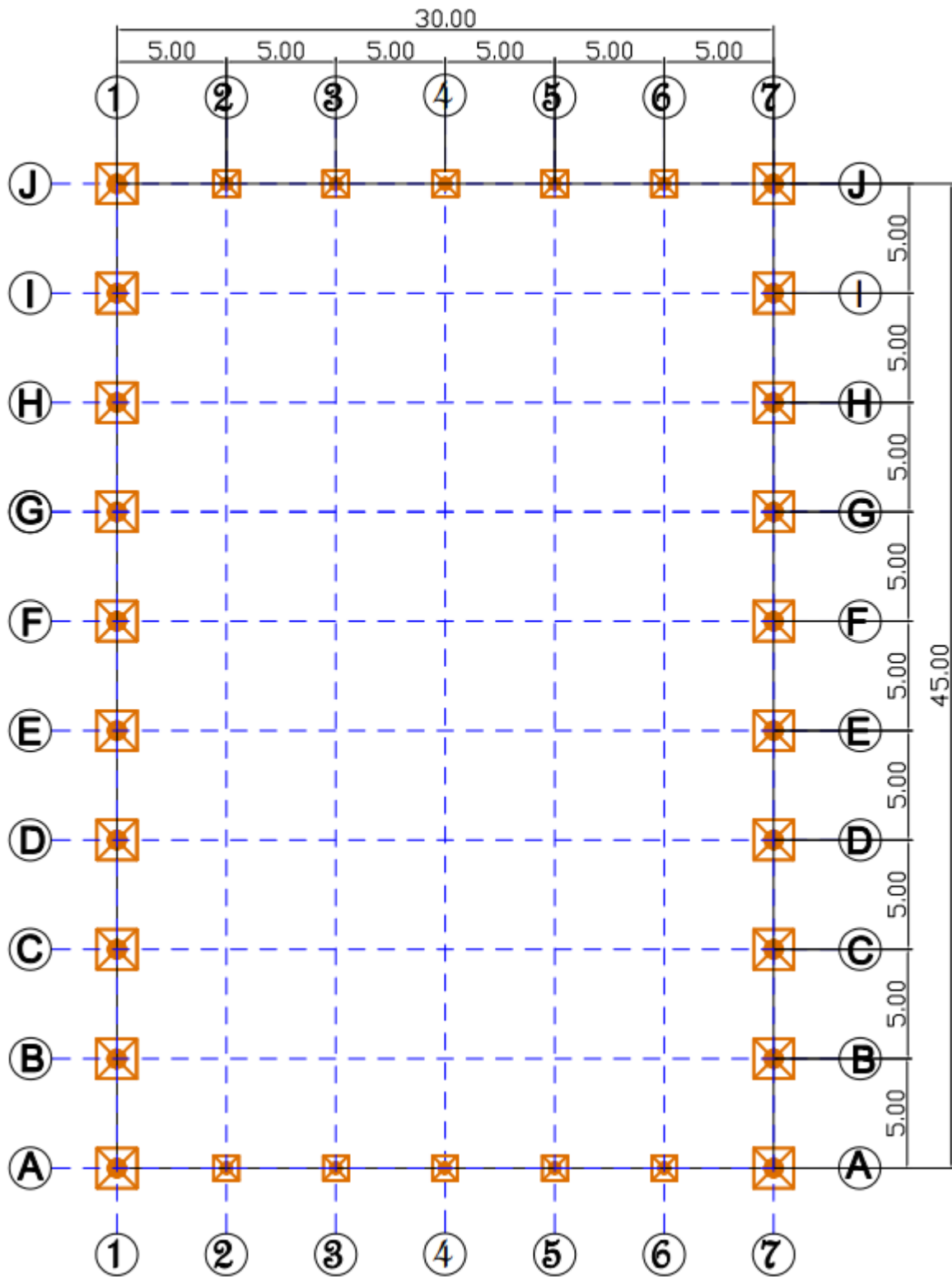


Figure 3.5. Floor plan of the store

The building consists of the following elements, from the foundation to the roof:

- Pad footing made of reinforced concrete for the foundation;
- An unarmred concrete paving;
- Ten portal frames of 5 m separating each of them. Each frame includes two IPE400 profile column of 6.50 m in height separated from each other by 30 m; two IPE400 rafter beams forming a half-range punch; and haunches at the rafter to column and rafter to rafter connection;
- IPE160 profiles for column on the front and back faces;
- 15x20x40 masonry block walls with 6.00 m height plastered from the outside only, stiffened by horizontal chains in reinforced concrete;
- IPE80 profile for purlins spaced 2.00 m apart;
- A ribbed sheet 7/10th aluminium cover;
- Angle bracing of 80x80x8 mm at the level of the columns (vertical direction) and 50x50x5 mm at the level of the purlins (horizontal bracing);
- Inside the store, there were metal shelves 6.0 m in high.

3.3.2. Characteristics of the materials

The structure is made of two main material, steel grade S235 as presented in table 3.1 for the structural elements and concrete C25/30 for the footing as illustrated in table 3.2.

Table 3.1. Steel structural sections material properties

Property	Value	Unit	Definition
Steel grade	S235	-	Gives the steel resistance
f_y	235	N/mm ²	Characteristic yield strength
f_u	360	N/mm ²	Characteristic ultimate strength
E	210 000	N/mm ²	Young modulus
G	80 769.23	N/mm ²	Shear modulus
ν	0.3	-	Poisson's ratio

INFLUENCE OF HIGH TEMPERATURE ON THE STRUCTURAL BEHAVIOUR OF STEEL
STRUCTURES AND SOLUTIONS : CASE OF PANZANI BUILDING

α	$12 \cdot 10^{-6}$	K^{-1}	Coefficient of thermal expansion
γ_{M0}	1	-	Safety factor for resistance whatever the section
γ_{M1}	1	-	Safety factor for resistance of members to instability
γ_{M2}	1.25	-	Safety factor for cross section in tension
f_{yb}	640	N/mm^2	Yield strength of bolt grade
f_{ub}	800	N/mm^2	Ultimate strength of the anchor

Table 3.2. Concrete and reinforcing steel material properties

Property	Value	Unit	Definition
Concrete class	C25/30	-	Concrete class
f_{ck}	25	N/mm^2	Cylindrical crushing strength
f_{ctk}	2.5	N/mm^2	Characteristic tensile strength of concrete
E_{cm}	31 000	N/mm^2	Secant modulus of elasticity of concrete
ϵ_{cu2}	0.35%	-	Ultimate compressive strain of concrete
γ_c	1.5	-	Safety factor for concrete
Reinforcing steel	B450C	-	Reinforcement steel type
f_{yk}	450	N/mm^2	Characteristic yield strength of reinforcing steel
E_s	210 000	N/mm^2	Modulus of elasticity of reinforcing steel
γ_s	1.15	-	Safety factor for steel
Q_{adm}	0.2	N/mm^2	Admissible soil bearing capacity

3.4. Loads determination

The building is meant for storage use, and according to this implies it falls under category E1 as shown in annex 3. The wind loads on the structure was determined using the equations mentioned in section 2.4.3.2, the results are shown in table 3.3.

Table 3.3. Wind load calculations

Wind force determination	
Designation	Value
Basic wind velocity (V_b)	22m/s
Basic velocity pressure (q_b)	0.3025 kN/m ²
Peak velocity pressure (q_p)	0.3025 kN/m ²
Exposure factor	1.133
Pressure coefficient on the windward ($C_{pe} + C_{pi}$)	1
Pressure coefficient on the leeward ($C_{pe} + C_{pi}$)	-0.6
Pressure coefficient on the roof ($C_{pe} + C_{pi}$)	0.6
Wind force per unit area on the windward side (w)	0.34 kN/m ²
Wind force per unit area on the leeward side (w)	-0.21
Wind force per unit area on the roof (w)	0.21 kN/m ²

3.4.1. Vertical loads

The vertical loads on the structure are generated due to the self-weight of the structural elements, self-weight of the roof, imposed load of the roof and the wind load acting on the roof. These loads are presented in table 3.4.

Table 3.4. Vertical loads

Nature	Description	Value	Unit
G_1	Self-weight of structural component	γA	kN/m
G_2	Self-weight of metal roof 7/10th	0.03	kN/m ²
Q_m	Maintenance on the roof	0.4	kN/m ²
$Q_{w(\text{roof})}$	Wind force per unit area on the roof	0.21	kN/m ²

3.4.2. Horizontal loads

The horizontal loads on the structure are generated due the wind loads. The winds loads applied on the structure are presented in table 3.5.

Table 3.5. Horizontal loads

Nature	Description	Value	Unit
Q_{windward}	Wind force per unit area on the windward side	0.34	kN/m ²
Q_{leeward}	Wind force per unit area on the leeward side	-0.21	kN/m ²

3.5. Design verifications of the steel structure

The design verifications of the building are done under the different actions on the building. It consists of obtaining the design solicitations on the members of the structure and the deflections after the model has been created in SAP2000 as shown in figure 3.6. The results of the design verifications will be discussed in this chapter.

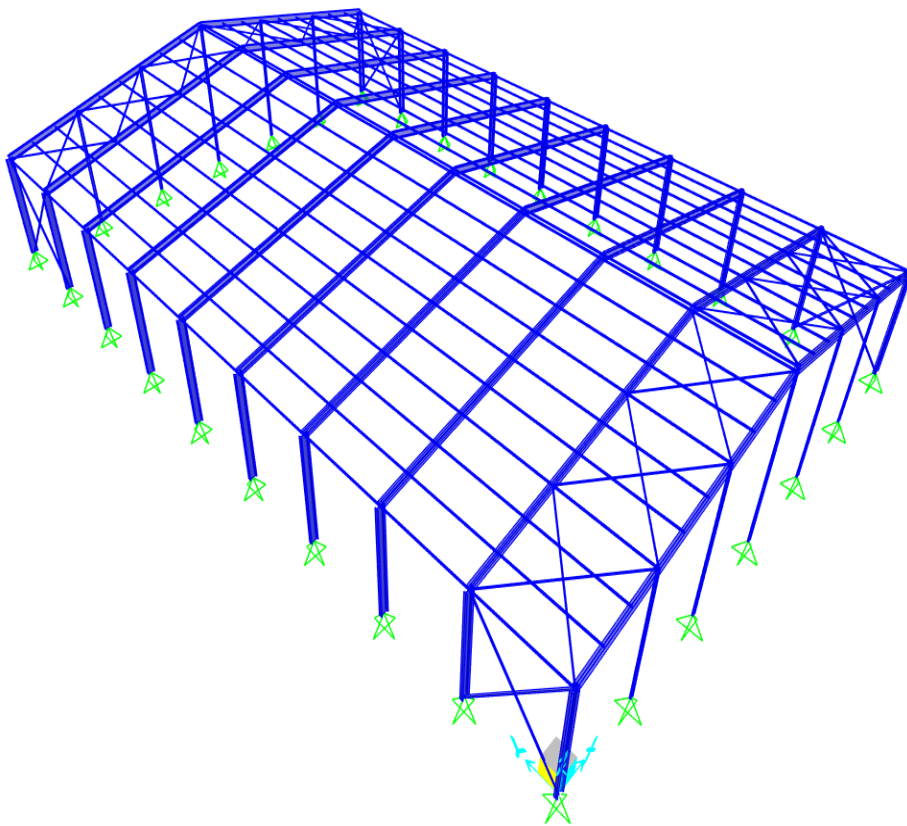


Figure 3.6. Building model from SAP2000

3.5.1. Purlin design verifications

The solicitations gotten from the analysis made on SAP2000 on a purlin are represented in table 3.6.

Table 3.6. Solicitations on the purlin

Solicitations	Value	Units
Bending moment	4.75	kNm
Shear force	3.8	kN

The section of the purlin element under study is IPE80 and its properties are shown in table 3.7.

Table 3.7. Properties of IPE80

	Depth (h)	80 mm
	Width (b)	46 mm
	Web thickness (t_w)	3.8 mm
	Flange thickness (t_f)	5.2 mm
	Root radius (r)	5 mm
	Weight (G)	6.00 kg/m
	Height of web (h_w)	59.6 mm
	Area (A)	764 mm ²
	Shear area z-z ($A_{v,z}$)	358 mm ²
	Moment of inertia (I_y)	801400 mm ⁴
	Radius of gyration (i_y)	32.4 mm
	Plastic section modulus ($W_{pl,y}$)	23.22*10 ³ mm ³
	Moment of inertia (I_z)	0.08489*10 ⁶ mm ⁴
	Radius of gyration (i_z)	10.5 mm
Plastic section modulus ($W_{pl,z}$)	5818 mm ³	

Firstly, the section needs to be classified as shown in table 3.8 and then the design verifications are presented in table 3.9.

Table 3.8. Classification of the purlin cross section

Designation	Verification	Value	Observation
Web in bending	$\frac{c}{t_w} \leq 72\varepsilon$	$15.7 \leq 72$	Class 1
Flange in compression	$\frac{c_f}{t_f} \leq 9\varepsilon$	$3.096 \leq 9$	Class 1

Table 3.9. Design verifications of the purlin

Designation	Verification	Value	Observation
Resistance in bending	$M_{c,Rd} \geq M_{Ed}$	5.46kNm > 4.75kNm	Verified
Resistance in shear	$V_{pl,Rd} \geq V_{Ed}$	48.48kN > 3.80 kN	Verified
Shear instability	$\frac{h_w}{t_w} < 72 \frac{\epsilon}{\eta}$	18.32 < 60	Shear instability is not required
Moment and shear interaction	$0.5V_{pl,Rd} \geq V_{Ed}$	24.24kN > 3.80kN	No bending moment reduction
Lateral torsional buckling	$M_{b,Rd} \geq M_{Ed}$	4.91kNm > 4.75kNm	Verified
Deflection check (SLS)	$f_{max} < \frac{L}{200}$	3.4mm < 20 mm	Verified

3.5.2. Rafter design verifications

The solicitations gotten from the analysis made on SAP2000 on a rafter are represented in table 3.10.

Table 3.10. Solicitations on the rafter

Solicitations	Value	Units
Maximum positive bending moment	152.37	kNm
Maximum negative bending moment	279.34	kNm
Shear force	63.48	kN
Axial force	63.69	kN

The section of the rafter element under study is IPE400 and its properties are shown in table 3.11.

Table 3.11. Properties of IPE400

	Depth (h)	400 mm
	Width (b)	180 mm
	Web thickness (t_w)	8.6 mm
	Flange thickness (t_f)	13.5 mm
	Root radius (r)	21 mm
	Weight (G)	66.3 kg/m
	Height of web (h_w)	331 mm
	Area (A)	8450 mm ²
	Shear area z-z ($A_{v,z}$)	4269 mm ²
	Moment of inertia (I_y)	231.3*10 ⁶ mm ⁴
	Radius of gyration (i_y)	165.5 mm
	Plastic section modulus ($W_{pl,y}$)	1307*10 ³ mm ³
	Moment of inertia (I_z)	13.18*10 ⁶ mm ⁴
	Radius of gyration (i_z)	39.5 mm
Plastic section modulus ($W_{pl,z}$)	229.0*10 ³ mm ³	

INFLUENCE OF HIGH TEMPERATURE ON THE STRUCTURAL BEHAVIOUR OF STEEL
STRUCTURES AND SOLUTIONS : CASE OF PANZANI BUILDING

Firstly, the section is classified as shown in table 3.12 and then the design verifications are presented in table 3.13.

Table 3.12. Classification of the rafter cross section

Designation	Verification	Value	Observation
Web subjected to bending and compression	$\frac{c}{t} \leq \frac{36\varepsilon}{\alpha}$	$38.49 \leq 72$	Class 1
Flange in compression	$\frac{c_f}{t_f} \leq 9\varepsilon$	$3.096 \leq 9$	Class 1

Table 3.13. Design verifications of the rafter

Designation	Verification	Value	Observation
Resistance in bending	$M_{c,Rd} \geq M_{Ed}$	$307.15 \text{ kNm} > 152.37 \text{ kNm}$	Verified
Resistance in shear	$V_{pl,Rd} \geq V_{Ed}$	$579.22 \text{ kN} > 63.48 \text{ kN}$	Verified
Shear instability	$\frac{h_w}{t_w} < 72 \frac{\varepsilon}{\eta}$	$38.49 < 60$	Shear instability verification is not required
Moment and shear interaction	$0.5V_{pl,Rd} \geq V_{Ed}$	$289.61 \text{ kN} > 63.48 \text{ kN}$	No bending moment reduction
Lateral torsional buckling	$M_{b,Rd} \geq M_{Ed}$	$187.69 \text{ kNm} > 152.37 \text{ kNm}$	Verified
Resistance in axial	$N_{pl,Rd} \geq N_{Ed}$	$1984.81 \text{ kN} > 63.69 \text{ kN}$	Verified
Buckling resistance	$N_{b,Rd} \geq N_{Ed}$	$1746.63 \text{ kN} \geq 63.69 \text{ kN}$	Verified
Axial verifications	$0.25N_{pl,Rd} \geq N_{Ed}$	$496.20 \text{ kN} > 63.69 \text{ kN}$	Axial forces doesn't affect moments
	$\frac{0.5h_w t_w f_y}{\gamma_{M0}} \geq N_{Ed}$	$334.48 \text{ kN} > 63.69 \text{ kN}$	
Moment and axial interaction	$\frac{N_{Ed}}{N_{pl,Rd}} + \frac{M_{Ed}}{M_{pl,Rd}} \leq 1$	$0.50 < 1$	No moment-axial interaction
Deflection check (SLS)	$f_{max} < \frac{L}{200}$	$30.4 \text{ mm} < 77 \text{ mm}$	Verified

The eave haunch found at the connection between the rafter and the column will take care of the negative moment found on the rafter. Its verification will be seen in section 3.5.5.1.

3.5.3. Column design verifications

The IPE400 and IPE160 columns found in the structure will be verified according to sections 3.5.3.1 and 3.5.3.2. The columns were verified taken in account the solicitations of the most loaded column of each set.

3.5.3.1. IPE400

The solicitations gotten from the analysis made on SAP2000 on a column are represented in table 3.14.

Table 3.14. Solicitations on the IPE400 column

Solicitations	Value	Units
Bending moment	152.37	kNm
Shear force	63.48	kN
Axial force	63.69	kN

The section of the column element under study is IPE400 and its properties are shown in table 3.11 and its classification is illustrated in table 3.12. The design verifications are presented in table 3.15.

Table 3.15. Design verifications of the IPE400 column

Designation	Verification	Value	Observation
Resistance in bending	$M_{c,Rd} \geq M_{Ed}$	307.15 kNm > 279.34 kNm	Verified
Resistance in shear	$V_{pl,Rd} \geq V_{Ed}$	579.22 kN > 47.99 kN	Verified
Shear instability	$\frac{h_w}{t_w} < 72 \frac{\epsilon}{\eta}$	38.49 < 60	Shear instability verification is not required
Moment and shear interaction	$0.5V_{pl,Rd} \geq V_{Ed}$	289.61 kN > 47.99 kN	No bending moment reduction
Resistance in axial	$N_{pl,Rd} \geq N_{Ed}$	1984.81 kN > 85.93 kN	Verified
Buckling resistance	$N_{b,Rd} \geq N_{Ed}$	1746.63 kN \geq 85.93 kN	Verified
Axial verifications	$0.25N_{pl,Rd} \geq N_{Ed}$	496.20 kN > 85.93 kN	Axial forces doesn't affect moments
	$\frac{0.5h_w t_w f_y}{\gamma_{M0}} \geq N_{Ed}$	334.48 kN > 85.93 kN	
Moment and axial interaction	$\frac{N_{Ed}}{N_{pl,Rd}} + \frac{M_{Ed}}{M_{pl,Rd}} \leq 1$	0.95 < 1	No moment-axial interaction
Deflection check (SLS)	$u_{max} < \frac{h}{300}$	21 mm < 22 mm	Verified

3.5.3.2. IPE160

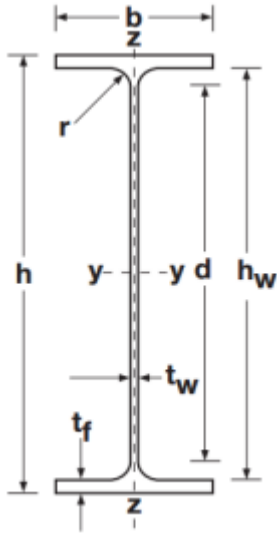
The solicitations gotten from the analysis made on SAP2000 on a column are represented in table 3.16.

Table 3.16. Solicitations on the IPE160 column

Solicitations	Value	Units
Bending moment	16.08	kNm
Shear force	6.43	kN
Axial force	46.70	kN

The section of the column element under study is IPE160 and its properties are shown in table 3.17.

Table 3.17. Properties of IPE160

	Depth (h)	160 mm
	Width (b)	82 mm
	Web thickness (t_w)	5.0 mm
	Flange thickness (t_f)	7.4 mm
	Root radius (r)	9 mm
	Weight (G)	15.8 kg/m
	Height of web (h_w)	127.2 mm
	Area (A)	2009 mm ²
	Shear area z-z ($A_{v,z}$)	966 mm ²
	Moment of inertia (I_y)	8.69*10 ⁶ mm ⁴
	Radius of gyration (i_y)	65.8 mm
	Plastic section modulus ($W_{pl,y}$)	123.9*10 ³ mm ³
	Moment of inertia (I_z)	0.68*10 ⁶ mm ⁴
	Radius of gyration (i_z)	18.4 mm
Plastic section modulus ($W_{pl,z}$)	26.10*10 ³ mm ³	

Firstly, the section is classified as shown in table 3.18 and then the design verifications are presented in table 3.19.

Table 3.18. Classification of the IPE160 column

Designation	Verification	Value	Observation
Web subjected to bending and compression	$\frac{c}{t} \leq \frac{36\varepsilon}{\alpha}$	25.44 ≤ 72	Class 1
Flange in compression	$\frac{c_f}{t_f} \leq 9\varepsilon$	3.99 ≤ 9	Class 1

Table 3.19. Design verifications of the IPE160 column

Designation	Verification	Value	Observation
Resistance in bending	$M_{c,Rd} \geq M_{Ed}$	29.11 kNm > 16.08 kNm	Verified
Resistance in shear	$V_{pl,Rd} \geq V_{Ed}$	131.6 kN > 6.43 kN	Verified
Shear instability	$\frac{h_w}{t_w} < 72 \frac{\varepsilon}{\eta}$	25.44 < 60	Shear instability verification is not required
Moment and shear interaction	$0.5V_{pl,Rd} \geq V_{Ed}$	65.8 kN > 6.43 kN	No bending moment reduction
Resistance in axial	$N_{pl,Rd} \geq N_{Ed}$	472.15 kN > 46.70 kN	Verified
Buckling resistance	$N_{b,Rd} \geq N_{Ed}$	165.25 kN \geq 46.70 kN	Verified
Axial verifications	$0.25N_{pl,Rd} \geq N_{Ed}$	118.04 kN > 46.70 kN	Axial forces doesn't affect moments
	$\frac{0.5h_w t_w f_y}{\gamma_{M0}} \geq N_{Ed}$	74.73 kN > 46.70 kN	
Moment and axial interaction	$\frac{N_{Ed}}{N_{pl,Rd}} + \frac{M_{Ed}}{M_{pl,Rd}} \leq 1$	0.65 < 1	No moment-axial interaction
Deflection check (SLS)	$u_{max} < \frac{h}{300}$	22.8 mm < 33 mm	Verified

3.5.4. Braces design verifications

The two types of braces used in the structures are horizontal and vertical braces. They will be verified according to sections 3.5.4.1 and 3.5.4.2.

3.5.4.1. Horizontal braces

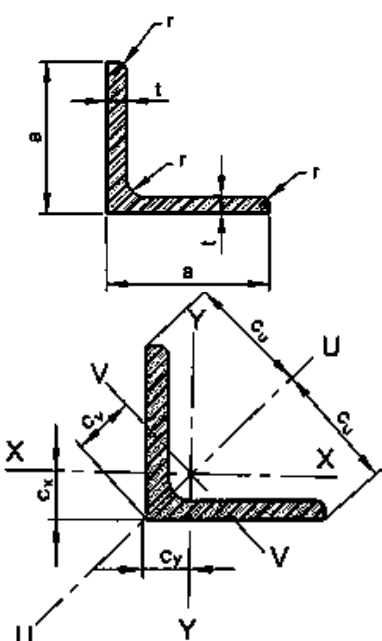
The solicitations gotten from the analysis made on SAP2000 on the horizontal braces are represented in table 3.20.

Table 3.20. Solicitation on the horizontal braces

Solicitation	Value	Units
Axial force	42.41	kN

The section of the horizontal braces used at the level of the roof under study is an angle section named L50*50*5 and its properties are shown in table 3.21.

Table 3.21. Properties of L50*50*5

	Depth (h)	50 mm
	Width (b)	50 mm
	Thickness (t)	5.0 mm
	Radius (r)	7.0 mm
	Weight (G)	3.77 kg/m
	Area (A)	480 mm ²
	Moment of inertia ($I_y=I_x$)	0.11*10 ⁶ mm ⁴
	Elastic section modulus ($W_{el,y} = W_{el,z}$)	3.05*10 ³ mm ³
	Radius of gyration ($i_x=i_y$)	15.1 mm
	Moment of inertia (I_u)	0.17*10 ⁶ mm ⁴
	Radius of gyration (i_u)	19.0 mm
	Moment of inertia (I_v)	0.05*10 ⁶ mm ⁴
	Elastic section modulus ($W_{el,v}$)	2.29*10 ³ mm ³
Radius of gyration (i_v)	9.73 mm ³	

L50*50*5 is a cross section of class 1 and its design verifications according to the case study are presented in table 3.22.

Table 3.22. Design verification of the horizontal braces

Designation	Verification	Value	Observation
Tensile resistance	$N_{t,Rd} \geq N_{Ed}$	112.8kN > 42.41kN	Verified

3.5.4.2. Vertical braces

The solicitations gotten from the analysis made on SAP2000 on the vertical braces are represented in table 3.23.

Table 3.23. Solicitation on the vertical braces

Solicitations	Value	Units
Axial force	32	kN

The section of the vertical braces used at the level of the columns under study is an angle section named L80*80*8 and its properties are shown in table 3.24.

Table 3.24. Properties of L80*80*8

	Depth (h)	80 mm
	Width (b)	80 mm
	Thickness (t)	8.0 mm
	Radius (r)	10.0 mm
	Weight (G)	9.63 kg/m
	Area (A)	1230 mm ²
	Moment of inertia ($I_y=I_x$)	$0.72 \cdot 10^6$ mm ⁴
	Elastic section modulus ($W_{el,y} = W_{el,z}$)	$12.6 \cdot 10^3$ mm ³
	Radius of gyration ($i_x=i_y$)	24.3 mm
	Moment of inertia (I_u)	$1.15 \cdot 10^6$ mm ⁴
	Radius of gyration (i_u)	30.6 mm
	Moment of inertia (I_v)	$0.30 \cdot 10^6$ mm ⁴
	Elastic section modulus ($W_{el,v}$)	$9.37 \cdot 10^3$ mm ³
	Radius of gyration (iv)	15.6 mm ³

L80*80*8 is a cross section of class 1 and its design verifications according to the case study are presented in table 3.25.

Table 3.25. Design verification of the vertical braces

Designation	Verification	Value	Observation
Tensile resistance	$N_{t,Rd} \geq N_{Ed}$	289.05 kN > 32 kN	Verified

3.5.5. Connections design verifications

The connections were verified according to the equations from section 2.5.6.

3.5.5.1. Beam-column connection

The type of connection used for this joint is an eave moment connection use to connect a rafter with a column since the building is made of a portal frame with eaves haunches. The solicitations gotten from the analysis made on SAP2000 on this connection are represented in table 3.26.

Table 3.26. Solicitations in the beam to column connection

Solicitations	Value	Units
Bending moment	279.3	kNm
Shear force	63.48	kN
Axial force	63.69	kN

The results obtained from the verification are presented in the table 3.27.

Table 3.27. Design verifications of the beam-column connection

Designation	Value/Verification	Observation
Numbers of bolts	12	/
Bolts diameter	24mm	/
Ultimate tensile strength of the bolt, f_{ub}	800 N/mm ²	/
Plate thickness	15 mm	/
Yielding strength of the steel profile, f_y	235 N/mm ²	/
Shear resistance per bolt, $F_{v,Rd}$	173.6 kN > 7.16 kN	Verified
Traction resistance per bolt, $F_{t,Rd}$	203.3 kN > 5.31 kN	Verified
Shear and traction Interaction of one bolt	0.06 < 1	Verified
Bearing resistance per bolt, $F_{b,Rd}$	259.2 kN > 7.16 kN	Verified
Total resisting moment,	280.87 kNm > 279.34 kNm	Verified

3.5.5.2. Beam-beam connection

The type of connection used for this joint connecting a rafter with another rafter is an apex moment connection since the building is made of a portal frame with an apex haunch. The solicitations gotten from the analysis made on SAP2000 on this connection are represented in table 3.28.

Table 3.28. Solicitations in the beam to beam connection

Solicitations	Value	Units
Bending moment	279.3	kNm
Shear force	63.48	kN
Axial force	63.69	kN

The results obtained from the verification are presented in the table 3.29.

Table 3.29. Design verifications of the beam-beam connection

Designation	Value/Verification	Observation
Numbers of bolts	10	/
Bolts diameter	24 mm	/
Ultimate tensile strength of the bolt, f_{ub}	800 N/mm ²	/
Plate thickness	15 mm	/
Yielding strength of the steel profile, f_y	235 N/mm ²	/
Shear resistance per bolt, $F_{v,Rd}$	173.6 kN > 6.35 kN	Verified
Traction resistance per bolt, $F_{t,Rd}$	203.3 kN > 6.37 kN	Verified
Shear and traction Interaction of one bolt	0.06 < 1	Verified
Bearing resistance per bolt, $F_{b,Rd}$	129.6 kN > 6.35 kN	Verified
Total resisting moment,	235.85 kNm > 137 kNm	Verified

3.5.5.3. Brace connection

These connections are used at the joints between the braces and the column/beam. The connection here is a shear connection, so no moment transmission. The solicitations present in this connection are represented in table 3.30.

Table 3.30. Solicitation in the beam to beam connection

Solicitation	Value	Units
Axial force	42.41	kN

The results obtained from the verifications are presented in the table 3.31.

Table 3.31. Design verifications of the brace connection

Designation	Value/Verification	Observation
Numbers of bolts	2	/
Bolts diameter	10 mm	/
Ultimate tensile strength of the bolt, f_{ub}	800 N/mm ²	/
Plate thickness	10 mm	/
Yielding strength of the steel profile, f_y	235 N/mm ²	/
Shear resistance per bolt, $F_{v,Rd}$	30.14 kN > 21.21 kN	Verified
Bearing resistance per bolt, $F_{b,Rd}$	49.15 kN > 21.21 kN	Verified

3.5.5.4. Column base connection

The column base connections are used at the joints between the columns and the foundation. The ground foundation is assumed to have a resistance of 2 N/mm². The solicitations present at the column base obtained from the software SAP2000 are presented in table 3.32.

Table 3.32. Solicitations at column base connection

Solicitations	Value	Units
Shear force	47.99	kN
Axial force (ULS)	85.93	kN
Axial force (SLS)	59.05	kN

The results obtained from the verifications are presented in the table 3.33.

Table 3.33. Design verifications of the column base connection

Designation	Value/Verification	Observation
Concrete class	C25/30	/
Section of the footing	60 cm x 60 cm	/
Height of the footing	30 cm	/
Bearing capacity resistance	$0.17 \text{ N/mm}^2 < 0.2 \text{ N/mm}^2$	Verified
Compressive resistance of the concrete block, f_{ck}	$0.76 \text{ N/mm}^2 < 14.17 \text{ N/mm}^2$	Verified
Section of the plate	25 cm x 45 cm	/
Tensile strength of the plate, f_{yp}	235 N/mm^2	/
Plate thickness	$15 \text{ mm} > 1.5 \text{ mm}$	Verified
Numbers of bolts	2	/
Bolts diameter	27 mm	/
Ultimate tensile strength of the anchor, f_{ub}	800 N/mm^2	/
Shear resistance per anchor, $F_{v,Rd}$	$183.22 \text{ kN} > 24 \text{ kN}$	Verified
Traction resistance per bolt, $F_{t,Rd}$	$264.38 \text{ kN} > 42.97 \text{ kN}$	Verified
Shear and traction interaction of one bolt	$0.40 < 1$	Verified
Bearing resistance per anchor, $F_{b,Rd}$	$291.6 \text{ kN} > 24 \text{ kN}$	Verified

3.6. Results of the fire analysis on the project

The analysis with the ABAQUS software was carried out following all the steps set out in the previous chapter and the results will be presented according to the different analyses made.

3.6.1. Local analysis on the roofing elements

The results of the heat analysis made on the roofing elements with temperatures arriving at around 500 °C are presented in figure 3.7 and figure 3.8. A one hour standard fire test with temperatures arriving at 945.34 °C was not conducted here because the melting point of the panel is less than 500 °C.

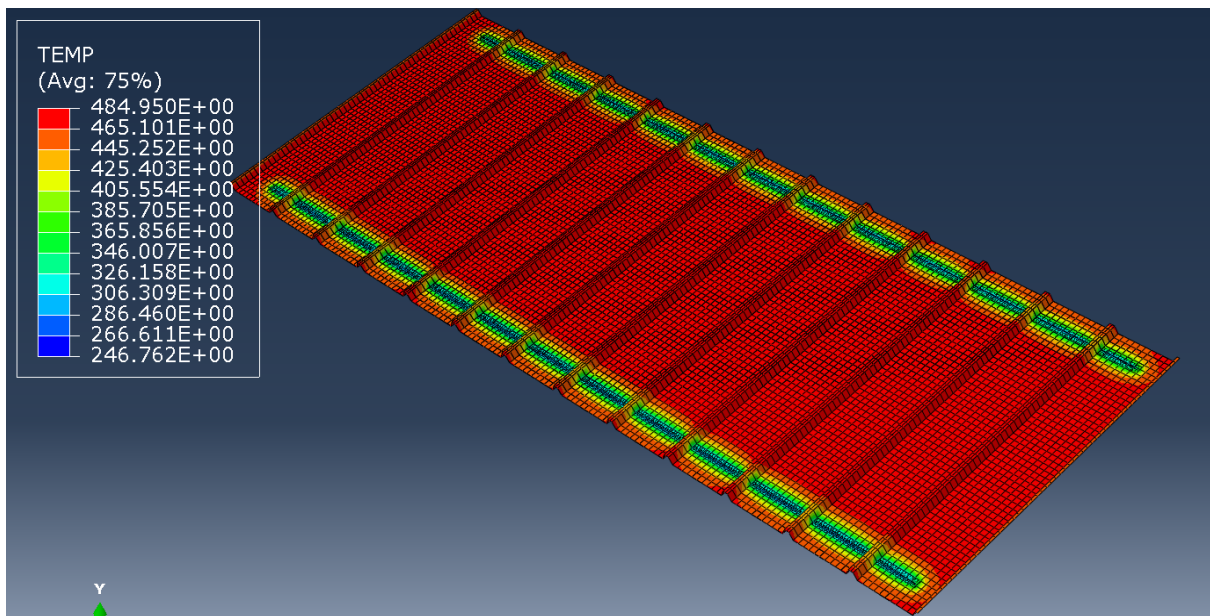


Figure 3.7. Front view of temperature distribution in the roofing elements

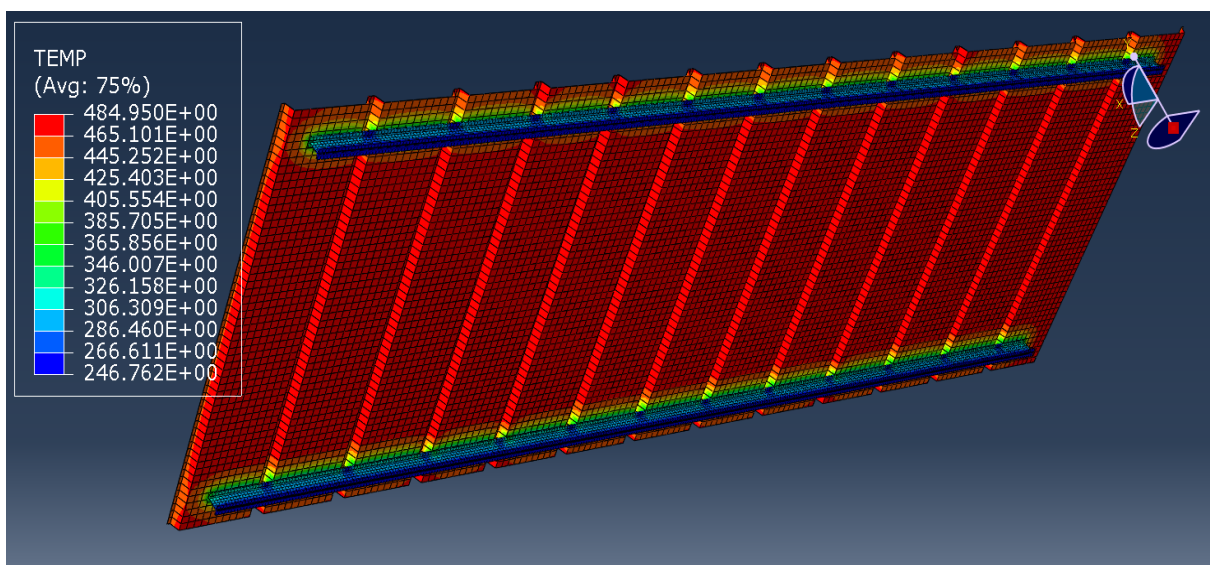


Figure 3.8. Back view of temperature distribution in the roofing elements

Due to the very high conductivity of aluminium zinc sheet as compare to the purlin made of steel, it is observed that the temperature of the aluminium zinc panel increases rapidly in contrast to the purlins supporting it. As seen, aluminium zinc sheet transmits the heat it receives to the top flange of the purlin by conductivity.

Just before melting, the deformation encountered by the roofing elements gotten from the stress analysis done directly after the thermal analysis are presented in figure 3.9.

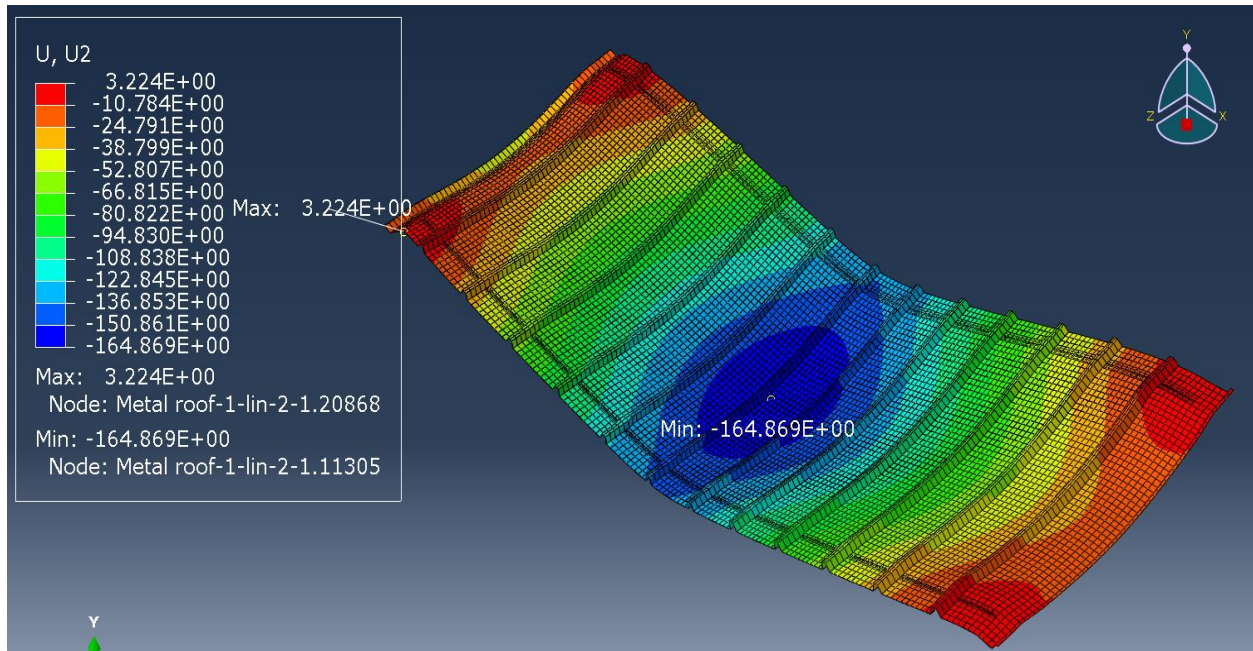


Figure 3.9. Deflection on the roofing elements

As it is been observed, the maximum vertical deflection is 164.9 mm and it is greater than the maximum vertical limit deflection for serviceability limit states which is equal to the length between the two purlins divided by 200.

$$f_{\max} = \frac{l}{200} = \frac{1700}{200} = 8.5 \text{ mm}$$

Therefore just before melting, the roofing elements didn't verify serviceability limit states and it was no more good for the structure. This is what has been observed during the fire damaged that happened in the structure as shown in figure 3.10. From these analyses, it is been observed that the greater the temperature the greater the deflection.



Figure 3.10. Damaged roofing elements due to fire

3.6.2. Global analysis on the structural elements

A global analysis of the structural elements was made and the results after the stress analysis are presented in figure 3.11 and figure 3.12, due to the fact that the aluminium zinc sheet used for roofing is a non-structural elements and that it doesn't really affects the other structural elements.

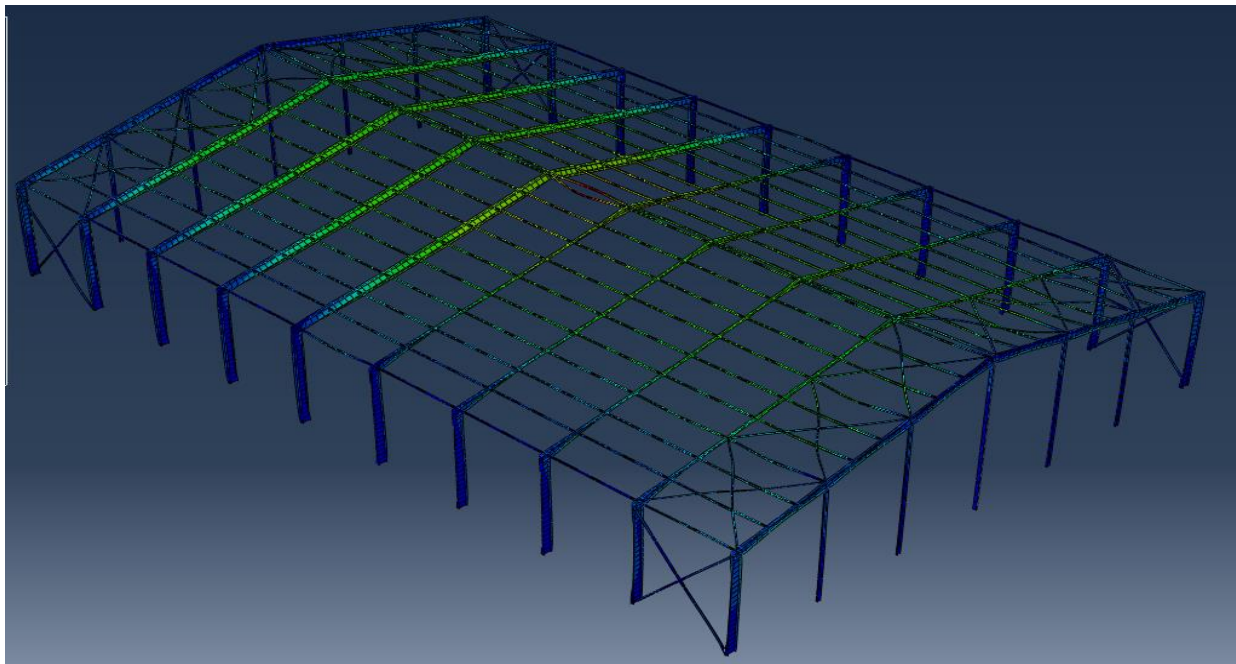


Figure 3.11. Displacement due to fire on the whole structure

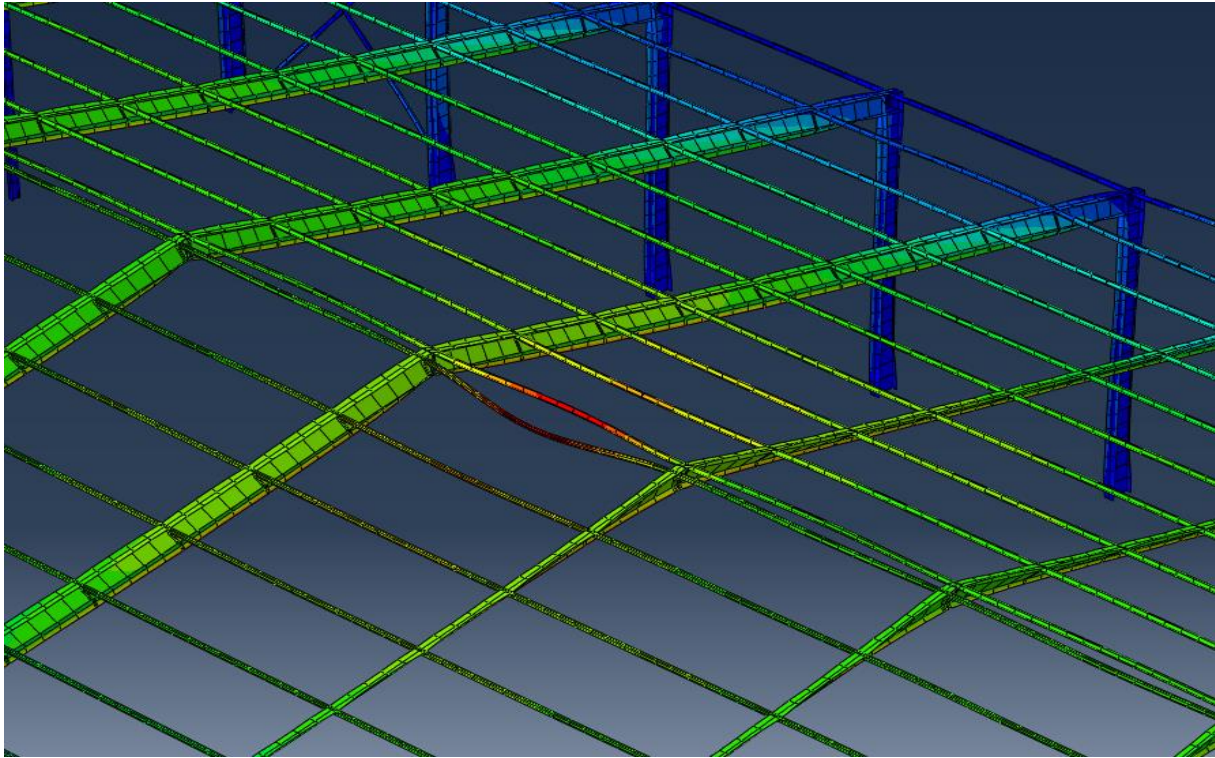


Figure 3.12. Zoomed image of the maximum displacement of the structure

From this analysis, it is observed that the most fragile element is the purlin due to its lower cross section as compare to the other elements. These results matches with what happen in the case study building as illustrated in figure 3.13.



Figure 3.13. Damaged roof elements of the Panzani's store

In order to better analyse in details how fire affects the structural elements of the building, a local analysis done in Abaqus was made on some of those structural elements.

3.6.3. Local analysis on the structural elements

This section present the results of the local analyses made on a simple supported IPE80 purlin and on a IPE400 column present in the Panzani's structure. And it also present the results gotten from the analysis made on different column's cross sections in order to analyse how they react due to a high thermal load.

3.6.3.1. Results of purlin

The results gotten from the heat analysis, where a standard fire of one hour was applied on one face (bottom flange) of the purlin, is presented in figure 3.14.

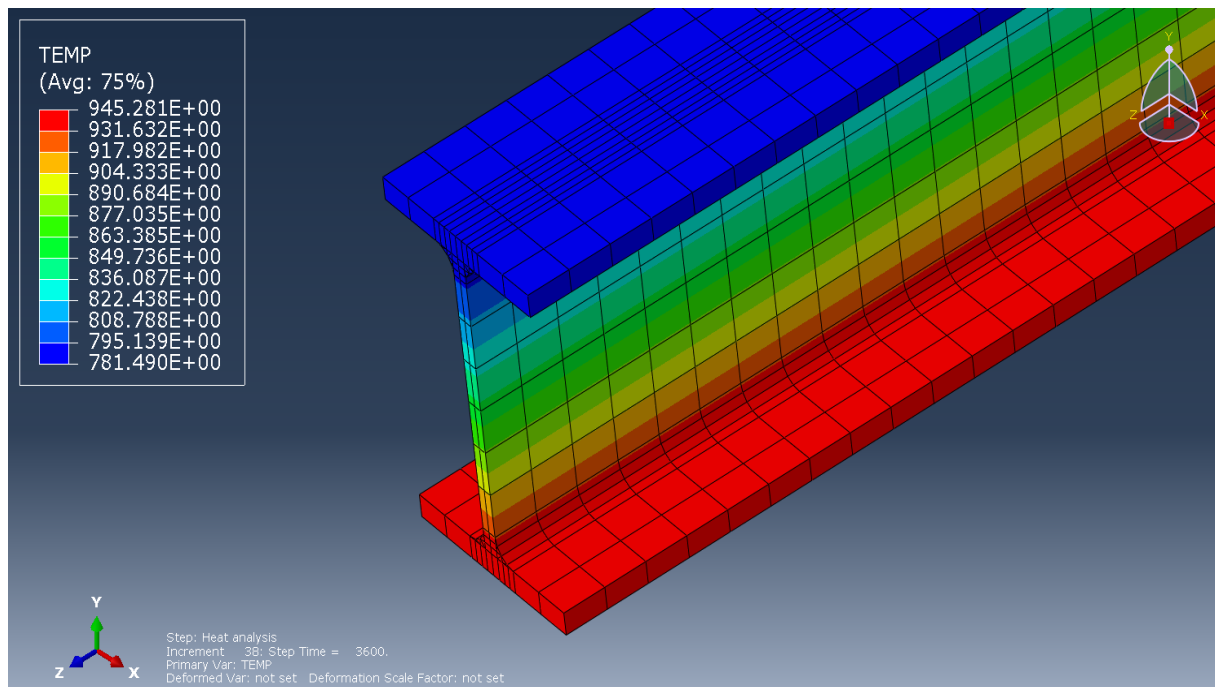


Figure 3.14. Temperature distribution in the purlin

It is observed that due to its small cross section and due to its high conductivity, the temperature in the elements rapidly increases and rapidly reaches the critical temperature of steel which 600 °C. The evolution temperature within the cross section of the purlin in function of time is illustrated in figure 3.15.

INFLUENCE OF HIGH TEMPERATURE ON THE STRUCTURAL BEHAVIOUR OF STEEL
STRUCTURES AND SOLUTIONS : CASE OF PANZANI BUILDING

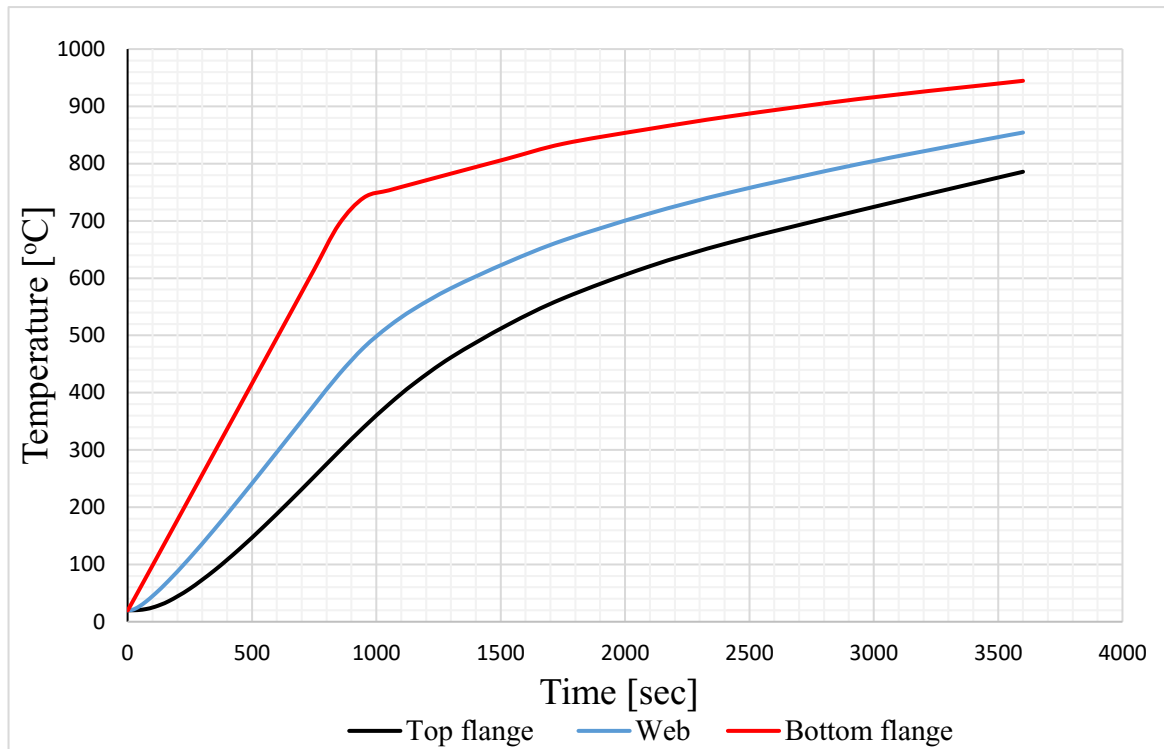


Figure 3.15. Temperature evolution in the IPE80 purlin's cross section

The results gotten from the stress analysis that was done on the same purlin is illustrated in figure 3.16.

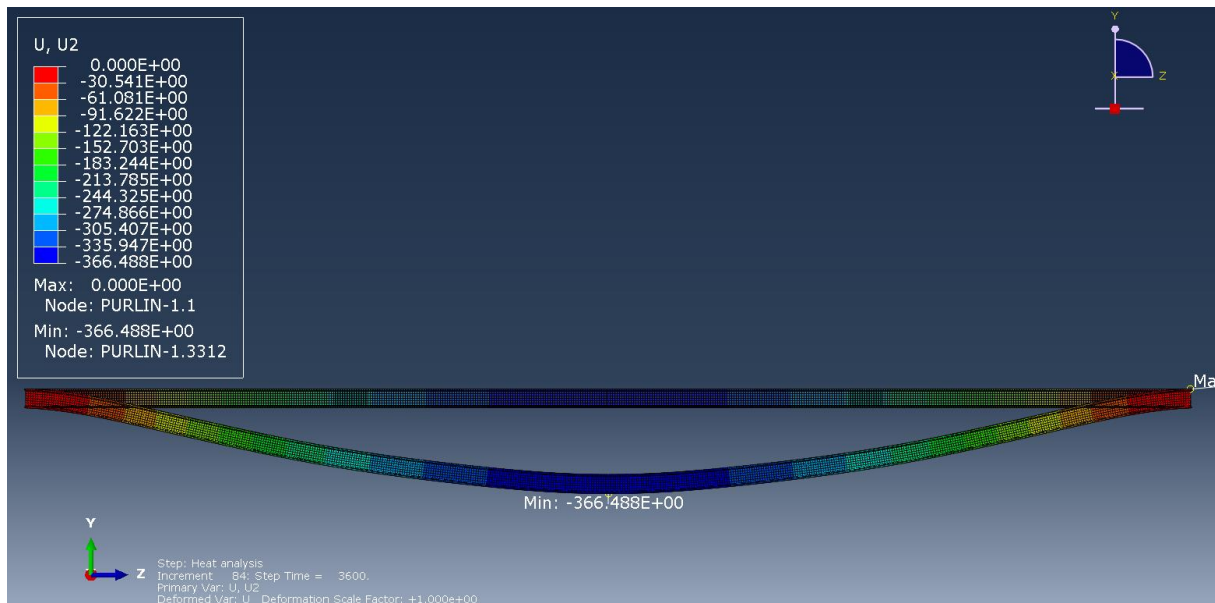


Figure 3.16. Undeformed and deformed shape of the purlin

As it is been observed, the maximum vertical deflection of the purlin is 366.5 mm and it is greater than the maximum vertical limit deflection for serviceability limit states which is equal to the length of the purlin divided by 200.

$$f_{\max} = \frac{l}{200} = \frac{5000}{200} = 25 \text{ mm}$$

Therefore the purlin doesn't verifies serviceability limit states and is no more good for the structure.

3.6.3.2. Results of column

The results gotten from the heat analysis, where a standard fire of one hour was applied on the three faces of the IPE400 column of the case study are presented in figure 3.17.

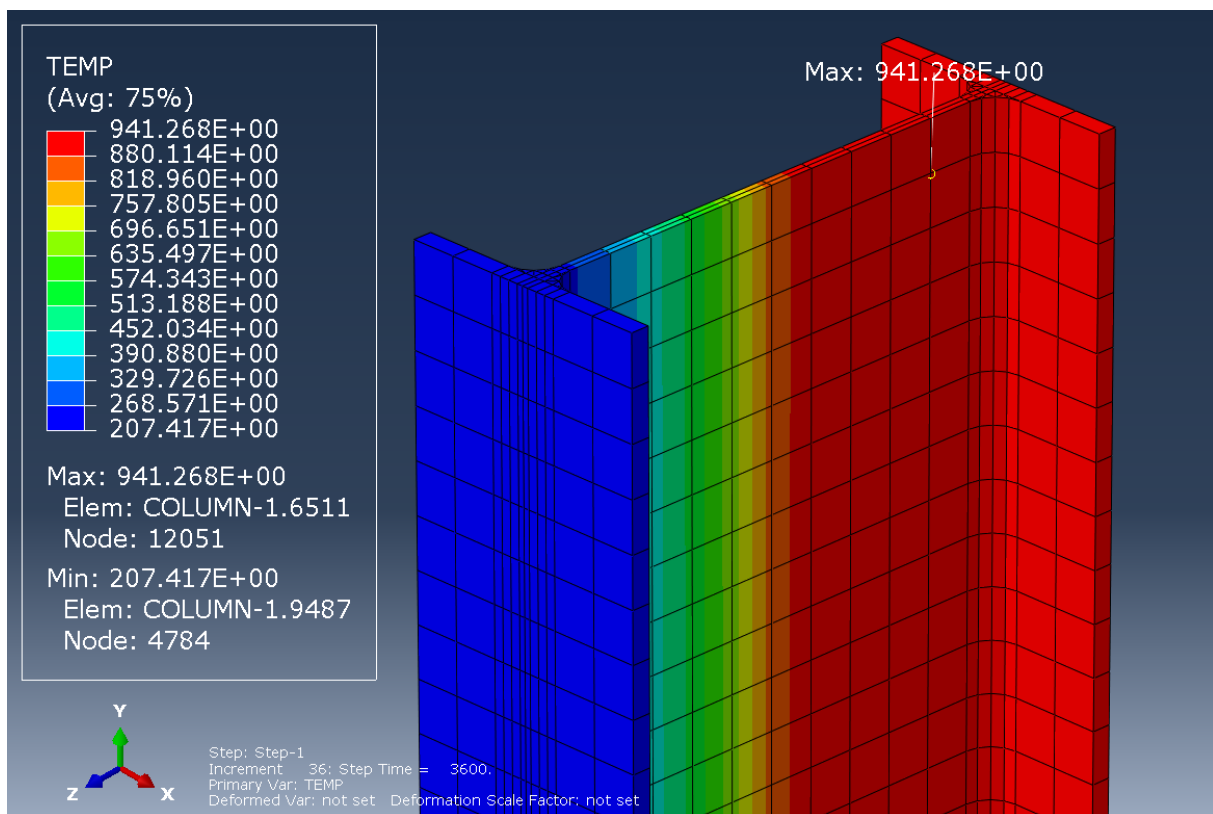


Figure 3.17. Temperature distribution in the IPE400 column

Due to the high conductivity of steel, the temperature in the elements rapidly increases and rapidly reaches the critical temperature of steel which is 600 °C. The evolution of temperature within the cross section of the column in function of time is illustrated in figure 3.18.

INFLUENCE OF HIGH TEMPERATURE ON THE STRUCTURAL BEHAVIOUR OF STEEL
STRUCTURES AND SOLUTIONS : CASE OF PANZANI BUILDING

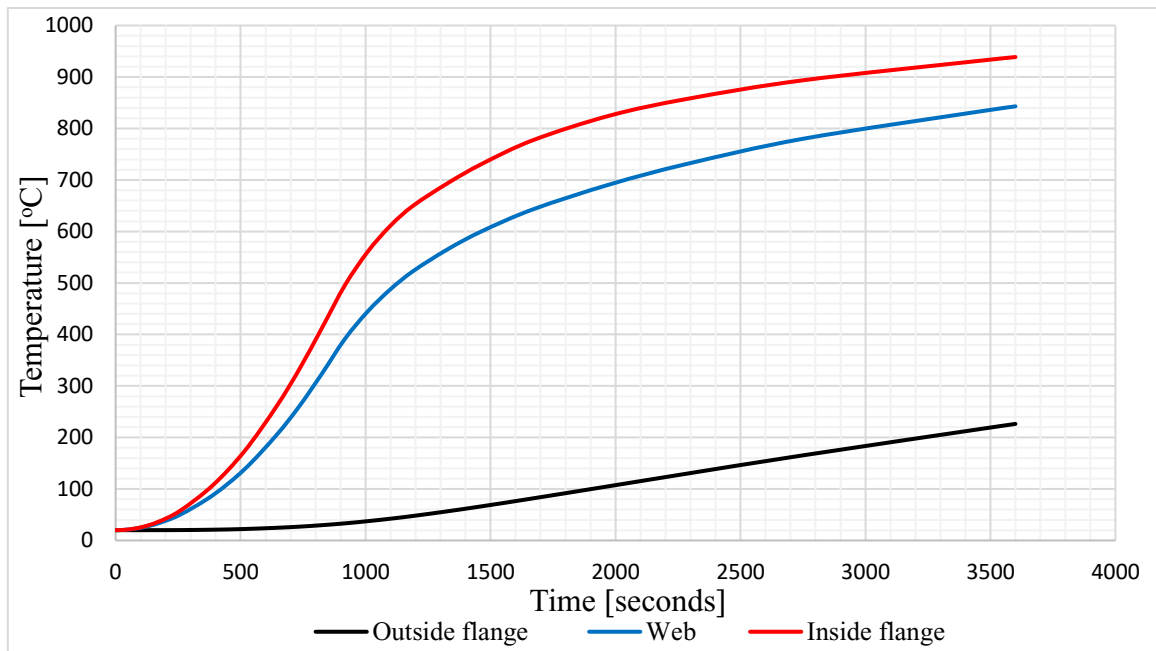


Figure 3.18. Temperature evolution in the IPE400 column's cross section

The results gotten from the stress analysis that was done on the same column is illustrated in figure 3.19.

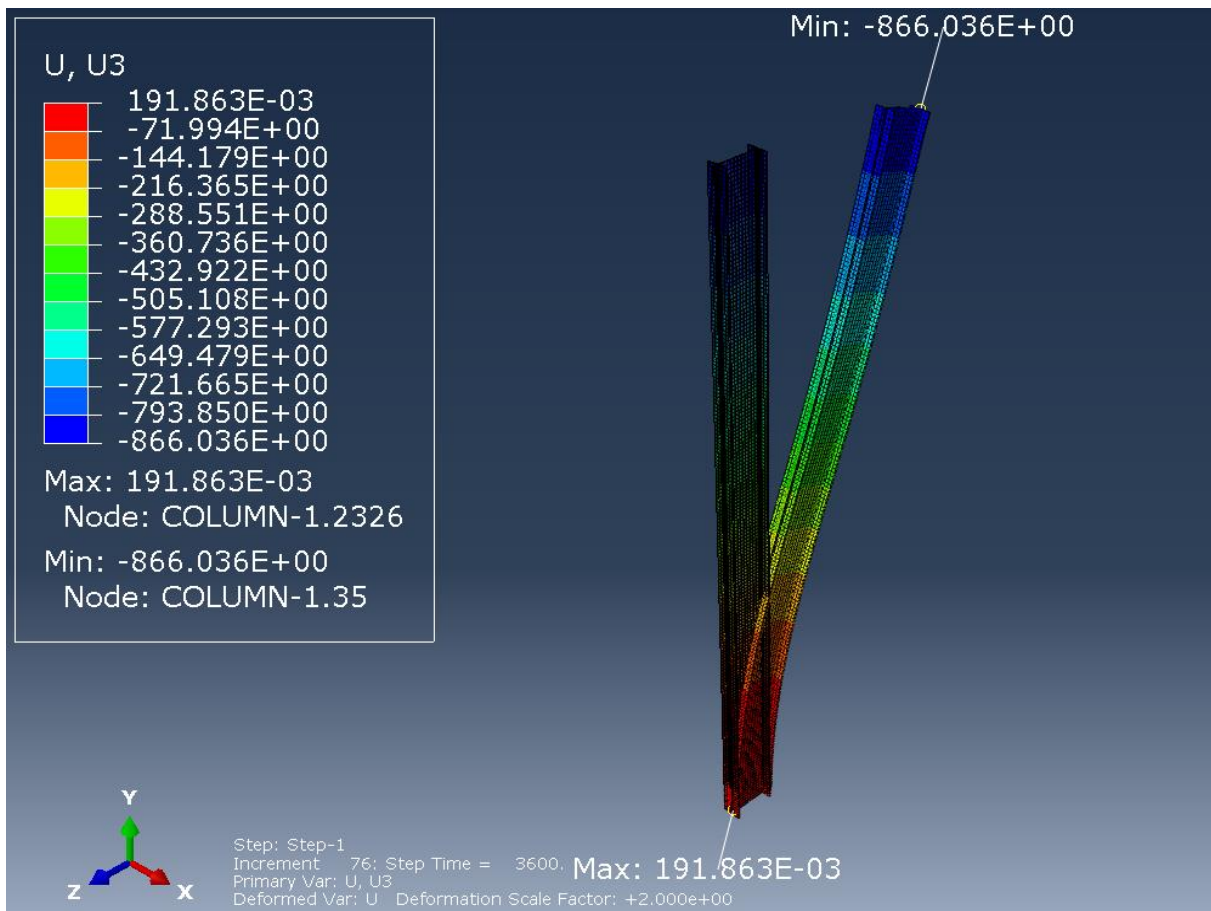


Figure 3.19. Displacement of the IPE column due to the fire effect

As it is been observed, the column deflects with a large value, showing that fire has a great effect on steel. The maximum horizontal deflection in question is 866.0 mm and it is way greater than the maximum horizontal limit deflection for serviceability limit states which is equal to the height of the column divided by 300.

$$u_{\max} = \frac{H}{300} = \frac{6500}{300} = 21.67 \text{ mm}$$

Therefore the column doesn't verifies serviceability limit states and cannot be used again.

As seen in figure 3.14 and figure 3.17, the column which had a larger cross section as compared to the purlin had a lower increase of temperature across the cross section even though it was heated on more faces than the purlin. This shows that the greater the cross section the lower the temperature evolution in the element. This remarks leads us to conduct a study on the effect of temperature on different type of cross sections that can be used for columns in such buildings. In order to use the SHS 260/16 and CHS 323.9/14.2 columns for the fire analysis, firstly a classification of their cross section was made as shown in table 3.34 and table 3.35.

Table 3.34. Classification of the SHS 260/16 column

Designation	Verification	Value	Observation
Web subjected to bending and compression	$\frac{c}{t} \leq \frac{36\varepsilon}{\alpha}$	$13.25 \leq 72$	Class 1

Table 3.35. Classification of the CHS 323.9/14.2 column

Designation	Verification	Value	Observation
Section in bending and compression	$\frac{c}{t} \leq 50\varepsilon^2$	$22.8 \leq 50$	Class 1

Then they were statically verified and the results of their verifications are presented in table 3.36 and table 3.37.

Table 3.36. Design verifications of the SHS 260/16 column

Designation	Verification	Value	Observation
Resistance in bending	$M_{c,Rd} \geq M_{Ed}$	320.31 kNm > 272.04 kNm	Verified
Resistance in shear	$V_{pl,Rd} \geq V_{Ed}$	1193.28 kN > 46.87 kN	Verified
Moment and shear interaction	$0.5V_{pl,Rd} \geq V_{Ed}$	596.6 kN > 46.87 kN	No bending moment reduction
Resistance in axial	$N_{pl,Rd} \geq N_{Ed}$	3246.76 kN > 89.9 kN	Verified
Buckling resistance	$N_{b,Rd} \geq N_{Ed}$	3019.49 kN \geq 89.9 kN	Verified
Axial verifications	$0.25N_{pl,Rd} \geq N_{Ed}$	811.69 kN > 89.9 kN	Axial forces doesn't affect moments
Moment and axial interaction	$\frac{N_{Ed}}{N_{pl,Rd}} + \frac{M_{Ed}}{M_{pl,Rd}} \leq 1$	0.88 < 1	No moment-axial interaction
Deflection check (SLS)	$u_{max} < \frac{h}{300}$	19.7 mm < 22 mm	Verified

Table 3.37. Design verifications of the CHS 323.9/14.2 column

Designation	Verification	Value	Observation
Resistance in bending	$M_{c,Rd} \geq M_{Ed}$	327.59 kNm > 270.18 kNm	Verified
Resistance in shear	$V_{pl,Rd} \geq V_{Ed}$	1040.78 kN > 46.58 kN	Verified
Moment and shear interaction	$0.5V_{pl,Rd} \geq V_{Ed}$	520.39 kN > 46.58 kN	No bending moment reduction
Resistance in axial	$N_{pl,Rd} \geq N_{Ed}$	3230.09 kN > 91.15 kN	Verified
Buckling resistance	$N_{b,Rd} \geq N_{Ed}$	3068.65 kN \geq 91.15 kN	Verified
Axial verifications	$0.25N_{pl,Rd} \geq N_{Ed}$	807.52 kN > 91.15 kN	Axial forces doesn't affect moments
	$\frac{0.5h_w t_w f_y}{\gamma_{M0}} \geq N_{Ed}$	488.8 kN > 91.15 kN	
Moment and axial interaction	$\frac{N_{Ed}}{N_{pl,Rd}} + \frac{M_{Ed}}{M_{pl,Rd}} \leq 1$	0.85 < 1	No moment-axial interaction
Deflection check (SLS)	$u_{max} < \frac{h}{300}$	20.9 mm < 22 mm	Verified

**INFLUENCE OF HIGH TEMPERATURE ON THE STRUCTURAL BEHAVIOUR OF STEEL
STRUCTURES AND SOLUTIONS : CASE OF PANZANI BUILDING**

The results gotten from the heat analysis, where a standard fire of one hour was applied on the SHS 260/16 column are presented in figure 3.20.

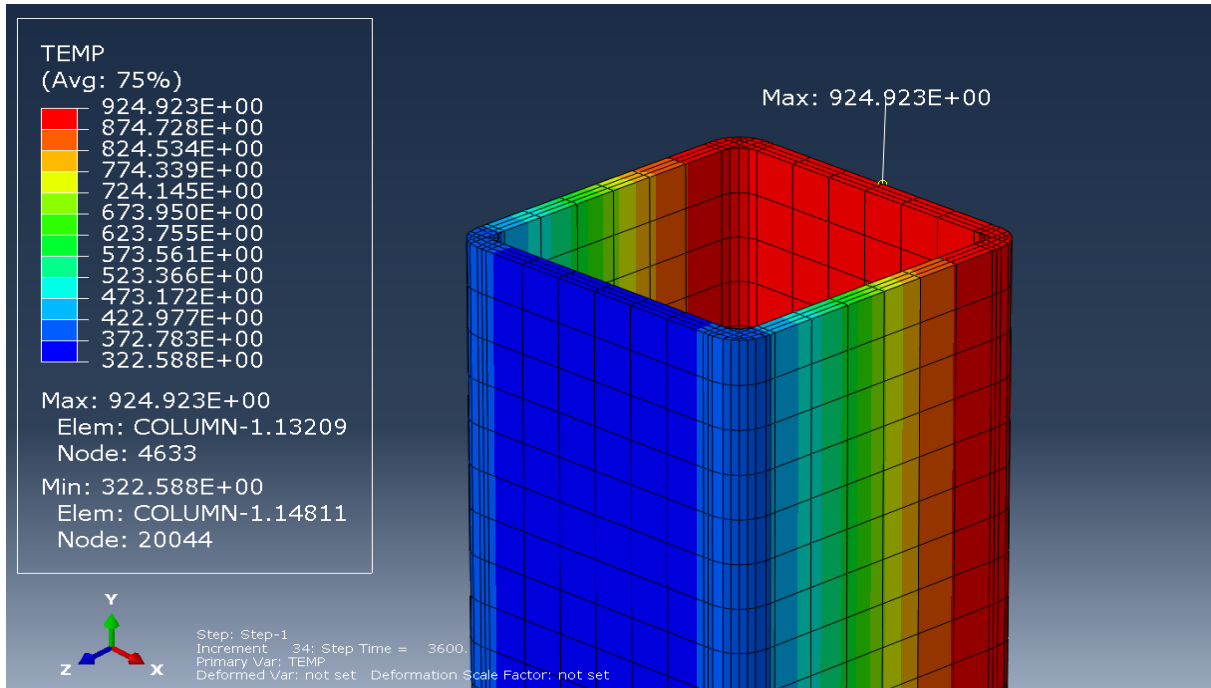


Figure 3.20. Temperature distribution in the SHS column due to fire effect

Due to the high conductivity of steel and the hollow form of the cross section, the temperature in the elements rapidly increases and rapidly reaches the critical temperature of steel which is 600 °C. The evolution of temperature within the cross section of the column in function of time is illustrated in figure 3.21.

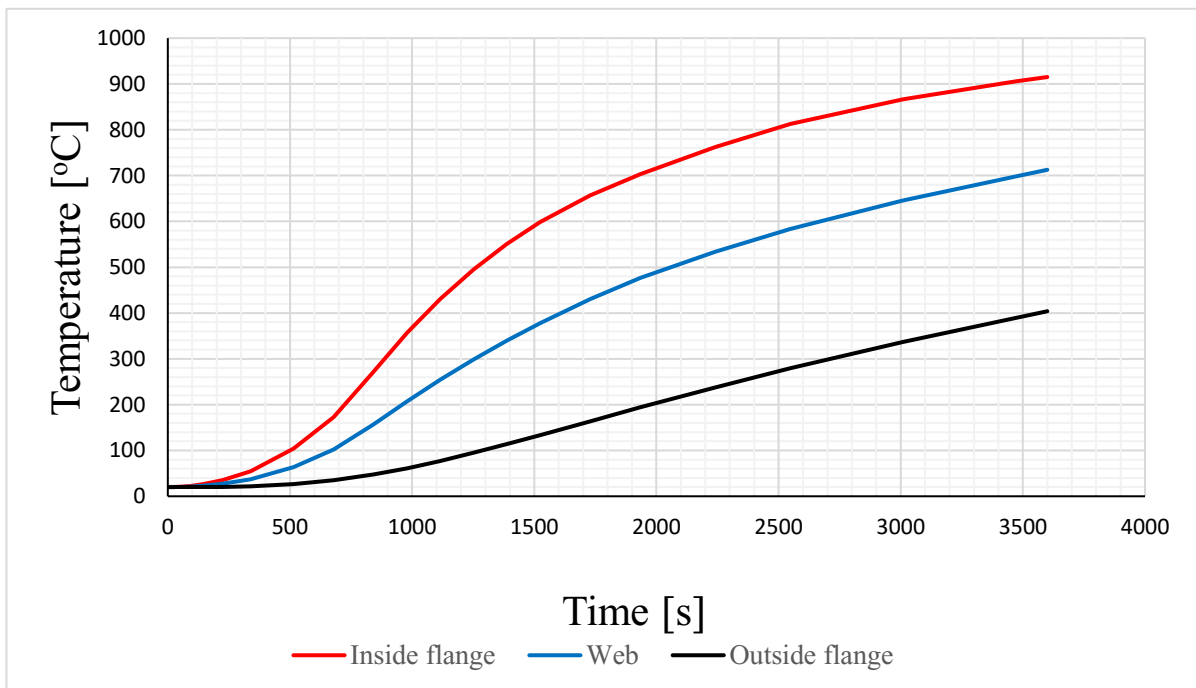


Figure 3.21. Temperature evolution in the SHS column's cross section

The result gotten from the stress analysis that was done on the SHS column is illustrated in figure 3.22.

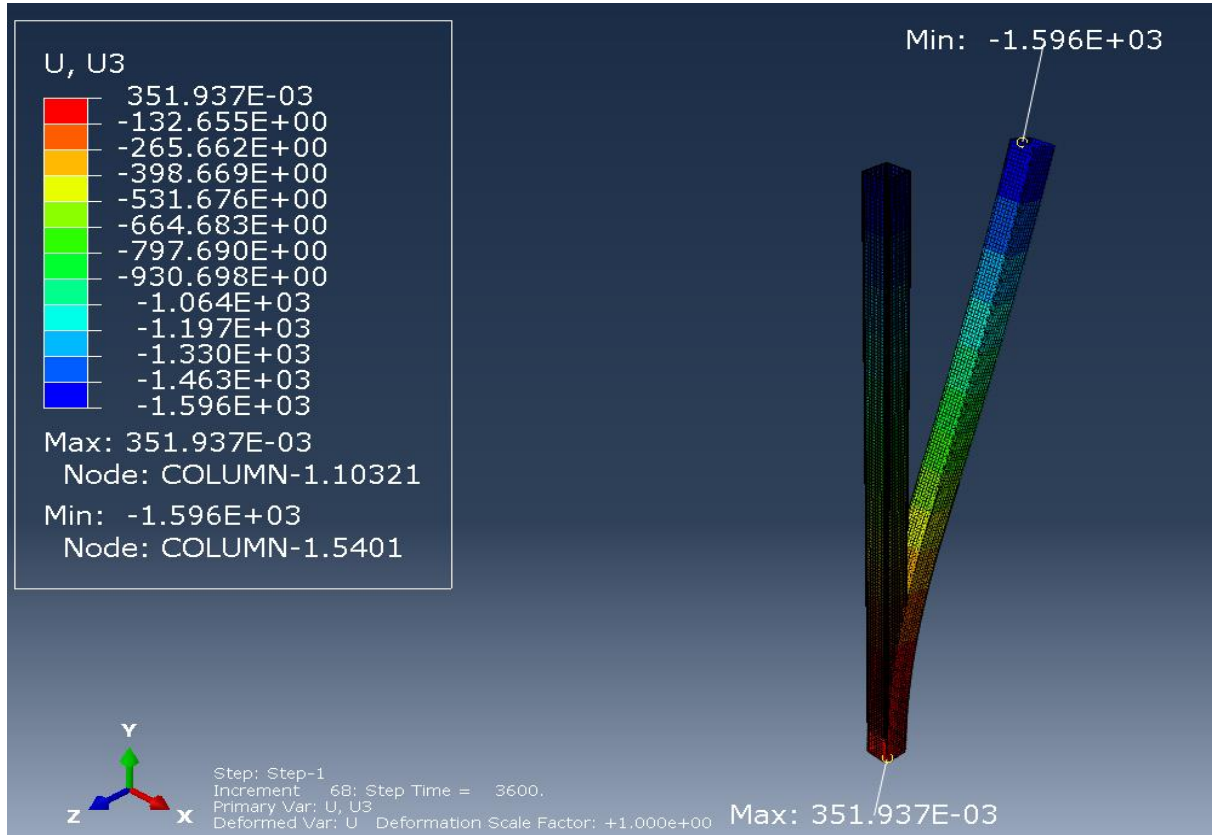


Figure 3.22. Displacement of the SHS column due to fire effect

Due to its hollow section, the column deflects with a very large value showing that fire has a great effect on this cross section as compare to an IPE cross section. The maximum horizontal deflection in question is 1596 mm and it is too much greater than the maximum horizontal limit deflection for serviceability limit states.

$$u_{\max} = \frac{H}{300} = \frac{6500}{300} = 21.67 \text{ mm}$$

Therefore the column doesn't verifies serviceability limit states and it is impossible to be used again.

The results gotten from the heat analysis, where a standard fire of one hour was applied on the CHS 323.9/14.2 column are presented in figure 3.23.

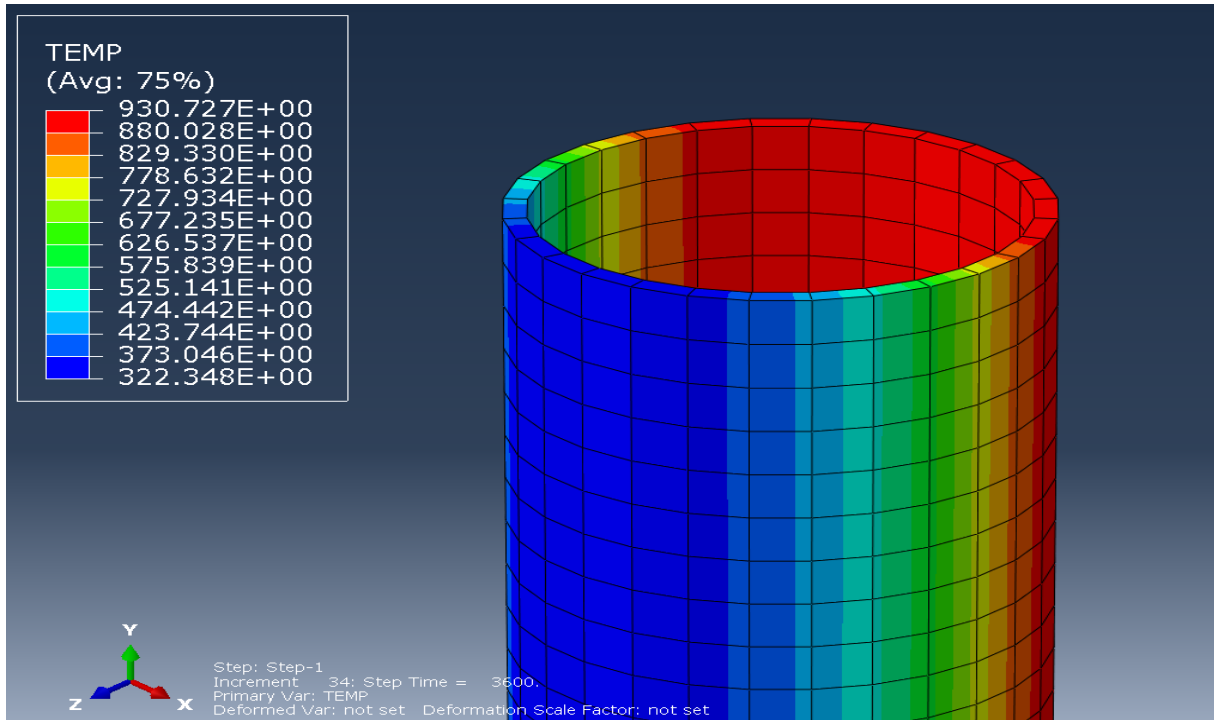


Figure 3.23. Temperature distribution in the CHS column due to fire effect

The high conductivity of steel and the hollow form of the cross section, induces the temperature in the elements to increase rapidly and then the critical temperature of steel which is 600 °C is rapidly reached. The evolution of temperature within the cross section of the column in function of time is illustrated in figure 3.24.

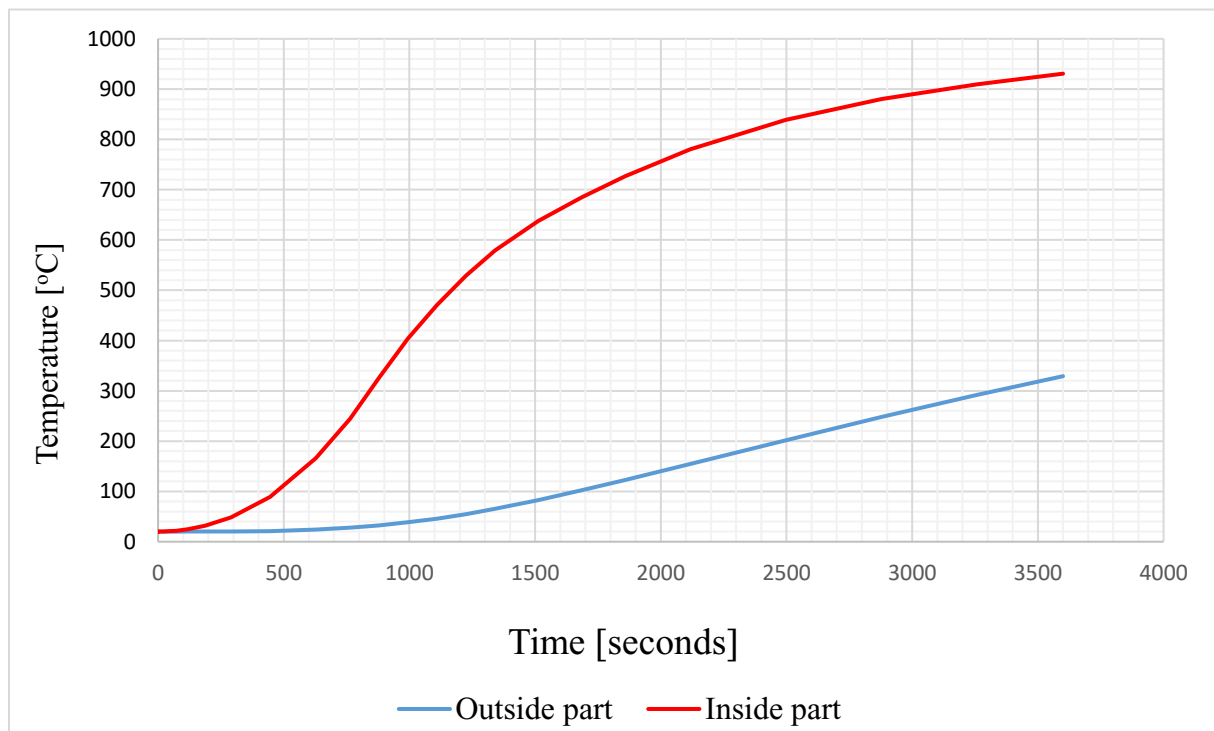


Figure 3.24. Temperature evolution in the CHS column's cross section

The result gotten from the stress analysis that was done on the CHS column is illustrated in figure 3.25.

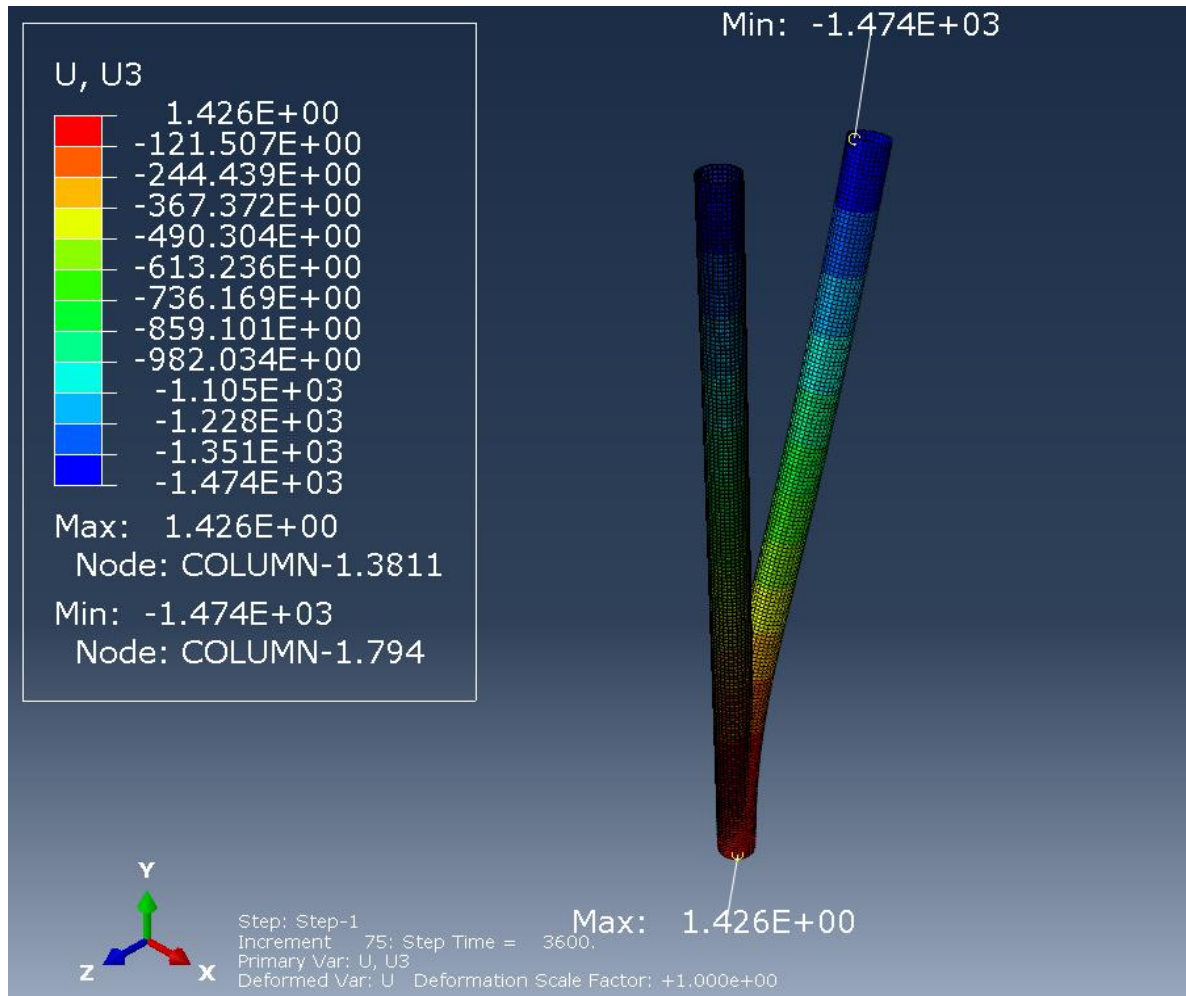


Figure 3.25. Displacement of the CHS column due to fire effect

The maximum horizontal deflection of the CHS 323.9/14.2 column is 1474 mm. This is due to its hollow section and geometry. This deflection is too much greater than the maximum horizontal limit deflection for serviceability limit states which is 21.67 mm. Therefore the column doesn't verify serviceability limit states and it is unusable.

3.7. Results of the analysis on the fire protective systems

Generally, the two types of fire protection that exist are active fire protection and passive fire protection systems. The recommendations made in this work will mainly concern passive fire protection system. A solid protection involving timber or concrete can be used to protect the columns. These solid elements can be partially or totally mixed with the column in order to insulate it and prevent the columns to reach their critical temperature. A heat analysis of this protection system was made in Abaqus and the results are presented in section 3.7.1 and 3.7.2.

3.7.1. Results of the hybrid steel-timber elements

The results gotten from the heat analysis, where a standard fire of one hour was applied on the partially protected steel-timber column are presented in figure 3.26.

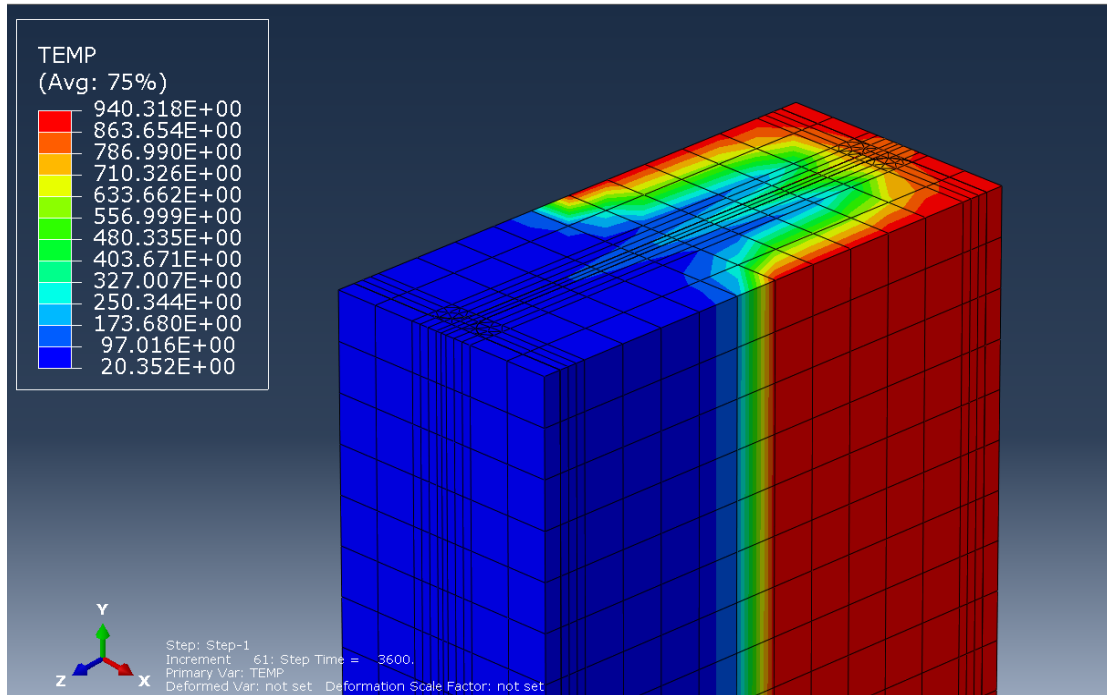


Figure 3.26. Temperature distribution in partially protected steel with timber

The evolution of temperature within the cross section of the steel column in function of time is illustrated in figure 3.27.

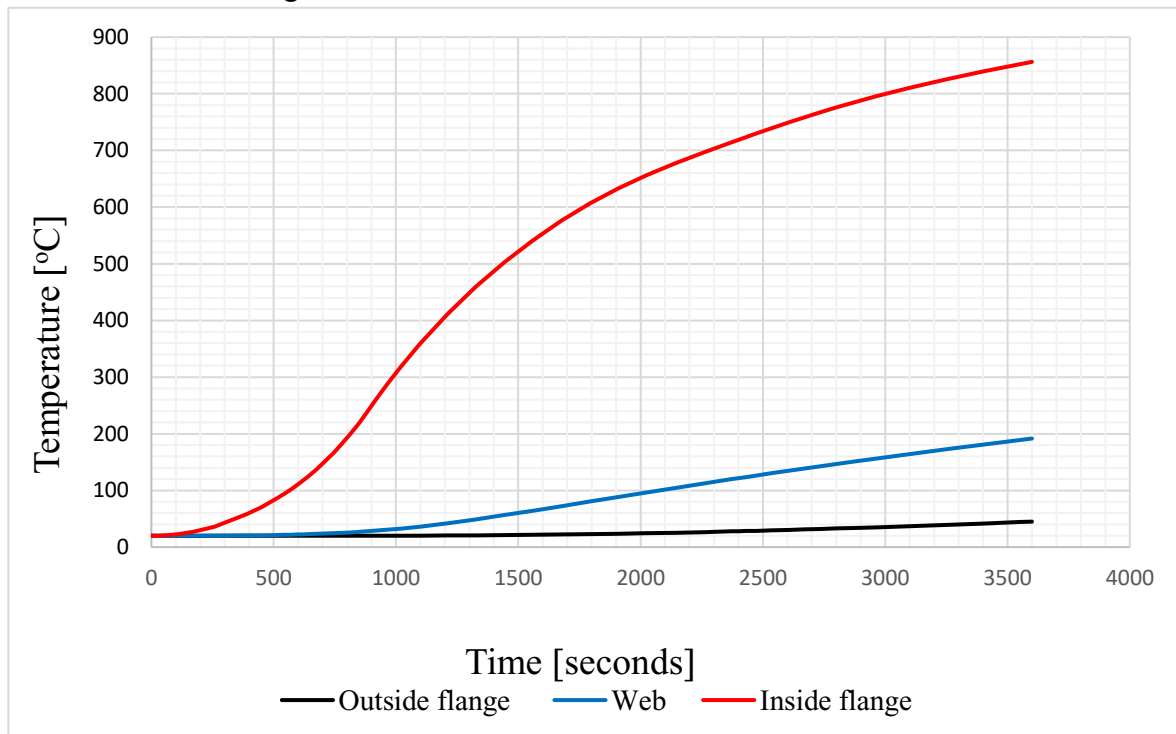


Figure 3.27. Temperature evolution in partially steel-timber cross section

INFLUENCE OF HIGH TEMPERATURE ON THE STRUCTURAL BEHAVIOUR OF STEEL STRUCTURES AND SOLUTIONS : CASE OF PANZANI BUILDING

Due to the very low conductivity of wood and the presence of char created on wood surface because of fire, the effect of fire on the steel column is reduced and the temperature inside the steel column doesn't increase rapidly as when the column wasn't protected as all, but the temperature of the inside flange of the column increases until it crosses the critical temperature because it is in direct contact with fire since the protection is only partial. Char wood is the residual black carbon material which comes from partly burned wood.

The results gotten from the heat analysis, where a standard fire of one hour was applied on the totally protected steel-timber column are presented in figure 3.28.

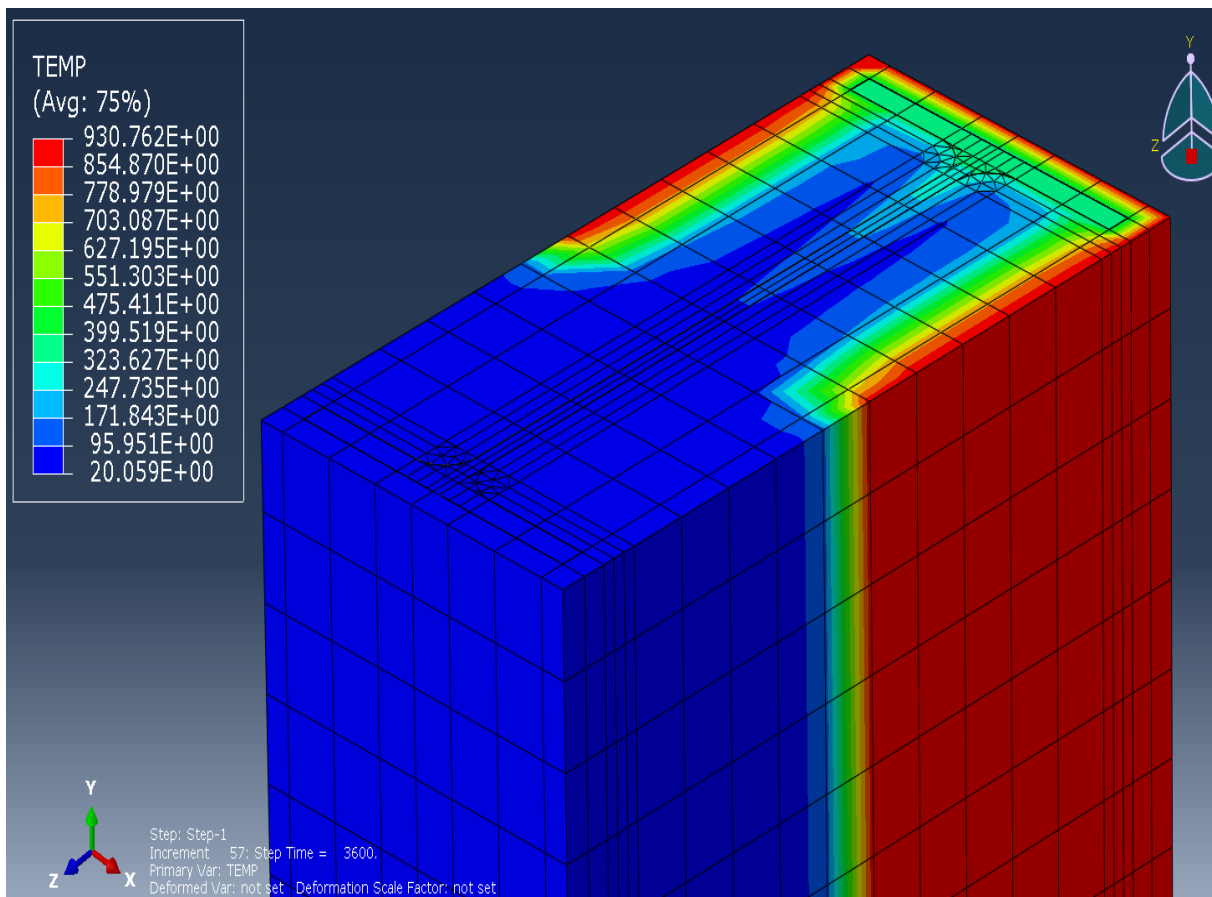


Figure 3.28. Temperature distribution in totally protected steel with timber

The evolution of temperature within the cross section of the steel column in function of time is illustrated in figure 3.29.

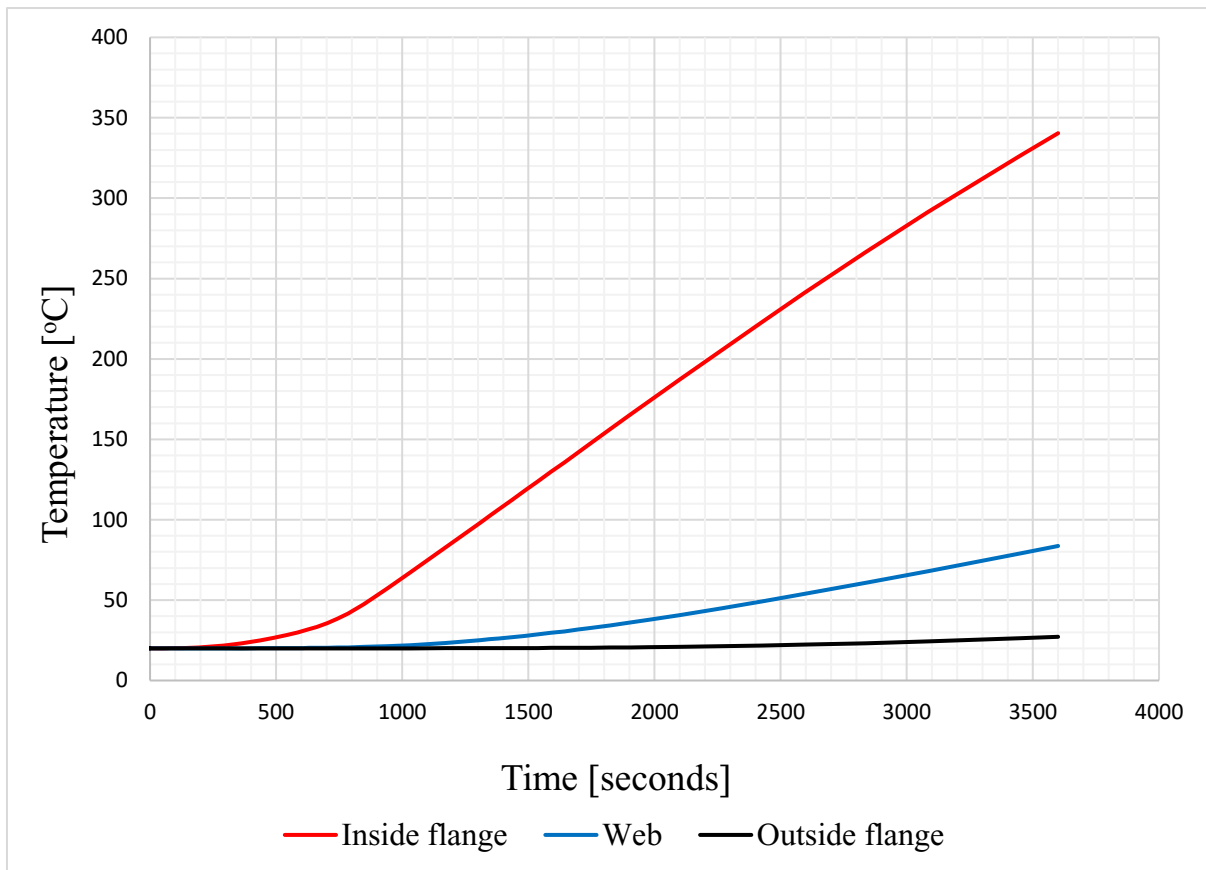


Figure 3.29. Temperature evolution in totally steel-timber cross section

This study shows that, in fire situation, the thermomechanical behaviour of steel beams is significantly improved when it is protected by timber elements. It appears that the failure of steel beams is slowed to a large extent, depending on the amount of steel surface protected by timber. Indeed, full timber protection seems to be twice as effective as partial timber protection. In these conditions, wood seems to be a possible solution to protect steel against fire. Furthermore, the advantage of timber, compared to other fire protection materials, is its ability to provide mechanical support to steel against buckling effects while its light weight does not significantly increase the weight of the element.

3.7.2. Results of the hybrid steel-concrete elements

The results gotten from the heat analysis, where a standard fire of one hour was applied on the partially protected steel-concrete member column are presented in figure 3.30.

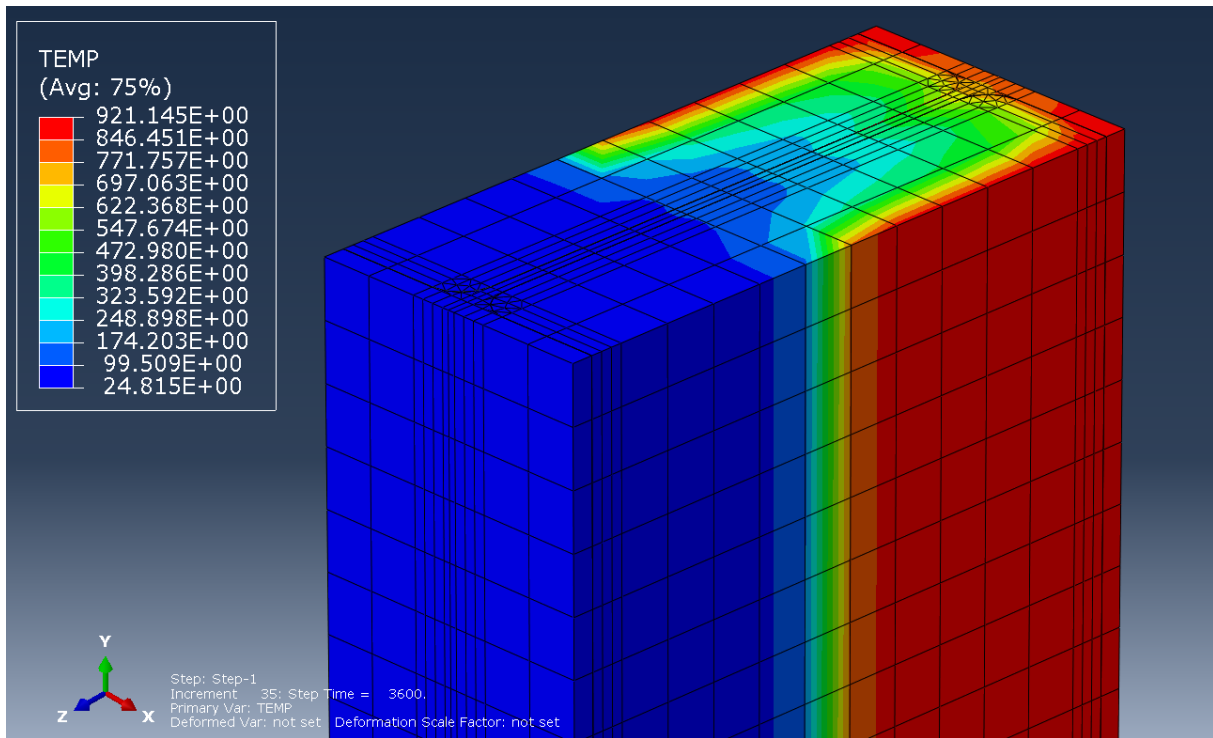


Figure 3.30. Temperature distribution in partially protected steel with concrete

The evolution of temperature within the cross section of the steel column in function of time is illustrated in figure 3.31.

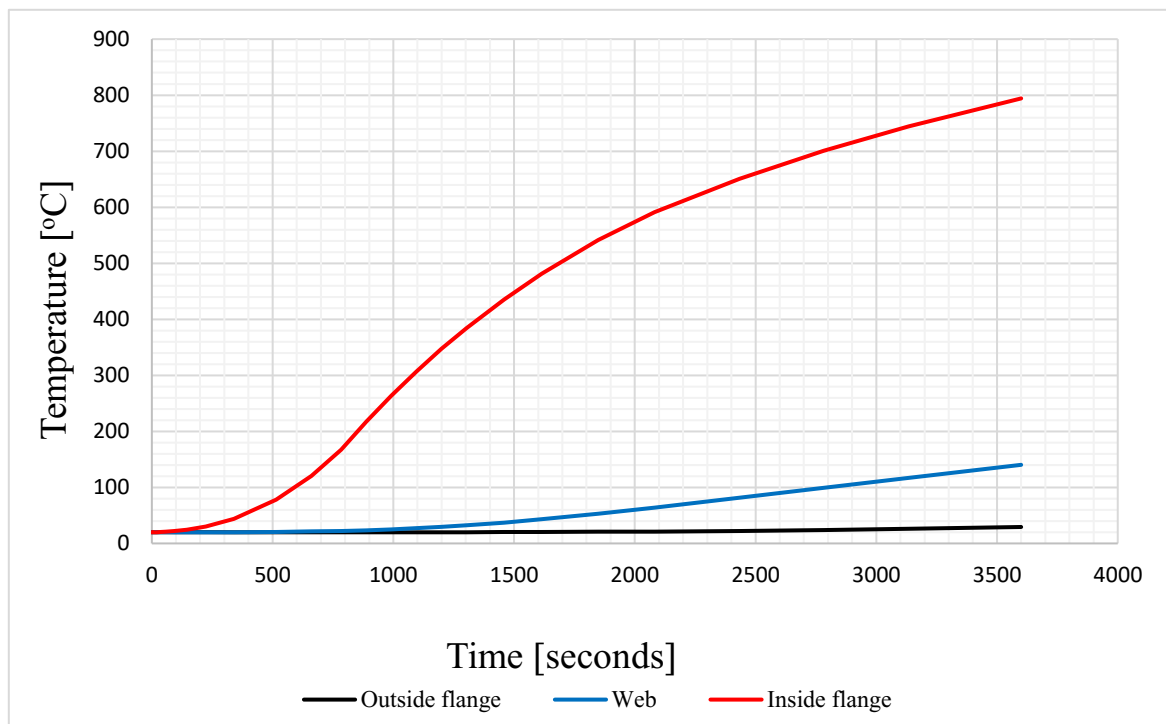


Figure 3.31. Temperature evolution in partially steel-concrete cross section

INFLUENCE OF HIGH TEMPERATURE ON THE STRUCTURAL BEHAVIOUR OF STEEL STRUCTURES AND SOLUTIONS : CASE OF PANZANI BUILDING

Due to the low conductivity of concrete as compare to steel and its material composition, the effect of fire on the steel column is reduced and the temperature inside the steel column doesn't increases rapidly as when the column wasn't protected as all, but the temperature of the inside flange of the column increases until it crosses the critical temperature because it is in direct contact with fire since the protection is only partial.

The results gotten from the heat analysis, where a standard fire of one hour was applied on the totally protected steel-concrete column are presented in figure 3.32.

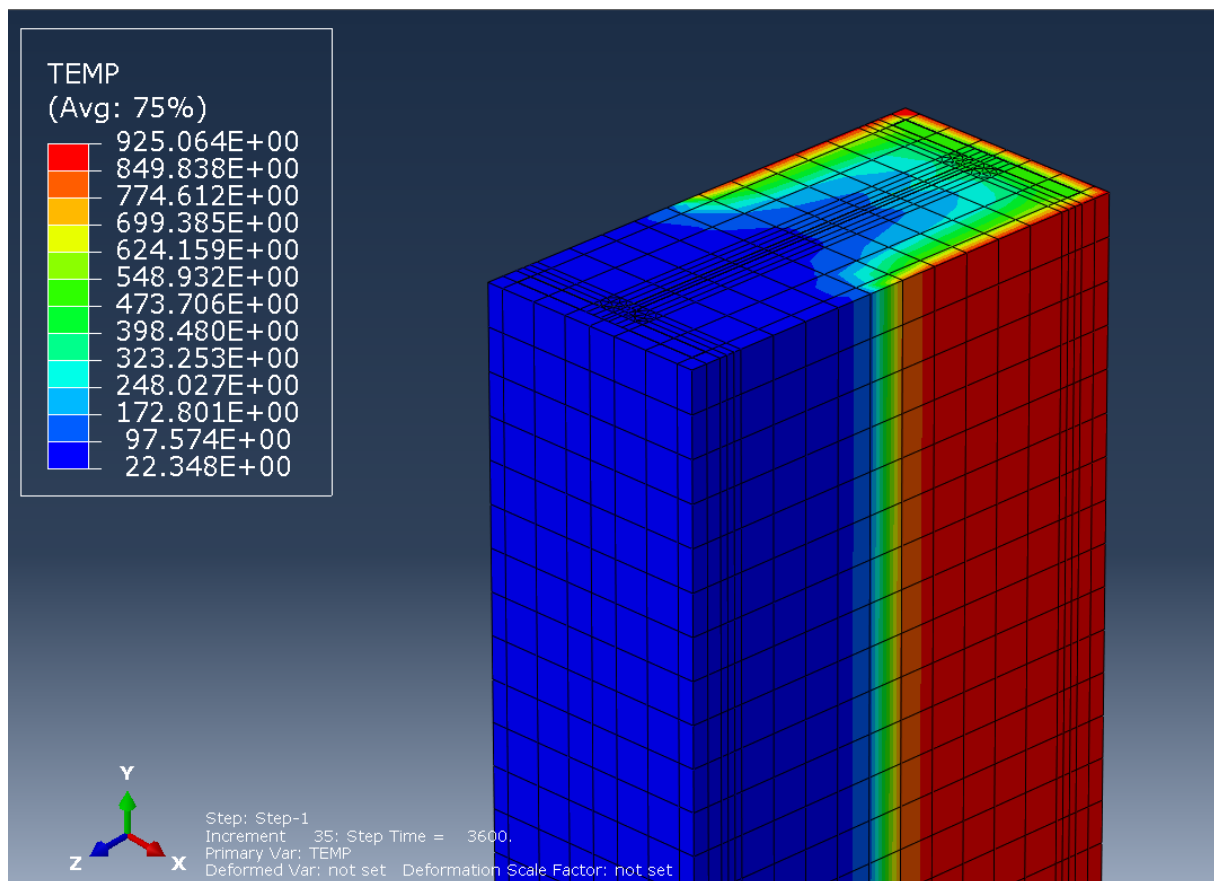


Figure 3.32. Temperature distribution in totally protected steel with concrete

The evolution of temperature within the cross section of the steel column in function of time is illustrated in Figure 3.33.

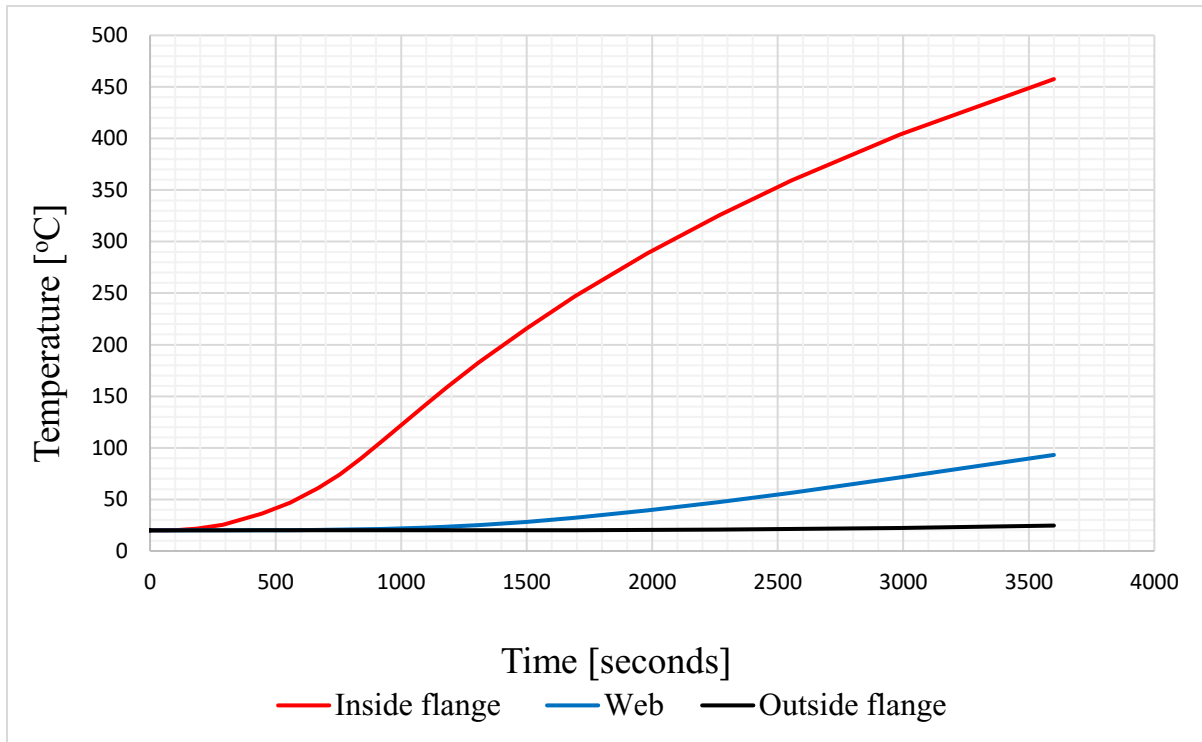


Figure 3.33. Temperature evolution in totally steel-concrete cross section

This study shows that, in fire situation, the behaviour of steel beams is quite improved when it is protected by concrete even though the conductivity of concrete is quite high as compared to timber since none of the part of the IPE column reached its critical temperature. It appears that the failure of steel beams is slowed to an extent, depending on the amount of steel surface protected by concrete. So, full concrete protects more as compare to partial concrete protection. In these conditions, concrete seems to be a possible solution to protect steel against fire.

The results of these analyses made using timber and concrete as protective materials for fire protection of steel showed that timber is a better material for fire protection as compare to concrete because it has a lower conductivity, therefore it conducts less heat and protect steel from rapidly reaching its critical temperature and the char produced due to fire prevents temperature to increase in the steel covered by it. Moreover, timber is an ecological renewable material, its transformation process produces less negative impacts to the environment and it is a material that confers beautiful aesthetics without being painted as compare to concrete. Other types of passive fire protection materials that can insulate steel structures from the effects of high temperatures proposed in this work are fire extinguisher balls (annex 9) that can be installed at significant heights on the walls with the help of mounting frames and intumescent coatings (annex 9) used for the purlins, the rafters and the inside part of aluminium zinc.

Conclusion

In this chapter, the main objective was to present the results of the static verification of the building, the numerical fire analyses made and interpret the results. Firstly, the structural members present in the case study were proven to be statically verified according to Eurocode prescriptions. Then, fire analysis made on the roofing elements showed that they were extremely affected by fire due to high deflection observed and the fact that their melting point arrived rapidly just after the beginning of the fire. Moreover, a global fire analysis of the structure was made and local analyses made on a purlin and a column of the case study showed that one hour of standard fire greatly affected those steel elements. Afterwards, the local analyses made on CHS and SHS columns showed that these two column cross sections are not efficient against fire as compare to an IPE due to their hollow sections. Finally, a protective fire system was proposed and the fire analyses made on the hybrid steel-timber column and hybrid steel-concrete column showed that they are good fire protective materials for steel and an analysis made between these two fire protective system resulted in favourable result for the system made with total timber in terms of conductivity, environmental effects and aesthetic.

GENERAL CONCLUSION

The main objective of this thesis was to study the impact of fire on the structural behaviour of steel and to propose some solutions in order to prevent this damage. To accomplish this, a steel building that was damaged by fire was used for the study. This study started with a static verification of the building in compliance with Eurocodes and fire analyses were made in the software Abaqus/CAE in order to observe how structural steel is affected by fire. The work was organised in three chapters, the first was a literature review on steel, steel structures, the effect of fire on steel structures and how structural analysis of fire in a structure can be made. The second chapter was the methodology, where the verification procedure of the building and the analyses process in Abaqus were explained. And in the third chapter, the results of the analyses were presented. We carried out numerical modelling by first performing a static analysis using SAP2000 and then fire analysis in Abaqus. All the members present in the case study were classified based on their cross section and then were proven to be statically verified according to Eurocode prescriptions. Then, fire analyses made on the roofing elements showed that they were extremely affected by fire due to high deflection observed and the fact that their melting point arrived rapidly just after the beginning of the fire. Moreover, a global fire analysis was made and it was observed that the most affected structures on it were the purlins due to their small cross sections as compare to the other structural elements. Afterwards, local analyses made on a purlin and a column showed that after one hour of fire, the purlin deflected with a value of 366.5 mm and the column with a value of 866 mm. Then, the analysis made on CHS and SHS columns showed that these two columns cross sections are not efficient against fire as compare to an IPE due to their hollow sections. The displacements observed after fire analyses on the SHS and CHS were 1596 mm and 1474 mm respectively. Finally, protective fire systems were analysed and only heat analyses were made on hybrid steel-timber and hybrid steel-concrete columns due to the high computational cost of stress analysis. These heat analyses results showed that they are good fire protective materials for steel and that the total hybrid steel-timber was the best configuration for fire protection. In view of all these results, even though steel is a non-combustible material, its mechanical properties decrease dramatically at elevated temperatures and it really need to be protected with timber or concrete, or with fire extinguisher balls and intumescent coatings in order to avoid severe damages. Studies following similar procedure can be carried out on the different connections of the buildings and a study of the behaviour of steel at the end of a fire event during the cooling phase in order to know if the steel elements could be reused or should be replaced could be the subject of other analyses.

BIBLIOGRAPHY

- Agarwal, A., & Varma, A. H. (2014). Fire Induced Progressive Collapse of Steel Building Structures: The Role of Interior Gravity Columns. *Engineering Structures*, 58, 129–140. <https://doi.org/10.1016/j.engstruct.2013.09.020>
- ASTM. (1980). *ASTM E119: Fire Tests of Building Construction and Materials*. American Society for Testing and Materials, Philadelphia, PA.
- Barraclough, K. (1990). *Steelmaking 1850–1900*, Institute of Metals, London.
- Bisby, L., Gales, J., & Maluk, C. (2013). *A contemporary review of large-scale non-standard structural fire testing*. 1–27.
- British Steel. (1999). *The Behaviour of Multi-storey Steel Framed Buildings in fire (British Steel).pdf*.
- Cameroon Tribune. (2019). *SONARA fire incident*.
- Davison, Buick; Graham, W. O. (2012). *STEEL DESIGNERS ' MANUAL*.
- Deo, Brahma; Boom, R. (1993). *Fundamentals of Steelmaking Metallurgy*. New York: Prentice Hall International.
- EN 1990. (2002). *Eurocode 0 : Basis of structural design*.
- EN 1991-1-1. (2002). *Eurocode 1 : Actions on structures — Part 1-1 : General actions — Densities, self-weight, imposed loads for buildings*.
- EN 1991-1-2. (2002). *Eurocode 1 : Actions on structures — Part 1-2 : General actions — Actions on structures exposed to fire*.
- EN 1991-1-4. (2002). *Eurocode 1 : Actions on structures — Part 1-4 : General actions — Wind actions*.
- EN 1992-1-2. (2004). *Eurocode 2 : Design of concrete structures — Part 1-2 : General rules — Structural fire design*.
- EN 1993-1-1. (2005). *Eurocode 3 : Design of steel structures — Part 1-1 : General rules and rules for buildings*.
- EN 1993-1-2. (2005). *Eurocode 3 : Design of steel structures — Part 1-2 : General rules — Structural fire design*.

- EN 1993-1-5. (2006). *Eurocode 3 : Design of steel structures — Part 1-5: Plated structural elements.*
- EN 1993-1-8. (2005). *Eurocode 3 : Design of steel structures — Part 1-8 : Design of joints.*
- EN 1995-1-2. (2005). *Eurocode 5 : Design of timber structures — Part 1-2 : General - Structural fire design.*
- EN 1999-1-1. (2007). *Eurocode 9 : Design of aluminium structures — Part 1-1: General structural rules.*
- EN 1999-1-2. (2007). *Eurocode 9 : Design of aluminium structures — Part 1-2 : Design of aluminium structures.*
- Gales, J., Maluk, C., & Bisby, L. (2012). *LARGE-SCALE STRUCTURAL FIRE TESTING – HOW DID WE GET HERE , WHERE ARE WE , AND WHERE ARE WE GOING ?* 1–22.
- Georgeta Baetu, ;, Teofil-Florin, G., & Baetu, S.-A. (2017). *Behaviour of steel structures under elevated temperature.* 181, 265–272. <https://doi.org/10.1016/j.proeng.2017.02.388>
- Jack C. McCormac, P.E; Stephen F. Csernak, P. . (2012). *structural steel design, 5th ed-signed.pdf.*
- Kamaya, M. (2014). Ramberg-Osgood type stress-strain curve estimation using yield and ultimate strengths for failure assessments. *International Journal of Pressure Vessels and Piping*, 137, 1–12. <https://doi.org/10.1016/j.ijpvp.2015.04.001>
- Landesmann, A., & Batista, E. D. M. (2005). *Implementation of advanced analysis method for steel-framed structures under fire conditions.* 40, 339–366. <https://doi.org/10.1016/j.firesaf.2005.02.003>
- Lennon, T., Moore, D. B., Wang, Y. C., & Bailey, C. G. (2007). *Designers ' guide to EN1991-1-2 ,.*
- Mbessa Michel. (2005). *Traité de génie civil Matériaux Volume 1.*
- PiT Project. (2000). *Main report of the Behaviour of steel framed structures under fire conditions.* June.
- Shi, Y., Tu, C., Wu, Y., Liu, D., Meng, L., & Ban, H. (2020). Numerical investigations of fire-resistant steel welded I-section columns under elevated temperatures. *Journal of Constructional Steel Research*, 177, 106464. <https://doi.org/10.1016/j.jcsr.2020.106464>

- Sylvain Andzong. (2020). *Business in Cameroon: SONARA's reconstruction depends on the effective restructuring of its over XAF700 bln debt, according to the MINEE.*
- T.J.MacGinley. (1998). *Steel Structures Practical design studies.*
- Tamboli, A. R. (2017). *Handbook of structural steel connection Design and Details, Third edition.*
- Thomas IR, Bennetts ID, Dayawansa PH, Proe DJ, L. R. (1992). *Fire Tests of the 140 William Street Office Building, BHP Research Report No. BHPR/ENG/ R/92/043/SG2C. BHP Billiton Limited, Melbourne.*
- Turkdogan. (1996). *Fundamentals of Steelmaking. London: Institute of Materials.*
- Wald, Moore, D. B., Lennon, T., Chladna, M., Santiago, A., Benes̃, M., & Borges, L. (2006). *Experimental behaviour of a steel structure under natural fire. 41, 509–522.*
<https://doi.org/10.1016/j.firesaf.2006.05.006>
- Wang, J. H., He, J., & Xiao, Y. (2019). Fire behavior and performance of concrete-filled steel tubular columns: Review and discussion. *Journal of Constructional Steel Research, 157,* 19–31. <https://doi.org/10.1016/j.jcsr.2019.02.012>
- World Steel Association. (2020). *World Steel in Figures.*

WEBOGRAPHY

<https://www.britannica.com/technology/crucible-process> consulted on 13 May 2021.

<https://www.britannica.com/technology/steel/Bessemer-steel> consulted on 13 May 2021.

https://www.steelconstruction.info/Corrosion_of_structural_steel#:~:text=Corrosion%20of%20structural%20steel%20The%20corrosion%20of%20structural,six%20times%20the%20volume%20of%20the%20original%20material consulted on 13 May 2021.

<http://www.iipinetwork.org/wp-content/letd/content/electric-arc-furnace.html> consulted on 13 May 2021.

<https://www.thoughtco.com/general-properties-of-steels-2340118> consulted on 13 May 2021.

<https://www.morecambemetals.co.uk/metals-and-their-properties-steel> consulted on 13 May 2021.

<https://www.structuralguide.com/preventcorrosion/#:~:text=%20How%20to%20Prevent%20Corrosion%20of%20Metal,employed%20to%20protect%20the%20steel.%20But...%20More%20> consulted on 04 June 2021.

<https://www.dreamstime.com/stock-photo-steel-pouring-hot-plant-image66078777> consulted on 02 July 2021.

<https://urbansplatter.com/2014/07/history-architecture-empire-state-building> consulted on 25 February 2021.

<https://www.aisc.org/modernsteel/news/2020/january/looking-back-on-a-decade-of-steel-construction> consulted on 25 February 2021.

<https://www.cameroon-tribune.cm/article.html/26030/fr.html/sonara-fire-incident-gov-t-assures-consumers-of-constant-supply> consulted on 25 February 2021.

<https://www.worldsteel.org/steel-by-topic/steel-markets/buildings-and-infrastructure.html> consulted on 25 February 2021.

<https://www.businessincameroon.com/public-management/0212-11086-cameroon-sonara-s-reconstruction-depends-on-the-effective-restructuring-of-its-over-xaf700-bln-debt-according-to-the-minee> consulted on 25 February 2021.

<https://www.steelincga.com/a-brief-history-of-steel-construction/> consulted on 25 January 2021.

ANNEXES

ANNEX 1. Section factor for unprotected and insulated steel section

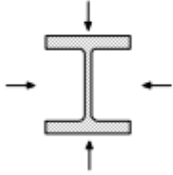
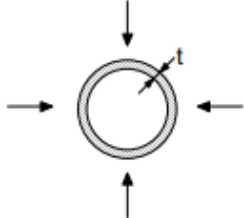
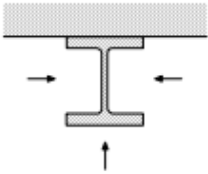

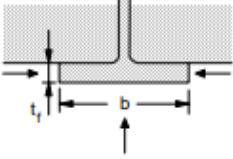
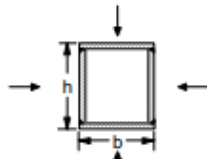
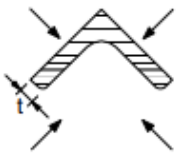
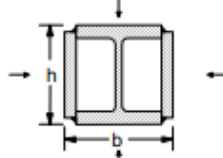
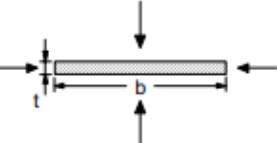
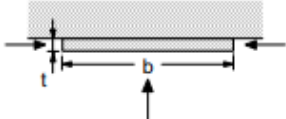
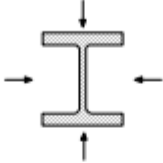
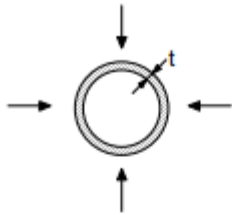
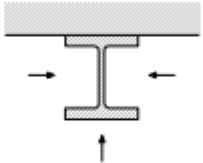
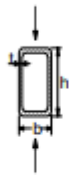
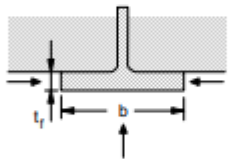
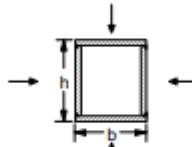
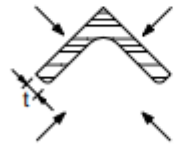
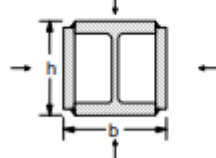
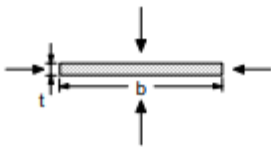
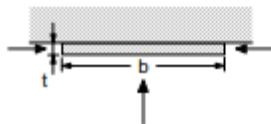
<p>Open section exposed to fire on all sides:</p> $\frac{A_m}{V} = \frac{\text{perimeter}}{\text{cross-section area}}$ 	<p>Tube exposed to fire on all sides: $A_m/V = 1/t$</p> 
<p>Open section exposed to fire on three sides:</p> $\frac{A_m}{V} = \frac{\text{surface exposed to fire}}{\text{cross-section area}}$ 	<p>Hollow section (or welded box section of uniform thickness) exposed to fire on all sides:</p> <p>If $t \ll b$: $A_m/V \approx 1/t$</p> 
<p>I-section flange exposed to fire on three sides:</p> $A_m/V = (b + 2t_f)/(bt_f)$ <p>If $t \ll b$: $A_m/V \approx 1/t_f$</p> 	<p>Welded box section exposed to fire on all sides:</p> $\frac{A_m}{V} = \frac{2(b + h)}{\text{cross-section area}}$ <p>If $t \ll b$: $A_m/V \approx 1/t$</p> 
<p>Angle exposed to fire on all sides:</p> $A_m/V = 2/t$ 	<p>I-section with box reinforcement, exposed to fire on all sides:</p> $\frac{A_m}{V} = \frac{2(b + h)}{\text{cross-section area}}$ 
<p>Flat bar exposed to fire on all sides:</p> $A_m/V = 2(b + t)/(bt)$ <p>If $t \ll b$: $A_m/V \approx 2/t$</p> 	<p>Flat bar exposed to fire on three sides:</p> $A_m/V = (b + 2t)/(bt)$ <p>If $t \ll b$: $A_m/V \approx 1/t$</p> 

Table 4.2: Section factor A_m/V for unprotected steel members.

<p>Open section exposed to fire on all sides:</p> $\frac{A_m}{V} = \frac{\text{perimeter}}{\text{cross-section area}}$ 	<p>Tube exposed to fire on all sides: $A_m/V = 1/t$</p> 
<p>Open section exposed to fire on three sides:</p> $\frac{A_m}{V} = \frac{\text{surface exposed to fire}}{\text{cross-section area}}$ 	<p>Hollow section (or welded box section of uniform thickness) exposed to fire on all sides:</p> <p>If $t \ll b$: $A_m/V \approx 1/t$</p> 
<p>I-section flange exposed to fire on three sides:</p> $A_m/V = (b + 2t_f)/(bt_f)$ <p>If $t \ll b$: $A_m/V \approx 1/t_f$</p> 	<p>Welded box section exposed to fire on all sides:</p> $\frac{A_m}{V} = \frac{2(b + h)}{\text{cross-section area}}$ <p>If $t \ll b$: $A_m/V \approx 1/t$</p> 
<p>Angle exposed to fire on all sides:</p> $A_m/V = 2/t$ 	<p>I-section with box reinforcement, exposed to fire on all sides:</p> $\frac{A_m}{V} = \frac{2(b + h)}{\text{cross-section area}}$ 
<p>Flat bar exposed to fire on all sides:</p> $A_m/V = 2(b + t)/(bt)$ <p>If $t \ll b$: $A_m/V \approx 2/t$</p> 	<p>Flat bar exposed to fire on three sides:</p> $A_m/V = (b + 2t)/(bt)$ <p>If $t \ll b$: $A_m/V \approx 1/t$</p> 

ANNEX 2. Critical temperature $\theta_{a,cr}$ for values of the utilization factor μ_0

μ_0	$\theta_{a,cr}$	μ_0	$\theta_{a,cr}$	μ_0	$\theta_{a,cr}$
0,22	711	0,42	612	0,62	549
0,24	698	0,44	605	0,64	543
0,26	685	0,46	598	0,66	537
0,28	674	0,48	591	0,68	531
0,30	664	0,50	585	0,70	526
0,32	654	0,52	578	0,72	520
0,34	645	0,54	572	0,74	514
0,36	636	0,56	566	0,76	508
0,38	628	0,58	560	0,78	502
0,40	620	0,60	554	0,80	496

ANNEX 3. Building category

Table 6.1 - Categories of use

Category	Specific Use	Example
A	Areas for domestic and residential activities	Rooms in residential buildings and houses; bedrooms and wards in hospitals; bedrooms in hotels and hostels kitchens and toilets.
B	Office areas	
C	Areas where people may congregate (with the exception of areas defined under category A, B, and D ¹⁾)	<p>C1: Areas with tables, etc. e.g. areas in schools, cafés, restaurants, dining halls, reading rooms, receptions.</p> <p>C2: Areas with fixed seats, e.g. areas in churches, theatres or cinemas, conference rooms, lecture halls, assembly halls, waiting rooms, railway waiting rooms.</p> <p>C3: Areas without obstacles for moving people, e.g. areas in museums, exhibition rooms, etc. and access areas in public and administration buildings, hotels, hospitals, railway station forecourts.</p> <p>C4: Areas with possible physical activities, e.g. dance halls, gymnastic rooms, stages.</p> <p>C5: Areas susceptible to large crowds, e.g. in buildings for public events like concert halls, sports halls including stands, terraces and access areas and railway platforms.</p>
D	Shopping areas	<p>D1: Areas in general retail shops</p> <p>D2: Areas in department stores</p>
<p>¹⁾ Attention is drawn to 6.3.1.1(2), in particular for C4 and C5. See EN 1990 when dynamic effects need to be considered. For Category E, see Table 6.3</p> <p>NOTE 1 Depending on their anticipated uses, areas likely to be categorised as C2, C3, C4 may be categorised as C5 by decision of the client and/or National annex.</p> <p>NOTE 2 The National annex may provide sub categories to A, B, C1 to C5, D1 and D2</p> <p>NOTE 3 See 6.3.2 for storage or industrial activity</p>		

Table 6.3 -Categories of storage and industrial use

Category	Specific use	Example
E1	Areas susceptible to accumulation of goods, including access areas	Areas for storage use including storage of books and other documents.
E2	Industrial use	

ANNEX 4. Safety factors for permanent and variable actions

Persistent and transient design situations	Permanent actions		Leading variable action (*)	Accompanying variable actions	
	Unfavourable	Favourable		Main (if any)	Others
(Eq. 6.10)	$\gamma_{Gj,sup} G_{kj,sup}$	$\gamma_{Gj,inf} G_{kj,inf}$	$\gamma_{Q,1} Q_{k,1}$		$\gamma_{Q,i} \psi_{0,i} Q_{k,i}$

(*) Variable actions are those considered in Table A1.1

NOTE 1 The γ values may be set by the National annex. The recommended set of values for γ are :

$$\gamma_{Gj,sup} = 1,10$$

$$\gamma_{Gj,inf} = 0,90$$

$$\gamma_{Q,1} = 1,50 \text{ where unfavourable (0 where favourable)}$$

$$\gamma_{Q,i} = 1,50 \text{ where unfavourable (0 where favourable)}$$

NOTE 2 In cases where the verification of static equilibrium also involves the resistance of structural members, as an alternative to two separate verifications based on Tables A1.2(A) and A1.2(B), a combined verification, based on Table A1.2(A), may be adopted, if allowed by the National annex, with the following set of recommended values. The recommended values may be altered by the National annex.

$$\gamma_{Gj,sup} = 1,35$$

$$\gamma_{Gj,inf} = 1,15$$

$$\gamma_{Q,1} = 1,50 \text{ where unfavourable (0 where favourable)}$$

$$\gamma_{Q,i} = 1,50 \text{ where unfavourable (0 where favourable)}$$

provided that applying $\gamma_{Gj,inf} = 1,00$ both to the favourable part and to the unfavourable part of permanent actions does not give a more unfavourable effect.

ANNEX 5. Recommended values of Ψ factors for buildings

Table A1.1 - Recommended values of ψ factors for buildings

Action	ψ_0	ψ_1	ψ_2
Imposed loads in buildings, category (see EN 1991-1-1)			
Category A : domestic, residential areas	0,7	0,5	0,3
Category B : office areas	0,7	0,5	0,3
Category C : congregation areas	0,7	0,7	0,6
Category D : shopping areas	0,7	0,7	0,6
Category E : storage areas	1,0	0,9	0,8
Category F : traffic area, vehicle weight $\leq 30\text{kN}$	0,7	0,7	0,6
Category G : traffic area, $30\text{kN} < \text{vehicle weight} \leq 160\text{kN}$	0,7	0,5	0,3
Category H : roofs	0	0	0
Snow loads on buildings (see EN 1991-1-3)*			
Finland, Iceland, Norway, Sweden	0,70	0,50	0,20
Remainder of CEN Member States, for sites located at altitude $H > 1000$ m a.s.l.	0,70	0,50	0,20
Remainder of CEN Member States, for sites located at altitude $H \leq 1000$ m a.s.l.	0,50	0,20	0
Wind loads on buildings (see EN 1991-1-4)	0,6	0,2	0
Temperature (non-fire) in buildings (see EN 1991-1-5)	0,6	0,5	0
NOTE The ψ values may be set by the National annex.			
* For countries not mentioned below, see relevant local conditions.			

ANNEX 6. Steel cross section's classification

Table 5.2 (sheet 1 of 3): Maximum width-to-thickness ratios for compression parts

Internal compression parts						
				Axis of bending		
				Axis of bending		
Class	Part subject to bending	Part subject to compression	Part subject to bending and compression			
1						
	$c/t \leq 72\varepsilon$	$c/t \leq 33\varepsilon$	when $\alpha > 0,5$: $c/t \leq \frac{396\varepsilon}{13\alpha - 1}$ when $\alpha \leq 0,5$: $c/t \leq \frac{36\varepsilon}{\alpha}$			
2	$c/t \leq 83\varepsilon$	$c/t \leq 38\varepsilon$	when $\alpha > 0,5$: $c/t \leq \frac{456\varepsilon}{13\alpha - 1}$ when $\alpha \leq 0,5$: $c/t \leq \frac{41,5\varepsilon}{\alpha}$			
3						
	$c/t \leq 124\varepsilon$	$c/t \leq 42\varepsilon$	when $\psi > -1$: $c/t \leq \frac{42\varepsilon}{0,67 + 0,33\psi}$ when $\psi \leq -1^*)$: $c/t \leq 62\varepsilon(1 - \psi)\sqrt{-\psi}$			
$\varepsilon = \sqrt{235/f_y}$	f_y	235	275	355	420	460
	ε	1,00	0,92	0,81	0,75	0,71

*) $\psi \leq -1$ applies where either the compression stress $\sigma \leq f_y$ or the tensile strain $\varepsilon_y > f_y/E$

Table 5.2 (sheet 2 of 3): Maximum width-to-thickness ratios for compression parts

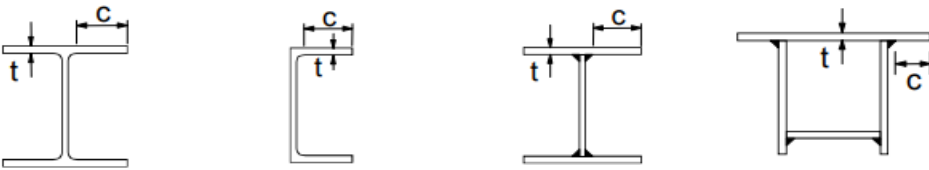
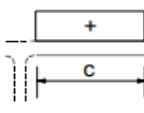
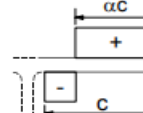
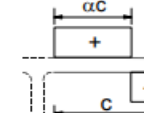
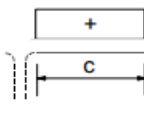
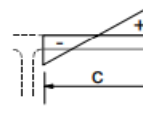
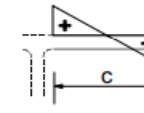
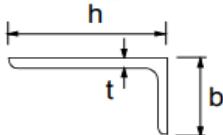
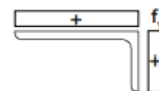
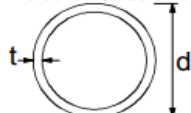
Outstand flanges						
						
Rolled sections			Welded sections			
Class	Part subject to compression	Part subject to bending and compression				
		Tip in compression		Tip in tension		
Stress distribution in parts (compression positive)						
1	$c/t \leq 9\epsilon$	$c/t \leq \frac{9\epsilon}{\alpha}$		$c/t \leq \frac{9\epsilon}{\alpha\sqrt{\alpha}}$		
2	$c/t \leq 10\epsilon$	$c/t \leq \frac{10\epsilon}{\alpha}$		$c/t \leq \frac{10\epsilon}{\alpha\sqrt{\alpha}}$		
Stress distribution in parts (compression positive)						
3	$c/t \leq 14\epsilon$	$c/t \leq 21\epsilon\sqrt{k_\sigma}$ For k_σ see EN 1993-1-5				
$\epsilon = \sqrt{235/f_y}$	f_y	235	275	355	420	460
	ϵ	1,00	0,92	0,81	0,75	0,71

Table 5.2 (sheet 3 of 3): Maximum width-to-thickness ratios for compression parts

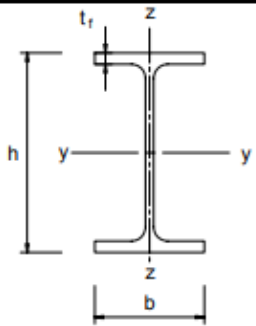
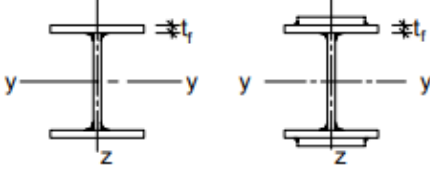

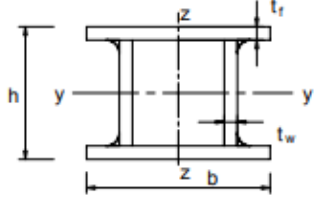
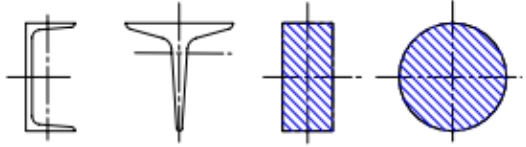
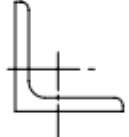
Angles							
Refer also to "Outstand flanges" (see sheet 2 of 3)					Does not apply to angles in continuous contact with other components		
		Section in compression					
Stress distribution across section (compression positive)							
3	$h/t \leq 15\epsilon; \frac{b+h}{2t} \leq 11,5\epsilon$						
Tubular sections							
							
		Section in bending and/or compression					
		1	$d/t \leq 50\epsilon^2$				
		2	$d/t \leq 70\epsilon^2$				
3	$d/t \leq 90\epsilon^2$						
NOTE For $d/t > 90\epsilon^2$ see EN 1993-1-6.							
$\epsilon = \sqrt{235/f_y}$	f_y	235	275	355	420	460	
	ϵ	1,00	0,92	0,81	0,75	0,71	
	ϵ^2	1,00	0,85	0,66	0,56	0,51	

ANNEX 7. Imperfection factor and buckling curve's selection tables

Table 6.1: Imperfection factors for buckling curves

Buckling curve	a ₀	a	b	c	d
Imperfection factor α	0,13	0,21	0,34	0,49	0,76

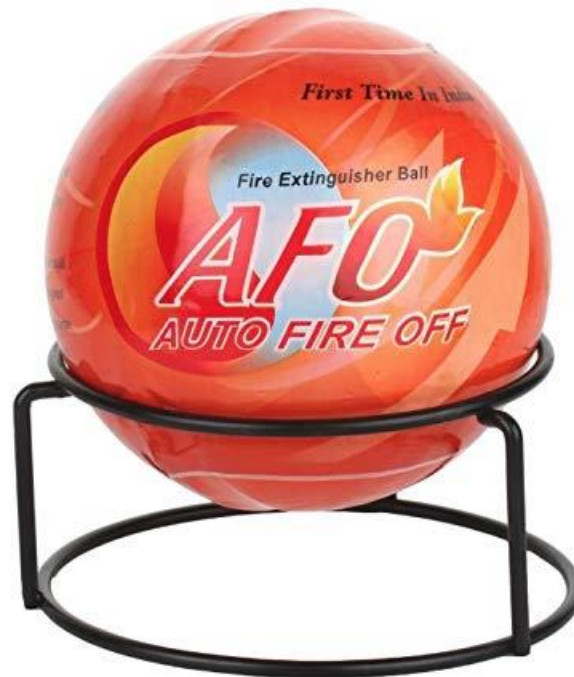
Table 6.2: Selection of buckling curve for a cross-section

Cross section	Limits	Buckling about axis	Buckling curve		
			S 235 S 275 S 355 S 420	S 460	
Rolled sections 	$h/b > 1,2$	y-y z-z	$t_f \leq 40$ mm	a b	a ₀ a ₀
			$40 < t_f \leq 100$	b c	a a
	$h/b \leq 1,2$	y-y z-z	$t_f \leq 100$ mm	b c	a a
			$t_f > 100$ mm	d d	c c
Welded I-sections 	$t_f \leq 40$ mm	y-y z-z	b c	b c	
	$t_f > 40$ mm	y-y z-z	c d	c d	
Hollow sections 	hot finished	any	a	a ₀	
	cold formed	any	c	c	
Welded box sections 	generally (except as below)	any	b	b	
	thick welds: $a > 0,5t_f$ $b/t_f < 30$ $h/t_w < 30$	any	c	c	
U-, T- and solid sections 		any	c	c	
L-sections 		any	b	b	

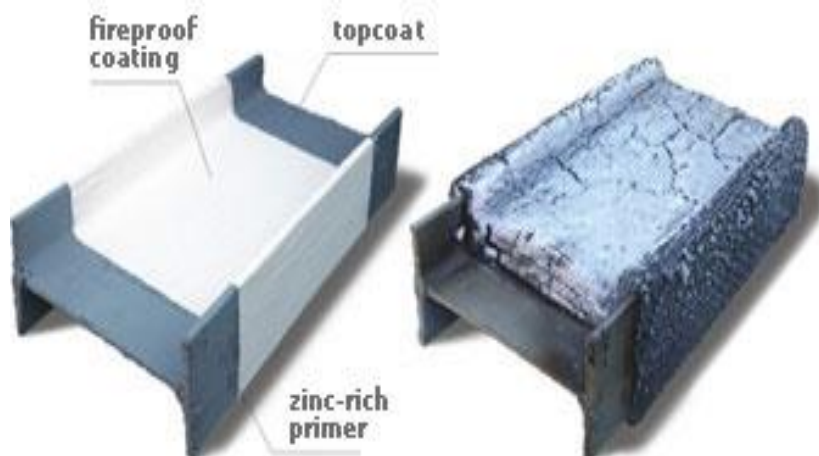
ANNEX 8. Effective length of the T-stub

Bolt-row Location	Bolt-row considered individually		Bolt-row considered as part of a group of bolt-rows	
	Circular patterns $\ell_{\text{eff,cp}}$	Non-circular patterns $\ell_{\text{eff,nc}}$	Circular patterns $\ell_{\text{eff,cp}}$	Non-circular patterns $\ell_{\text{eff,nc}}$
Inner bolt-row	$2\pi m$	$4m + 1,25e$	$2p$	p
End bolt-row	The smaller of: $2\pi m$ $\pi m + 2e_1$	The smaller of: $4m + 1,25e$ $2m + 0,625e + e_1$	The smaller of: $\pi m + p$ $2e_1 + p$	The smaller of: $2m + 0,625e + 0,5p$ $e_1 + 0,5p$
Mode 1:	$\ell_{\text{eff,1}} = \ell_{\text{eff,nc}}$ but $\ell_{\text{eff,1}} \leq \ell_{\text{eff,cp}}$		$\sum \ell_{\text{eff,1}} = \sum \ell_{\text{eff,nc}}$ but $\sum \ell_{\text{eff,1}} \leq \sum \ell_{\text{eff,cp}}$	
Mode 2:	$\ell_{\text{eff,2}} = \ell_{\text{eff,nc}}$		$\sum \ell_{\text{eff,2}} = \sum \ell_{\text{eff,nc}}$	

ANNEX 9. Fire extinguisher ball and intumescent coating



Fire extinguisher ball



Fireproof coating system
before and after fire exposure

Intumescent coating